# NAVAL POSTGRADUATE SCHOOL
## Monterey, California

DTIC FILE COPY

DTIC
ELECTE
FEB 0 4 1991
S B D

## THESIS

SEPARATING BOUNDARY LAYER RESPONSE TO AN
UNSTEADY TURBULENT ENVIRONMENT

by

David J. Gwilliam Jr.

December, 1989

Thesis Advisor:          Richard M. Howard

Approved for public release; distribution is unlimited

# REPORT DOCUMENTATION PAGE

Form Approved
OMB No 0704-0188

| 1a REPORT SECURITY CLASSIFICATION UNCLASSIFIED | 1b RESTRICTIVE MARKINGS |
|---|---|

| 2a SECURITY CLASSIFICATION AUTHORITY | 3 DISTRIBUTION AVAILABILITY OF REPORT |
|---|---|
| 2b DECLASSIFICATION DOWNGRADING SCHEDULE | Approved for public release; distribution is unlimited |

| 4 PERFORMING ORGANIZATION REPORT NUMBER(S) | 5 MONITORING ORGANIZATION REPORT NUMBER(S) |
|---|---|

| 6a NAME OF PERFORMING ORGANIZATION Naval Postgraduate School | 6b OFFICE SYMBOL (If applicable) Code 67 | 7a NAME OF MONITORING ORGANIZATION Naval Postgraduate School |
|---|---|---|

| 6c ADDRESS (City, State, and ZIP Code) Monterey, California 93943-5000 | 7b ADDRESS (City, State, and ZIP Code) Monterey, California 93943-5000 |
|---|---|

| 8a NAME OF FUNDING SPONSORING ORGANIZATION | 8b OFFICE SYMBOL (If applicable) | 9 PROCUREMENT INSTRUMENT IDENTIFICATION NUMBER |
|---|---|---|

| 8c ADDRESS (City, State, and ZIP Code) | 10 SOURCE OF FUNDING NUMBERS | | | |
|---|---|---|---|---|
| | PROGRAM ELEMENT NO | PROJECT NO | TASK NO | WORK UNIT ACCESSION NO |

11 TITLE (Include Security Classification)
SEPARATING BOUNDARY LAYER RESPONSE TO AN UNSTEADY TURBULENT ENVIRONMENT

12 PERSONAL AUTHOR(S)
Gwilliam, David J. Jr.

| 13a TYPE OF REPORT Master's Thesis | 13b TIME COVERED FROM ____ TO ____ | 14 DATE OF REPORT (Year, Month Day) 1989, December | 15 PAGE COUNT 143 |
|---|---|---|---|

16 SUPPLEMENTARY NOTATION
The views expressed in this thesis are those of the author and do not reflect the official policy or position of the Department of Defense or the U.S. Government.

| 17 COSATI CODES | | | 18 SUBJECT TERMS (Continue on reverse if necessary and identify by block number) |
|---|---|---|---|
| FIELD | GROUP | SUB-GROUP | Separated; Boundary Layer Response to Disturbance; Unsteady Aerodynamics |
| | | | |

19 ABSTRACT (Continue on reverse if necessary and identify by block number)

An experimental investigation of the separating boundary layer of a wing subjected to periodic turbulent disturbances was conducted.

Turbulence pulses were generated by a non-thrusting spinning rod placed upstream of the test airfoil at the reduced frequencies of .09 and .47.

Time-varying velocity measurements were made at various heights above the 70% chord location at 12 degrees angle of attack (nearly separated flow) and 22 degrees angle of attack (fully separated flow). Split-film anemometry was used to determine flow speed and direction. The flow responses were compared to the quasi-steady state of undisturbed separated flow.

| 20 DISTRIBUTION AVAILABILITY OF ABSTRACT ☒ UNCLASSIFIED UNLIMITED ☐ SAME AS RPT ☐ DTIC USERS | 21 ABSTRACT SECURITY CLASSIFICATION Unclassified |
|---|---|
| 22a NAME OF RESPONSIBLE INDIVIDUAL Prof. Richard M. Howard | 22b TELEPHONE (Include Area Code) (408) 646-2870 | 22c OFFICE SYMBOL Code 67Ho |

#19 - ABSTRACT - (CONTINUED)

Variation of reduced frequency had a dramatic influence on the effects which the periodic disturbance had on the flow response. At a reduced frequency of .47 the periodic disturbance had no noticeable influence. Imposition of periodic disturbance of the same reduced frequency on attached flow near separation (12 degrees angle of attack) once again caused no apparent destabilizing effects. The lack of sensitivity of the separated boundary layer to the pulses generated at the higher reduced frequency of .47 apparently resulted from its inability to resolve turbulent pulses from one another. Imposition at 22 degrees angle of attack of a pulse at the reduced frequency of .09, however, first stabilized the flow, then greatly intensified the original separation before allowing the flow to return to its undisturbed separated state.

| Accession For | |
| --- | --- |
| NTIS GRA&I | ☑ |
| DTIC TAB | ☐ |
| Unannounced | ☐ |
| Justification | |

By_____

Distribution/

Availability Codes

| Dist | Avail and/or Special |
| --- | --- |

Separating Boundary Layer Response to an Unsteady
Turbulent Environment

by

David J. Gwilliam Jr.
Lieutenant, United States Navy
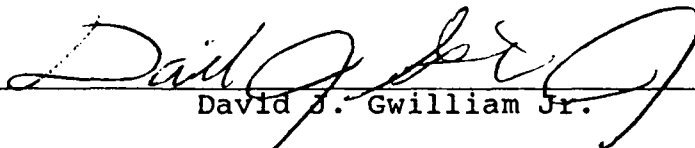B.S., United States Naval Academy, 1983

Submitted in partial fulfillment of the
requirements for the degree of

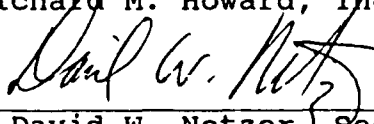MASTER OF SCIENCE IN ENGINEERING SCIENCE

from the
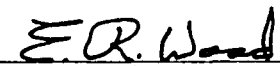
NAVAL POSTGRADUATE SCHOOL
December, 1989

Author: _____
David J. Gwilliam Jr.

Approved by: _____
Richard M. Howard, Thesis Advisor

_____
David W. Netzer, Second Reader

_____
E. Roberts Wood, Chairman
Department of Aeronautics and Astronautics

iii

## ABSTRACT

An experimental investigation of the separating boundary layer of a wing subjected to periodic turbulent disturbances was conducted.

Turbulence pulses were generated by a non-thrusting spinning rod placed upstream of the test airfoil at the reduced frequencies of .09 and .47.

Time-varying velocity measurements were made at various heights above the 70% chord location at 12 degrees angle of attack (nearly separated flow) and 22 degrees angle of attack (fully separated flow). Split-film anemometry was used to determine flow speed and direction. The flow responses were compared to the quasi-steady state of undisturbed separated flow.

Variation of reduced frequency had a dramatic influence on the effects which the periodic disturbance had on the flow response. At a reduced frequency of .47 the periodic disturbance had no noticeable influence. Imposition of periodic disturbance of the same reduced frequency on attached flow near separation (12 degrees angle of attack) once again caused no apparent destabilizing effects. The lack of sensitivity of the separated boundary layer to the pulses generated at the higher reduced frequency of .47 apparently resulted from its inability to resolve turbulent pulses from one

another. Imposition at 22 degrees angle of attack of a pulse
at the reduced frequency of .09, however, first stabilized the
flow, then greatly intensified the original separation before
allow-ing the flow to return to its undisturbed separated
state.

# TABLE OF CONTENTS

# LIST OF FIGURES

## ACKNOWLEDGMENTS

I wish to thank my thesis advisor Dr. Rick Howard for his expert guidance throughout this entire project. His continued patience was an integral factor in its completion.

I also wish to thank the following members of the NPS Aeronautical Engineering Department whose technical assistance contributed to the completion of this thesis: Pat Hickey--Laboratory Supervisor; John Moulton--Metal Model Shop Technician; and Tony Cricelli--Computer Engineer.

I most of all wish to thank my wonderful wife Tricia who not only provided constant support during this work but also spent countless hours helping with data collection and typing.

# I.  INTRODUCTION

## A.  BACKGROUND

At extremely high Reynolds numbers, the transition from laminar to turbulent flow over an airfoil surface is fairly predictable.  Below Reynolds numbers of 500,000, however, the nature of the boundary layer becomes difficult to predict. The flow may separate near the leading edge, transition as a separated shear layer, and reattach as a turbulent boundary layer, forming the well-known laminar separation bubble.  At low Reynolds numbers the transition region may be a significant fraction of the chordlength, and transition and separation may become very sensitive to freestream disturbances, such as turbulence or the presence of contaminants.

Low Reynolds number boundary layer phenomena under steady state conditions have been thoroughly studied over many years. Recent investigations made by Meir and Kreplin [Ref. 1], Potter [Ref. 2], and Kindelspire [Ref. 3] have well documented the effects of freestream turbulence on airfoil performance.

The analysis performed by Meir and Kreplin indicated a strong correlation between airfoil performance and the intensity of induced turbulence.  The dependence was most pronounced when the length scales were similar to the boundary layer thickness.  Potter found that freestream turbulence

1

intensity spread into the entire boundary layer. Later, Kindelspire verified that increased levels of freestream turbulence caused an early transition to a turbulent boundary layer.

The effects of an unsteady flowfield have been studied to a much lesser degree than the effects of steady flow. Most studies on an unsteady flowfield involve a pitching airfoil, associated with the dynamic stall phenomenon, or a streamwise sinusoidal velocity variation over a stationary airfoil. A review of the former is given by Carr [Ref. 4], a a recent study of the latter is described by Brendel [Ref. 5]. In both of these cases, it is a variation of the mean flowfield that characterizes the flow condition. Brendel discovered that the mean boundary layer thickness was not altered by a sinusoidal modulation of the freestream. Carr documented the effects of dynamic stall associated with those airfoils which experience unsteady motion. Dynamic stall begins when a pitching airfoil passes the static-stall angle without any noticeable change in the flow. Further increases in the angle of attack cause the surface flow on the aft portion of the airfoil to reverse. As the pitch angle of the airfoil continues to increase, the reversal of flow progresses up the airfoil surface. At a certain angle, depending on many factors, the viscous flow no longer remains attached and a strong vortical flow develops. Then, as the angle of attack decreases, fully separated flow develops. Of all the effects

produced by this phenomenon the most important one documented by Carr was that of an increase in maximum lift coefficient. Carr states that an airfoil's lift coefficient is increased by pitching it rapidly in a freestream and that this is due to the vortex formed during unsteady motion.

This thesis deals with the response of a separating boundary layer of a wing to periodically-varying turbulent disturbances in the mean flow. The study is similar to Carr's analysis in that it involves an oscillating disturbance which impinges the airfoil's surface. Unsteady turbulent flowfields may in practice be periodic, as in the case of a propeller slipstream over an aircraft wing, or they may be single-event occurrences, such as wind gusts or control surface disturbances. In either case, the effects of such flowfields can be studied by characterizing the boundary layer response through high speed data acquisition and ensemble-averaging of periodic data. Previous work in this area by Miley, Howard, and Holmes [Ref. 6], and by Howard and Miley [Ref. 7] was concerned with the propeller slipstream flowfield over a laminar wing boundary layer. In these studies thrusting and freewheeling propellers induced the disturbances. A more generic source of periodic turbulence with a greater application toward single event disturbances was sought. Such disturbances are of concern when dealing with the wing disturbance from canard control surfaces or maneuvering

3

aircraft, whose lifting surfaces may penetrate another aircraft's wake.

The result of such disturbances may be particularly important for an aircraft operating near stall or in the post-stall flight regime during aggressive maneuvering, since a change in wing boundary layer behavior may affect the ability of the flow to remain attached during the maneuver and a loss of lift over one of the surfaces could adversely affect aircraft control. The use of large-deflection control surfaces at low speeds and dynamic stall for augmented lift, and the possible operation at post-stall flight angles of attack, make enhanced configurational aerodynamics a consideration in the design of advanced fighter aircraft. Unfortunately, the effect of single-event freestream disturbances at supermaneuvering conditions is largely unknown.

In 1987 Howard [Ref. 8] placed a rotating propeller upstream of an airfoil in order to study the effects of a periodic turbulent disturbance on an attached boundary layer. As expected, passage of the propeller wake (a transient free-stream disturbance) over the wing caused the boundary layer flow to vary from laminar to turbulent. Within this transition, however, he discovered a distinct relaminarization process indicated by decreased turbulence and an increased surface velocity just after the turbulent pulse passed. He also discovered that the average drag coefficient was actually

lower than what it would have been in undisturbed laminar flow! Somehow the turbulent pulse caused part of the cycle to become more stable than undisturbed freestream flow. The reduction in drag, increase in stability, and the presence of a relaminarization effect were all unexpected responses to such a transient disturbance as a propeller pulse in the slipstream.

Renoud [Ref. 9] further investigated the mechanics behind Howard's discoveries utilizing a wing boundary layer subjected to nonthrusting turbulent pulses. By measuring the velocity profiles, turbulence intensities, velocity spectra, and total spectral power at three representative chord locations (laminar, transitional/turbulent, fully turbulent) he found the boundary layer to exhibit a cyclic transitional response. The response began as undisturbed flow, changed to turbulent during the passage of the pulse itself, then returned to undisturbed flow. Intuitively, a recovery to laminar flow was expected over the forward wing section; but the recovery mechanism brought a relaminarization also to the aft section. The aft region actually showed less turbulence during the recovery phase of the cycle than it did under steady freestream conditions. In addition to lower turbulence levels this recovery was characterized by reduced boundary layer thickness, confirming the stabilizing effects discovered by Howard. Renoud hypothesized that this laminarization resulted from "rapid acceleration of the near surface flow within the

boundary layer due to turbulence induced momentum transfer down through the boundary layer and local flow acceleration following the velocity deficit of the turbulence pulse." By using a nonthrusting cylindrical rod to generate the disturbance he also proved that the unusual recovery discovered by Howard's propeller work was not a function of thrust mechanisms.

B.  THESIS OBJECTIVES

The research described in the previous section dealt with the effect of time-dependent turbulent disturbances on attached wing boundary layers.  The goal of this thesis was to further study the stabilizing effect of periodic turbulence on flow near separation.  Renoud's work was to be continued by investigating the response to periodic freestream disturbances at high angles of attack.

This investigation was to be performed with the same apparatus used by Renoud.  An airfoil operating in a free-stream at a Reynolds number of 500,000 was to be subjected to periodic disturbances generated by a spinning cylindrical rod. Prior to data collection, flow visualization techniques were to be utilized to determine the angle of attack at which separation/stall first occurs.  These observations would dictate the angle of attack to be used for the investigation. In addition, flow visualization would yield the chord location at which separation begins.  All data were to be collected in

the separated region in the form of velocity measurements using thermal anemometry and high-speed data acquisition.

Turbulent pulses were to be generated at a lower rate for one set of runs to investigate the response of the airfoil to changes in reduced frequency. The purpose of this was to document the ability of a separating boundary layer to respond to various disturbance frequencies. In order to sense the expected flow reversal (a phenomenon not encountered in Renoud's low angle of attack work), this study would utilize a split-film probe instead of a conventional single sensor hotwire.

After ensemble averaging, non-stationary mean velocity profiles and time histories at various heights above the surface will be presented. The analysis will attempt to determine whether a stabilizing effect for flows near separation exists similar to the one found to be associated with attached boundary layers.

Future work in this subject area will be concerned with the actual control of unsteady separated flow. Research in unsteady aerodynamics will expand the boundaries which currently limit fighter aircraft maneuverability. The consistent control of unsteady, separated flow will be required if fighter pilots are to utilize these expanded flight envelopes.

## II.  EXPERIMENTAL EQUIPMENT

### A.  APPARATUS

The major pieces of equipment used for this experiment are:

1. low speed wind tunnel

2. wing section and its supports

3. periodic turbulence generator

4. split-film probe

5. IFA 100 anemometer system

6. split-film calibration equipment

7. traversing mechanism

8. IBM personal computer.

The operation of this equipment is described in this chapter.

#### 1.  Wind Tunnel

The Naval Postgraduate School wind tunnel located in the northwest corner of the Halligan Hall basement was used for the entire investigation.  Built by the Aerolab Development Company in the 1950's, this wooden tunnel is of the closed circuit variety, with 64 feet of length and a width varying between 21.5 and 25.5 feet.  Capable of generating wind speeds of up to 200 mph, the tunnel has a 100-hp electric motor coupled to a three-bladed variable fan via a four speed truck transmission.  For this investigation the transmission

8

was left in third gear for all data runs, yielding a fan shaft speed of 750 RPM.  The fan is operated in a duct of roughly constant cross sectional area so that the air pressure is increased rather than the velocity (the velocity is later increased by constriction).  Downstream of the blades is a set of eight flow straighteners whose function is to remove fan swirl in order to reduce turbulence and pressure losses. Turning vanes are placed at the tunnel corners to reduce the loss of kinetic energy associated with duct flow around a bend.

After passing through three sets of turning vanes the flow travels into a settling chamber.  This section has the largest cross sectional area of the tunnel and therefore the lowest velocity.  The following acceleration of the flow into the test section decreases turbulence.  There are also two fine wire screens mounted in the settling chamber which help break up turbulent fluctuations.

The next section is a 10:1 area ratio contraction cone, which accelerates the flow to the required velocity and helps produce a uniform distribution within the test section. The test section itself has a cross sectional area of 8.75 square feet, a rectangular design, and frosted-light glass corner fillets which provide illumination of the wing.  The walls of the test section are slightly divergent to counter the effective contraction due to boundary layer growth.  This section also is equipped with a full size reflection plane

mounted four inches above the floor. Hinged windows on each side permit viewing and easy access while plywood-supported Plexiglas covers the top of the test section. The Plexiglas, which allows viewing and photography from above, has a narrow ten inch slit to permit passage of the split-film probe via a traversing mechanism.

The diffuser of the tunnel is a gradually widening duct downstream of the test section which converts the kinetic energy of the air into pressure energy. This section also houses a foreign object damage screen to protect the fan. The tunnel-operating instructions used for this investigation are contained in Ref. 10. The velocity is controlled by electrically setting the blade pitch angle at the controls adjacent to the test section. To measure tunnel speed two sets of static pressure port rings are installed. One set is placed just upstream of the contraction cone while the other is located at the entrance of the test section. A pressure differential is indicated on an installed manometer located near the controls. A calibration can be performed to obtain the test section dynamic pressure based upon the pressure differential. A wind tunnel velocity calibration was conducted by Renoud and is discussed in Chapter III.

2. <u>Wing Section and Wing Mount Assembly</u>

The airfoil, a section of a Bell helicopter tail rotor, has a ten inch chord and a 24 inch span. A photograph of the wing and its assembly is included in Figure 1 while the

Figure 1.  Wing and Mount Assembly

section coordinates are listed in Appendix A.  The airfoil was

stripped to bare metal, filled, and sanded prior to use.  For

flow visualization the surface was finished in a high gloss

white to ensure high contrast between it and the black

pigmentation of the flow visualization medium.  For all other

work the section was finished with high gloss black lacquer

and buffed with silver polish in order to maximize the

reflectivity of its surface.  A reflective surface was

required to ensure accurate sensor positioning.  By

simultaneously viewing the probe and its reflection through a

sighting level telescope and comparing the two positions, the probe's distance above the wing surface was determined within 0.0032 inches. This probe positioning procedure developed by Renoud is described in further detail in Ref. 10.

The wing mount assembly, which secures the wing section within the wind tunnel, consists of two vertical aluminum supports which hold opposite sides of the wing. Each support has horizontal plates above and below which are secured by bolts to the test section's floor and ceiling. Circular inserts within the supports allow for 45° rotation of angle of attack. Rough angle of attack settings were made by matching the degree etchings of the moveable inserts with a horizontal marker on the vertical support. After setting a rough angle of attack, the heights of the leading and trailing edges of the wing above the reflection plane were measured. In this way the angle of attack could be solved for analytically. No corrections were made for tunnel upflow.

All data collected during this investigation were taken 1.0 inch left of mid span due to damage on the wing surface at the mid span line. This offset was far enough from any disturbances generated by surface imperfections but not far enough to detect any support effects.

3. Split-Film Probe

Due to the reversal associated with separation, measurement of the flow direction in this study was just as important as the measurement of flow speed. Since hotwires

12

lack directional sensitivity, the split-film probe shown in Figure 2 was used instead. The split-film also offered the following advantages in addition to directional sensitivity:

1. less prone to damage than hotwires

2. much less sensitive to contamination effects

3. good frequency response

4. ability to measure turbulence when the intensity would be too high for other probes to do so

5. better spatial resolution than hotwires.

The split-film probe consists of two electrically independent films placed on a common quartz fiber. Each film and its associated anemometry circuit behaves essentially in the same manner as a single hotwire circuit. The presence of two separate sensors located on the same fiber, however, yields flow direction as well as speed. Such a capability was deemed crucial for this investigation due to the reversal associated with separated flow.

Each film of the probe is maintained at a constant temperature by a feedback circuit discussed in Section 5. If the films are subject to the flow of a lower temperature fluid, heat is removed. The amount of current required to maintain a constant temperature within either of the films is proportional to the velocity of flow across the probe. For an ideal sensor the amount of heat dissipated to the environment by each film is the same if the flow is directed at the split. If the flow is not directed at the split,

13
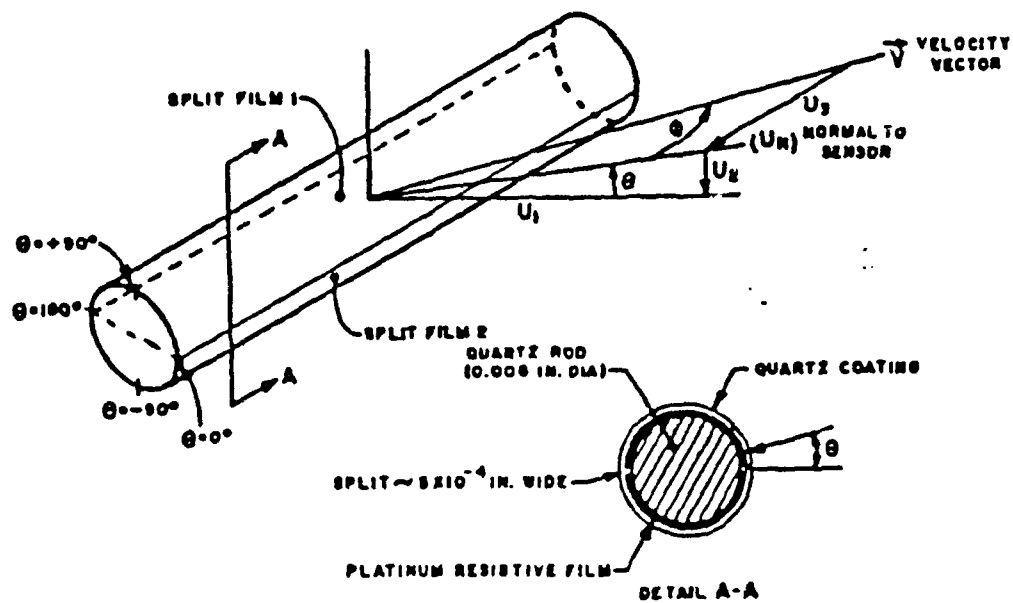
a.   Enlarged View of Probe Fiber
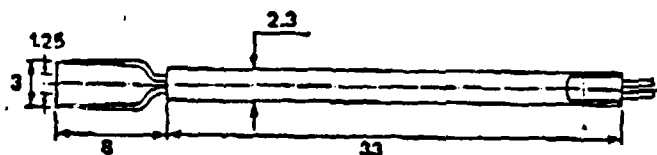


b.   Longitudinal View of Probe (units in mm)

Figure 2.   Split-Film Probe [Ref. 11]

14

a greater amount of heat will be dissipated by the upstream facing film.

For a given wind speed, the heat transfer from the upstream film to the flow will reach a maximum when the flow impinges on its center. Therefore the difference in heat transfer rates between the two films and their surroundings is related to the velocity component perpendicular to the plane of the split.

The total heat transfer from the two films yields the magnitude of the flow velocity. Since the heat transfer Q is proportional to the square of the flow velocity, King's law is written:

$$\frac{E_4^2 + E_3^2}{\Delta T} = A + B \, \overline{V}^{1/2} \tag{1}$$

With A, B, and $\Delta T$ constant, the voltages, which can be read from an LED, depend only on the velocity magnitude.

As just discussed, the direction of the flow velocity is related not to the sum but to the difference of heat transfer rates:

$$\frac{E_4^2 - E_3^2}{\Delta T} = C\theta \tag{2}$$

where $E^2$ is related to the heat transfer rate Q, $\theta$ is the flow angle, and C is a nonlinear function of flow speed.

15

## 4. Probe Calibration Support Apparatus

In order to rotate the split-film probe around its fiber axis (a procedure required for sensor calibration, discussed in Chapter III), a new support apparatus was needed. The axis of the split-film fiber (shown previously in Figure 2) had to be rotated in such a way as to form incremental angles with respect to the freestream from positive to negative 90 degrees. The vertical sections used to support the wing (previously discussed) provided an excellent foundation for such an apparatus. These supports were modified to hold a horizontal aluminum cylindrical rod (in much the same manner as they had supported the wing during Renoud's work). Unfortunately, the circular inserts within the supports allowed only 45 degrees of rotation. By removing the two holding bolts from each circular insert, full rotation was now possible. A clamp was installed to secure the inserts and the rod at the desired angle of attack.

One end of the rod was machined to form a key fit with its respective rotational insert in order to prevent rotation during operation. A 360-degree protractor was installed on one of the inserts to indicate the angle of the split film probe axis with respect to freestream flow. A depression was machined in the center of the rod which acted as a cradle for the probe holder. A cover and two small set screws secured the probe holder in place. When installed, the cover fit the contour of the rod so as to minimize external flow

disturbances. The split-film sensor could be inserted and removed from the front of the probe holder at will between calibration runs. The two wires of the probe holder were run along the rod, downstream of the supports, and out the bottom of the wind tunnel to form an electrical connection with the anemometer circuit. Figure 3 shows the probe calibration support apparatus and the split-film probe.
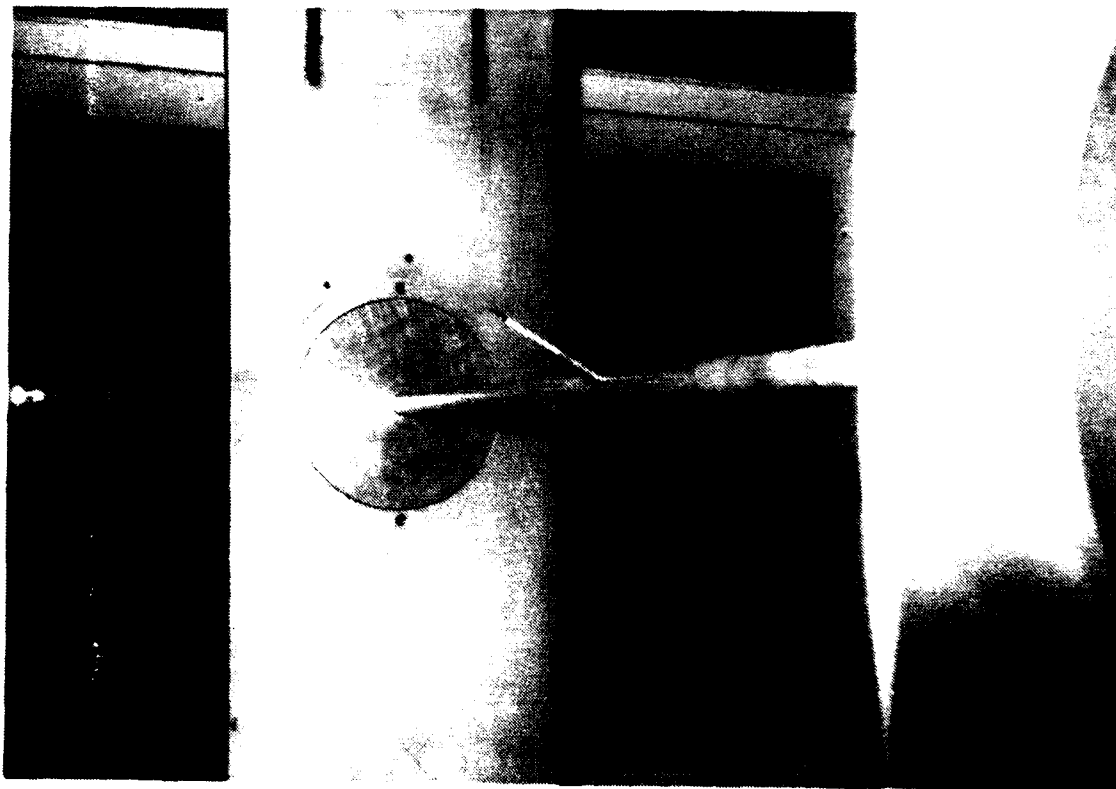


Figure 3. Probe Calibration Support Apparatus and Split-Film Probe

## 5. Anemometer Cir... ry

Velocity was measured by a TSI IFA 100 System Model 150 Constant Temperature Anemometer and Model 157 Signal Conditioner. This equipment is shown in Figure 4. The Model 150 is a high performance, low noise, constant temperature anemometer. Two of the anemometer's transducers (or channels) were connected to the hotfilm, a Dantec 55 R 55 Split Film Probe. The probe actually consists of two separate sensors: thin nickel films deposited on a single 200 mm quartz fiber. The fiber is soldered to four tapered gold plated stainless steel prongs which are embedded in a ceramic probe body. These prongs pass through the ceramic body and connect with similar prongs within the probe holder, allowing electrical current to flow from the films to attached wires and finally through 15-foot coaxial cables to the anemometer.

As air flows past the probe the films are cooled and heat is removed. The anemometer compensates this heat loss by increasing the flow of current to the films, thus maintaining a constant temperature. Each feedback circuit consists of a voltage bridge and an amplifier. The amplifier controls the current through the probe by means of the voltage on top of the bridge. Since the current required to maintain the sensor at constant temperature is related directly to this bridge voltage, the voltage itself is a function of flow velocity across the sensor. Because the probe used in this investigation was of the split-film variety, each of the two
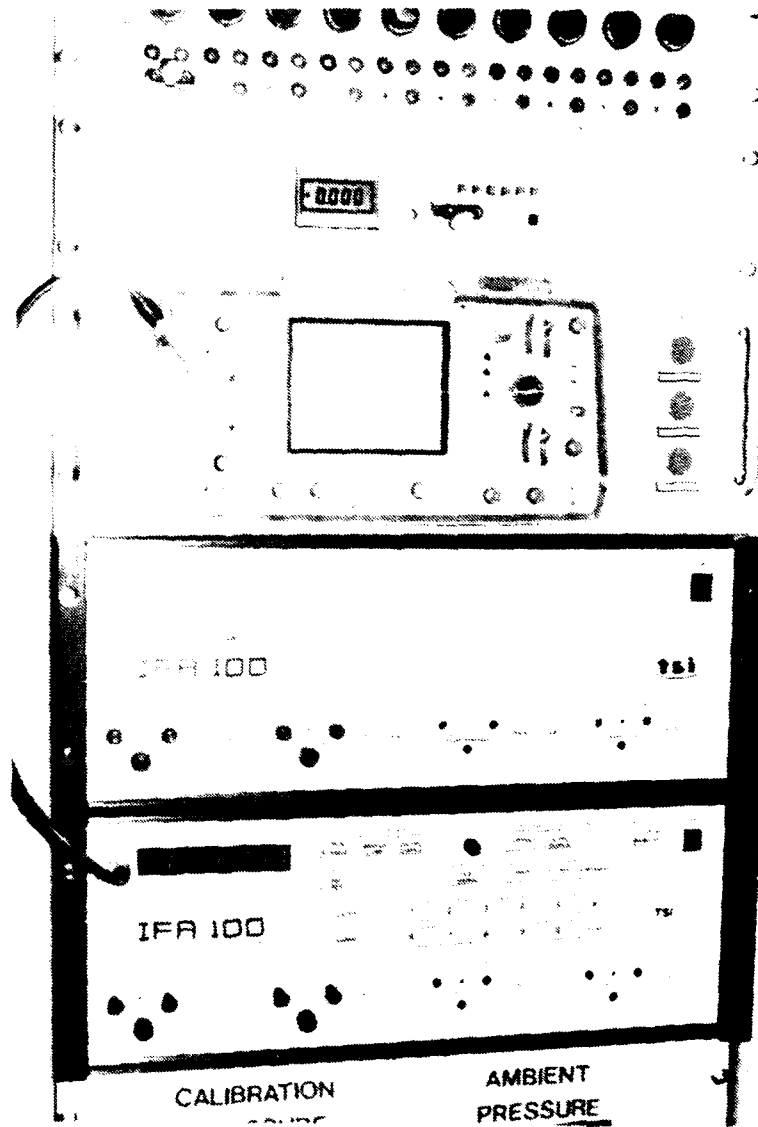
Figure 4.   IFA-100 Anemometer System

films required a separate anemometry circuit. The presence of these two films, each cooling at rates which are dependent on flow angle, enables the formulation of an expression for flow velocity direction as well as magnitude.

The anemometer module was operated in the standard one bridge configuration. Its output (bridge voltage) was fed into the Model 157 signal conditioner in order to provide low pass filtering.

The low pass filter was set at the Nyquist cut off frequency of 10 KHz as calculated by the following equation:

$$f_n = f_s/2 = 20,000/2 = 10,000 \text{ Hz}$$

where $f_s$ is the frequency at which the digital computer samples the output of the signal conditioner. A sampling rate of 50,000 Hz had been used by Renoud, who subsequently found that little useful spectral information was contained at those frequencies above 19 KHz. Based on this finding and in order to reduce data processing time, the rate for this investigation was reduced to 20 KHz.

In addition to providing low pass filtering, the signal conditioner was capable of applying an offset and gain to the bridge voltage. This capability was desirable for the investigation since it would improve velocity resolution by increasing the range of voltages used in the associated mathematical relations. However, calibration data showed that

20

the unconditioned range of one film's bridge voltage varied from 2.67 to 3.87 volts while the other film varied from 1.93 to 2.56 volts. The analog to digital (A to D) conversion band meanwhile had a range set at zero to five volts. Unfortunately, there are no combinations of gain and offset which could be applied simultaneously to both bridge voltages without causing one or the other to fall outside the A to D range of zero to five volts (only negative integral offsets and positive integral gains are allowed in the signal conditioner). With no gain or offset and an A to D voltage resolution of 2.44 volts, a velocity magnitude resolution of 0.03 ft/sec was obtained.

A problem associated with the IFA 100 system was encountered during the first test of automated data collection. Although the system theoretically was capable (under the configuration used by the author) of transmitting four active data channels simultaneously to the data acquisition system, in practical use with a split-film probe only one active channel could be transmitted at a given time. According to an applications engineer for TSI Incorporated, use of the system with split-film sensors is limited. Channels within the IFA 100 system are placed by the operator in one of two modes: run or standby. According to the engineer, heat conducted from one nickel film to the other across the quartz fiber of the probe fools the IFA system into thinking that both channels are in run. This effectively

21

locks one channel into the standby mode making it impossible to read both parts of a split-film probe simultaneously. The problem was circumvented by data analysis software discussed later. The voltage to velocity conversion procedure will be covered in Chapter III.

The unconditioned output of one of the two anemometer channels was connected to an oscilloscope at all times during data collection. This oscilloscope was mounted on the IFA 100 equipment rack in order to monitor the instantaneous signal.

### 6. Turbulent Pulse Generator

Periodic turbulence pulses were generated by spinning a cylindrical metal rod in the freestream just forward of the wing section. The apparatus is fully described in Ref. 10. The rod, which resembles a non-thrusting propeller and is shown in Figure 5, is supported by a hub and vertical strut. The cylindrical rod is 18 inches long and has a .375 inch diameter. The hub and strut were connected to a motor by a flexible drive shaft. Although the spinning rod was mounted slightly upstream of the wing section, its driving motor was mounted well downstream of the wing. The motor, which is shown in Figure 6, was run at two different speeds in order to study the response of the airfoil to changes in reduced frequency.

A proximity transducer was installed adjacent to a ferrous pickup wheel located on the motor shaft. This transducer senses any discontinuities, such as gear teeth or

22
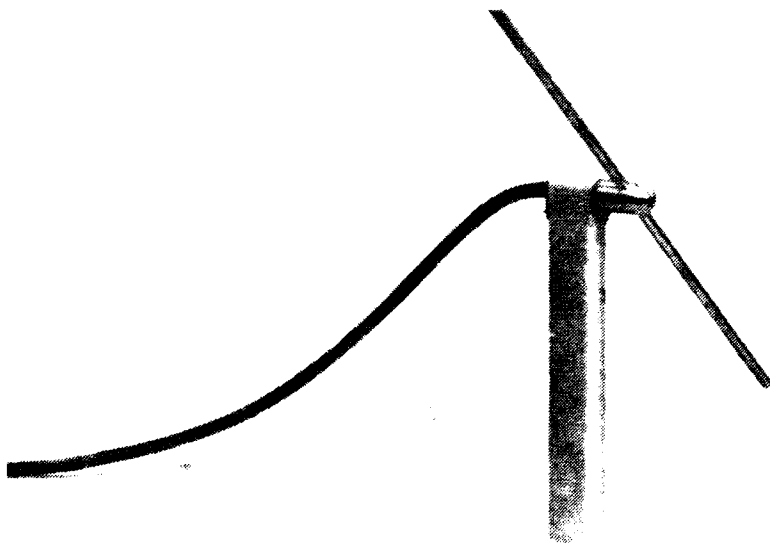
Figure 5. Turbulent Pulse Generator
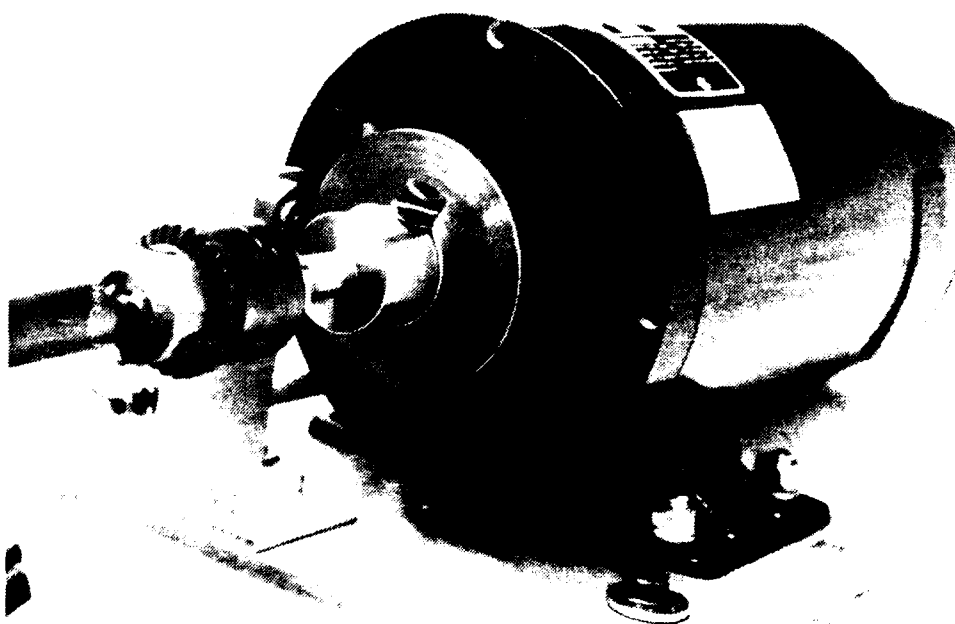


Figure 6. Electric Motor

23

slots. The pickup wheel has two teeth on its circumference which correspond to the position of each end of the spinning rod. An electrical pulse was generated twice each revolution as the rod passed in front of the wing section, providing a signal used to set the pulse generation frequency and to synchronize the data acquisition process.

7. **Three Dimensional Traverser**

The Velmex 8300 Control/Driver 3D traverser system used to position the split-film probe at various heights above the wing surface is shown in Figure 7. The traverser configuration used was the same as that incorporated and described by Kindlespire [Ref. 3].

The traverser was mounted on top of the test section allowing the split-film probe to be moved chordwise, spanwise, or vertically. All measurements were taken at the same span and chord locations. The traversing mechanism was capable of discerning incremental movements of 0.000125 inches. An IBM PC/AT (separate from the one used for data acquisition) was used to control the traverser. The incorporated program is described later in Chapter II.

8. **Data Acquisition System**

Conditioned signals from the IFA 100 System were collected by an IBM PC/AT via a Metrabyte DAS16F A to D converter card.

The personal computer had a 40 megabyte hard disk, high and low density disk drives, and 1.4 megabytes of RAM.

24
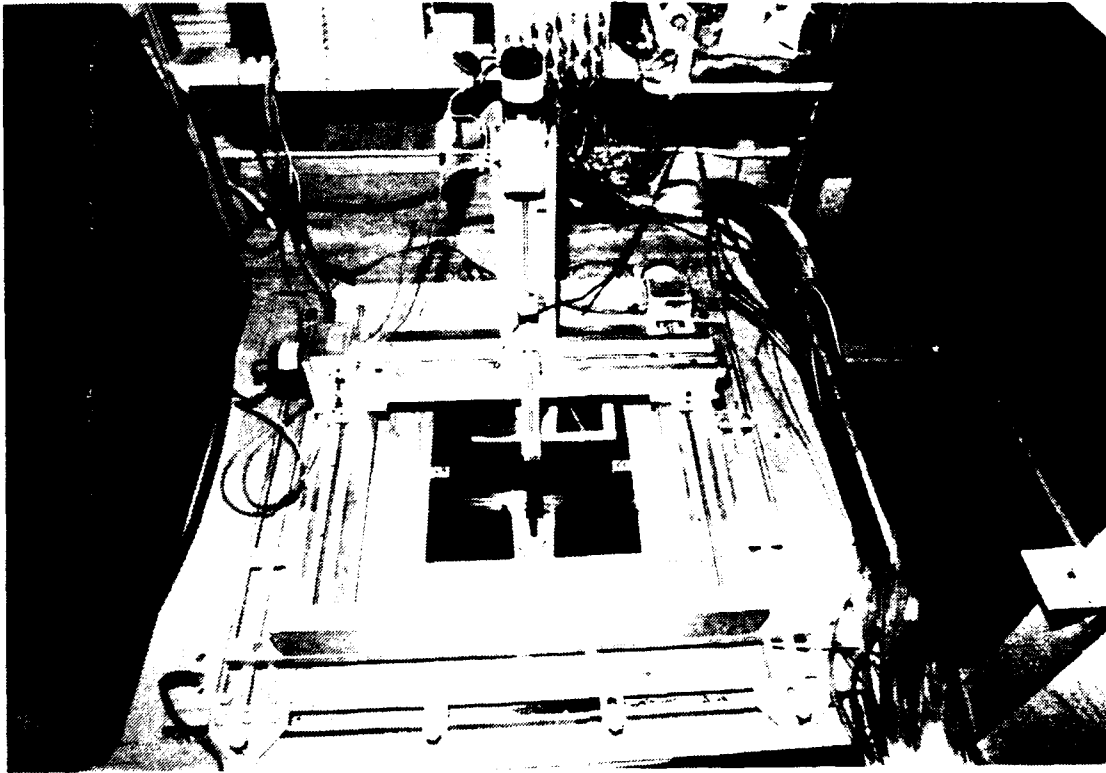
Figure 7. Traverser

A large temporary storage capacity was desired to process the large volume of data collected during each run of the investigation. At a sampling rate of 20,000 Hz over a period of one second, 20,000 data points would be collected on each of three channels requiring temporary storage for 60,000 data points. During data acquisition testing several weeks prior to actual data collection, over 80,000 points were successfully collected, temporarily stored within random access memory, and downloaded to either floppy or hard disk. Unfortunately, during the first actual use of the system, a

large portion of the RAM capacity suddenly was occupied by an unknown entity. After several unsuccessful attempts to free RAM capacity, the problem was circumvented by making two data runs under identical conditions and then combining the two sets of data into one file. This method, while time consuming, did allow for the collection of the 60,000 samples per data run.

The DAS16F, a very high speed A to D interface board, was installed directly into one of the expansion slots of the computer. Output from the IFA-100 Signal Conditioner was fed via cable to a Metrabyte STA-16 terminal accessory board. The STA-16 then relayed the unmodified analog signal to the DAS16F via ribbon cable. The DAS16F A to D conversion was triggered by keyboard command using the compatible LABTECH NOTEBOOK software. The card was used in the unipolar mode with its clock set at ten MHz and an input range of zero to five volts.

The DAS16F was configured to read three different channels (the two anemometer channels corresponding to each half of the split-film and a timing pulse) over the input range of zero to five volts.

B. SOFTWARE

The IBM PC/AT was used for all phases of data collection and analysis. One PC was dedicated solely to operating the traverser mechanism while the other processed and analyzed data. All programs used for this investigation are described

in this section. Those programs which were written or modified by the author are listed in Appendices B through D.

1. Data Collection Software

The following programs were used in the data collection process.

| NAME | FUNCTION |
|------|----------|
| TRAVERSE.BAS | 3 Dimensional Traverser Control |
| LABTECH NOTEBOOK | A to D Board Control |

a. Program TRAVERSE.BAS

This program provides automated or discrete control of the traverser via IBM PC/AT keyboard commands. It was written by Kindelspire [Ref. 3:pp. 27-30] and modified by Renoud to remove manual data entry requirements and to improve the accuracy of the motor stepping routines. The program allows the user to input discrete movement commands (manual control) or to choose automated movement sequences (computer control). Prior to each data run discrete movements were used to position the probe at the 70% chord location, 1.0 inches left of mid span, at a height above the surface which depended on the conditions of that particular run. Upward vertical movement for subsequent runs at greater heights was also made by manual traverser control. This system provided great position accuracy once the probe's initial location was sighted optically. The automated boundary layer sequencing capability of this program was not used since the investigation dealt with unattached flow.

b. LABTECH NOTEBOOK

A commercial software package developed by Laboratory Technologies Corporation called LABTECH NOTEBOOK was used for control of the DAS16F A to D board. This package allows the user to select the manner of data collection and storage during a given run. The sampling rate, run duration, number of channels, mode of storage, triggering mechanism, output file format and various display parameters are rapidly selected and modified using a menu-driven interactive format. For this investigation the high speed sampling mode was selected. While this selection limited the program's display capabilities, it allowed an increase of the sampling rate to the desired value of 20,000 Hz.

Prior to each data run the appropriate parameters were chosen from the menus and an appropriate name was given to the output file. Although the runs all lasted less than a few seconds in duration, it took several minutes for data transfer from RAM to the respective floppy disk, due to the high volume of data collected. While waiting for this transfer, the next data run parameters were chosen. Each floppy, which contained data from one or two runs, depending on the number of data points involved, was labeled and stored following data transfer. Instructions for the use of LABTECH NOTEBOOK are contained in Ref. 13.

## 2. Data Analysis Software

Data analysis was performed with software written by Johnson [Ref. 14], Renoud [Ref. 10], and the author. A description of these programs is provided below.

### a. Program CONVERTS.FOR

This FORTRAN program was written by the author to convert the bridge voltages of the anemometer circuitry into flow speed and direction. It applies only to the data runs in which the turbulence generator was not used. The program reads data from two input files, each of which contains voltage values on an active channel and on an inactive channel. One file contains active data in its first column (channel 3) while the other file contains active data in its second column (channel 4). The program combines the active channels of the two files into a third file and disregards the two inactive channels (columns). For every sampling point it then converts the split-film bridge voltages into flow speeds based on King's Law. After calculating the flow speed the subroutine INTERP is called to determine flow direction. With entering arguments of velocity magnitude and $(E_4^2 - E_3^2)$, INTERP scans a calibration table (previously loaded into the program) and determines a value for $\theta$ (see Figure 2). This value, which represents the direction of flow (from -90 to 90 degrees) with respect to the plane of the split, is returned to the main program. An interpolation method was required due

to the following relation between flow speed, flow direction, and bridge voltages:

$$\frac{E_4^2 - E_3^2}{\Delta T} = C\theta \qquad (3)$$

Because C represents not a variable but a nonlinear function of velocity magnitude, calculation of direction could not be performed by a single algorithm. After flow velocity magnitude and direction are found for each pair of voltages, their values are written to an output file of the user's choice.

b. Program PROPCONV.FOR

This program, written in FORTRAN by the author, is a modification of the previously discussed program CONVERTS.FOR. In addition to performing all the functions contained within that program, PROPCONV.FOR synchronizes data taken from two different channels at different times and provides ensemble averaging. As mentioned during the discussion of the IFA 100 system, only one channel could be read from the anemometer at a time. PROPCONV.FOR matches data from different bridge voltage channels by using the synchronization pulse of a third magnetic transducer channel. An algorithm in PROPCONV.FOR changes the sensor voltage of this third channel into a single synchronization pulse. The program then arranges data from both channels to match this pulse. As in the program CONVERTS.FOR, the subroutine INTERP

30

calculates flow direction based on calibration data within the file CAL.DAT. As the flow speeds and directions are calculated, their values are added to the holding bin (whose length equals that of the shortest pulse) for ensemble averaging. By dividing the velocity sums within the bin by the number of pulses, an ensemble averaged single pulse is determined. The flow direction and velocity magnitudes of this pulse are written to an output file of the user's choice.

c.   Program READIN.FOR

This program, written in FORTRAN by the author, creates the calibration data file used by the programs CONVERTS.FOR and PROPCONV.FOR. It instructs the user to input velocities, probe angle, and the manually read bridge voltage calibration data from both channels. This information is written to a file for later use by the voltage/velocity conversion programs.

d.   Program SMOOTH.FOR

This program, written by Johnson [Ref. 14:pp. 158-166], computes the time varying mean of a non-stationary, periodic time series. The data, which had been ensemble averaged by PROPCONV.FOR, are transformed via a Fast Fourier Transform (FFT) into the frequency domain. By applying a low pass filter the data are then smoothed. The user can specify the degree of smoothing by selecting the smoothing window size (a function of cutoff frequency and sampling frequency). An

inverse FFT transforms the data back into the time domain before they are finally written to an output file.

## III. EXPERIMENTAL PROCEDURE

### A. WIND TUNNEL TEST SECTION CALIBRATION

The first parameter which had to be quantified for this investigation was the airspeed in the wind tunnel test section. Placing a pitot-static tube in the center of the section would disturb the airflow around the wing, while placement of such a device to the side would yield an incorrect velocity due to blockage effects. The best way to determine test section airspeed, therefore, was through an indirect method. A tunnel calibration can be used to correlate contraction cone pressures (easily measured without disturbing the model) to test section airspeeds. By making some simplifying assumptions and utilizing the continuity and the energy equations, Ref. 11 shows that the pressure change across the contraction cone is directly proportional to the measured dynamic pressure in the test section. Expressed symbolically:

$$q = F \Delta p \qquad (4)$$

where F is referred to as a tunnel calibration factor. This principle was used by Renoud to perform a tunnel calibration in 1988. Pressure across the contraction cone ($\Delta p$) was measured using the permanently-installed manometer. The

33

dynamic pressure of the test section, q, was measured by placing a pitot-static tube inside the section and connecting a differential micromanometer across its total and static ports. Values of q were plotted versus p yielding the slope, or tunnel calibration constant F. With the relation q = F$\Delta$p, measurement of $\Delta$p yields a value for q. This dynamic pressure can be related to the velocity of the test section as follows:

$$q = \frac{\rho V^2}{2} \tag{5}$$

where $\rho$ is the density of the air. In this way test section velocity can be specified by setting the proper differential-pressure contraction cone value.

During his calibration, Renoud, using an airspeed range of 40-140 ft/sec, plotted q versus $\Delta$p and found the tunnel calibration constant F to be 1.126 (Figure 8).

B. FLOW VISUALIZATION

In order to study the stabilizing effects of periodic turbulence on flow near separation for a particular airfoil, the following parameters first had to be identified:

1. the angles of attack over which separation/stall developed

2. the location of the separated flow region at these angles of attack.
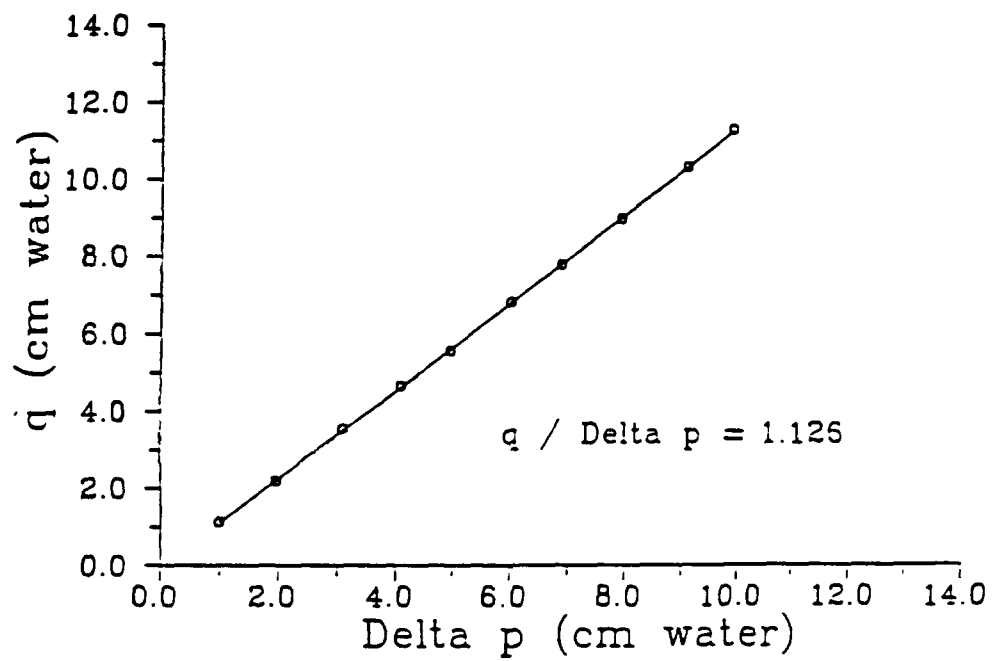
Figure 8. Wind Tunnel Test Section Calibration [Ref. 9]

The best way to identify both of these parameters was through flow visualization. A 12:1 mixture of Mobil 10W-40 motor oil and black tempera pigmentation was applied evenly to the upper surface of the wing section. The wing had been painted white to guarantee a high degree of contrast between the surface and the dark mixture. Runs were made at nine angles of attack ranging from 8 to 24 degrees. Two to three black and white photographs were taken at each angle of attack through the Plexiglas top of the test section. Selected photographs are shown in Figures 9-13. The flow patterns indicated by these photographs were compared with an oil flow visualization photograph of a Clark Y airfoil (roughly geometrically similar to the airfoil under investigation) known to be just beyond stall (Figure 14). Of all the photographs taken, the ones at 22 degrees angle of attack best conformed to the Clark Y fully-stalled pattern. These photographs also showed the 70 percent chord location to be well within the separated flow region at 22 degrees of angle of attack.

Based on these discoveries the investigation would thus involve the imposition of periodic turbulence on a wing section at 22 degrees angle of attack. Measurements would take place at the region where Renoud noticed the most pronounced stabilizing effects of imposed periodic turbulence. An additional run at 12 degrees angle of attack would be
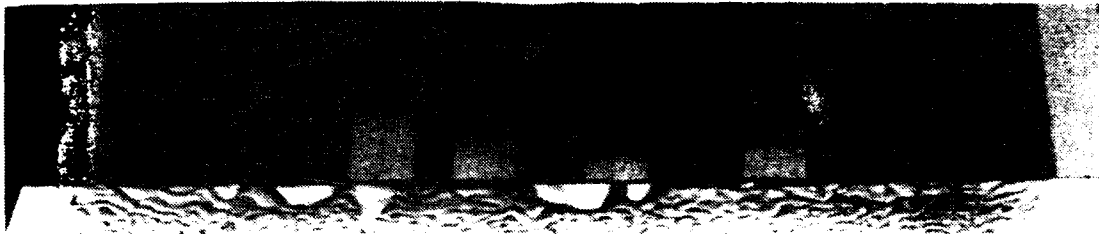
Figure 9.   Flow Visualization Pattern, 12° Angle of Attack



Figure 10.   Flow Visualization Pattern 14° Angle of Attack
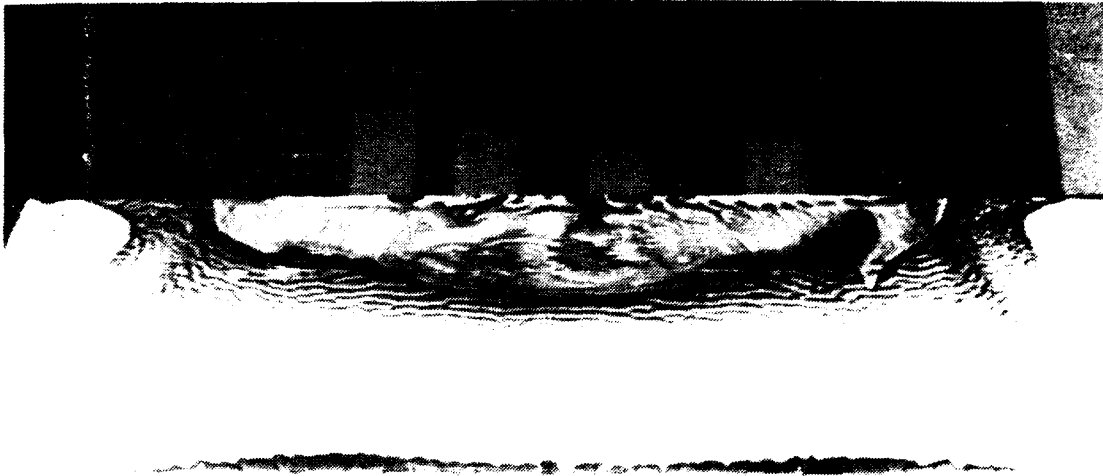
Figure 11.   Flow Visualization Pattern 16° Angle of Attack
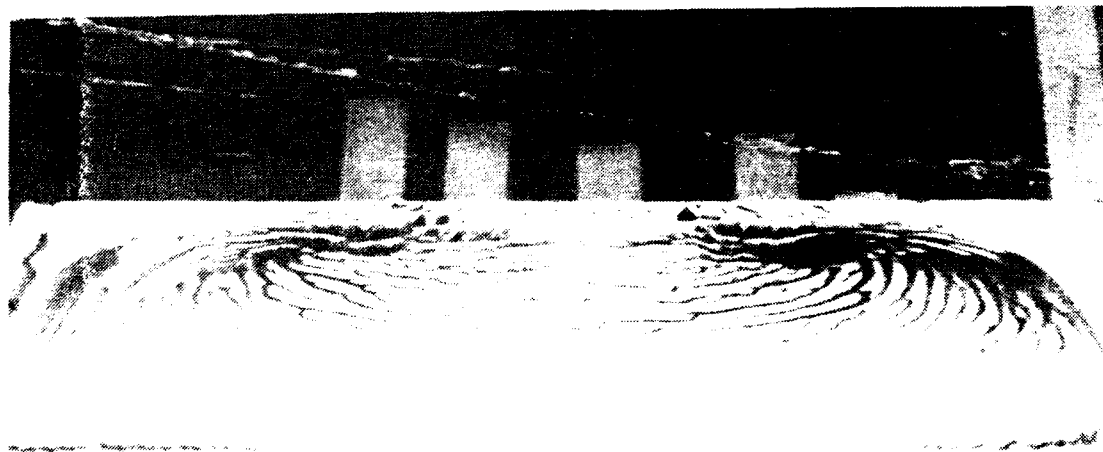


Figure 12.   Flow Visualization Pattern 20° Angle of Attack
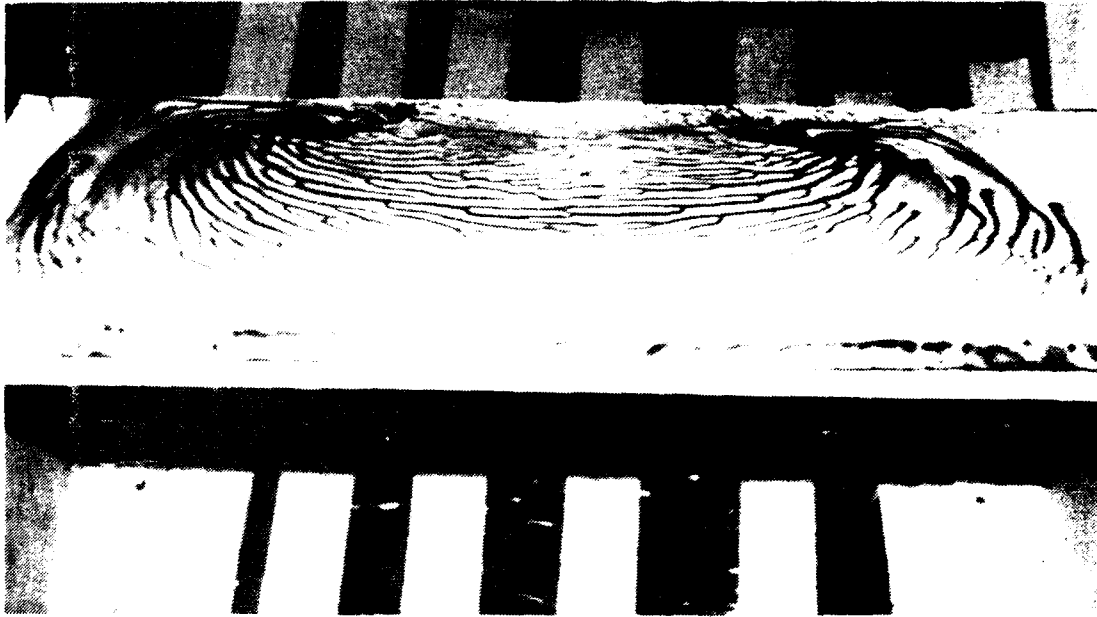
Figure 13.   Flow Visualization Pattern 22° Angle of Attack
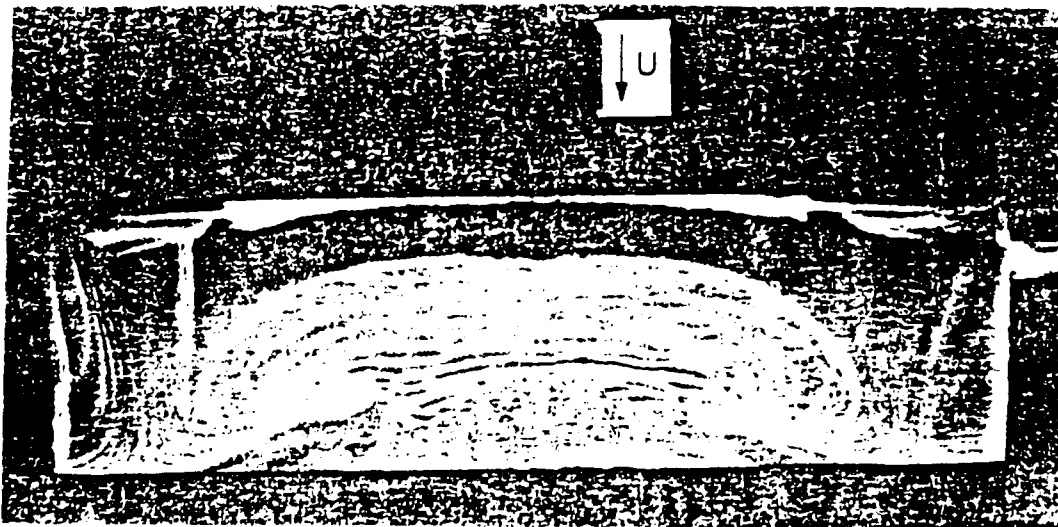


Figure 14.   Clark Y Airfoil Showing Stall Development
             (C = 3.5 inches, Aspect Ratio = 3.5,
             AOA = 22.8°, $Re_c$ = 245,000)

performed to determine if the periodic turbulence might promote separation of an attached flow near separation.

## C.  SPLIT-FILM ANEMOMETER CALIBRATION

Split-film calibration was performed in order to accomplish the following:

1. to determine an equation relating the output bridge voltages to flow speed

2. to develop the calibration curves relating the output bridge voltages and flow speeds to flow direction.

The calibration process consisted of the following steps:

1. IFA 100 System setup and initialization

2. manual calibration data acquisition

3. curve plotting

4. writing of the FORTRAN subroutine INTERP.

Initialization procedures for the IFA-100 system were in accordance with the directions of the instruction manual [Ref. 12].

Channels three and four of the anemometer were used for calibration and data collection.  The following parameters were used during all operations:

| | |
|---|---|
| OVERHEAT RATIO: | 1.5 |
| BRIDGE: | STANDARD CONFIGURATION |
| HIGH PASS FILTER: | NOT USED |
| LOW PASS FILTER: | SET AT ONE HALF THE NYQUIST FREQUENCY |
| VOLTAGE OFFSET: | ZERO |
| VOLTAGE GAIN: | ONE |

40

The next step, in accordance with Ref. 15, was to find a value of E3/E4 which remained essentially constant over the entire velocity range. This was done by changing the velocity from one extreme to the other and readjusting the operating resistance knob of one channel until E3/E4 did not vary. Operating resistances of 8.2 ohms and 11.6 ohms for channels three and four, respectively, accomplished this. These settings also remained constant for all operations.

During the second set of data runs (in which the turbulence generator was first introduced) the hotfilm associated with channel four was damaged. The calibration procedure was therefore repeated for a second split-film. This second set of calibration data applies to all measurements taken in which the turbulence generator was involved. The original calibration curves apply only to the baseline runs in which the turbulence generator was not used.

The split-film was calibrated against the installed manometer which measures the differential pressure across the contraction cone (see tunnel calibration procedure). The probe was supported by the calibration stand discussed in Chapter II.

To determine an equation relating voltage data to flow speed, the probe was maintained at a constant angle while the velocity of the tunnel was allowed to vary incrementally from zero to 148 ft/sec (the expected velocity magnitudes). The sum of the squared bridge voltages were plotted against the

41

tunnel velocity. A linear least-squares fit of these data yielded the calibration constants A and B for use in the conversion programs (see Appendix E).

The angle of the split with respect to freestream flow was then changed from -90 to 90 degrees in ten degree increments. At each angle the velocity was once again varied from zero to 148 ft/sec. A matrix of bridge voltage calibration data was collected manually from the anemometer output. The values, which fluctuated only slightly during calibration, were read with a precision of plus or minus .01 volts. All calibration data are plotted in graphical form in Appendix E.

The final step of calibration involved finding a way to relate bridge voltages and flow speed to flow direction. The FORTRAN subroutine INTERP was written to perform this task and is described in Chapter II.

D. SPLIT-FILM POSITIONING

In order to thoroughly investigate all aspects of flow at the 70 percent chord location it was desired to place the split-film as close to the wing surface as possible. The optical sighting method used by Kindelspire and perfected by Renoud was chosen for this purpose. A detailed explanation of the procedure is contained in Ref. 10.

The high angle of attack used in this investigation caused a large area of probe support tubing to be subjected to turbulent separated flow. This caused the probe to oscillate

quite violently during data collection. A danger of collision between the film and the wing surface therefore existed when the probe was at its closest positions to the wing. To prevent collision, the wind tunnel and turbulence generator were energized before positioning the probe. The probe, now oscillating, was gradually lowered until it appeared through the telescope that it had reached its minimum safe distance from the wing. The tunnel and pulse generator were then de-energized and the initial probe position was measured. The data collection process could then begin.

In spite of the prudence inherent within this procedure, during one of the first data runs the split-film was damaged. Although it was not determined whether there was an actual collision or if damage was caused by oscillation of the film itself, as a precautionary measure during subsequent runs the second probe was not lowered as close to the wing.

E. ACQUISITION OF EXPERIMENTAL DATA

1. Experimental Setup

Four different setups were used to support the goals of this experiment. While many parameters were common to all four setups, there were several which varied from one to another. Table 1 lists those parameters which varied.

## TABLE 1

### SUMMARY OF EXPERIMENTAL PARAMETERS

| Setup Number | Angle of Attack | Duration | $f_s$ | Turbulent Pulse Freq. | Generator Motor Speed | Freestream duration between Pulses |
|---|---|---|---|---|---|---|
| First Row | 22.4° | 0.1 sec | 20 KHz | None | N/A | N/A |
| Second Row | 22.4° | 1.0 sec | 20 KHz | 17 Hz | 510 RPM | 67" |
| Third Row | 22.4° | 5.67 sec | 3.53 KHz | 3 Hz | 180 RPM | 397" |
| Fourth Row | 12° | 1.0 sec | 20 KHz | 17 Hz | 510 RPM | 67" |

All data were collected at a Reynolds number of 500,000. Freestream velocity for a given Reynolds number is given by:

$$V = \frac{Re\ \mu}{\rho c} \tag{6}$$

where:

$\mu$ = viscosity

c = chord length

$\rho$ = density

Re = Reynolds number.

Solving this equation using typical Halligan Hall basement environmental conditions (temperature 60 degrees, pressure 1015 mbar) where Re = 500,000 and c = ten inches yields a test section velocity of 94.75 ft/sec. All data runs were made at this reference freestream velocity. This corresponds to about 4.6 cm of water as measured by the contraction cone manometer (see tunnel calibration procedure).

Parameters and conditions that remained constant throughout the investigation are as follows:

| | |
|---|---|
| Analog Channels Sampled (when pulses were generated) | 3 |
| First Split Film Voltage (Transducer Channel 3) | PC Channel 1 |
| Second Split Film Voltage (Transducer Channel 4) | PC Channel 2 |
| Synchronization Pulse (only used with pulse generation) | PC Channel 3 |
| Number of Pulse Periods Sampled | 17 |
| Chord location | 70 percent |

## 2. Data Acquisition System

Figure 15 is a flow chart which diagrams the transfer of information within the equipment.

Split-
Film
```
┌─────────────┬─────────────┐
│   film      │   film      │
│   #1        │   #2        │
└─────────────┴─────────────┘
```

3D
Traverser

IFA-100
System

```
┌─────────────┬─────────────┐
│ transducer  │ transducer  │
│    #3       │    #4       │
│             │             │
│  signal     │  signal     │
│ condition   │ condition   │
│    #3       │    #4       │
└─────────────┴─────────────┘
```

Velmex
controller

STA-16
Terminal Accuracy
Board

IBM
PC/AT

IBM PC/AT

Operator

RPM
counter

Installed
manometer

Magnetic
transducer

Wind
tunnel
speed
control

Electric
motor

Motor
controller

Wind
tunnel
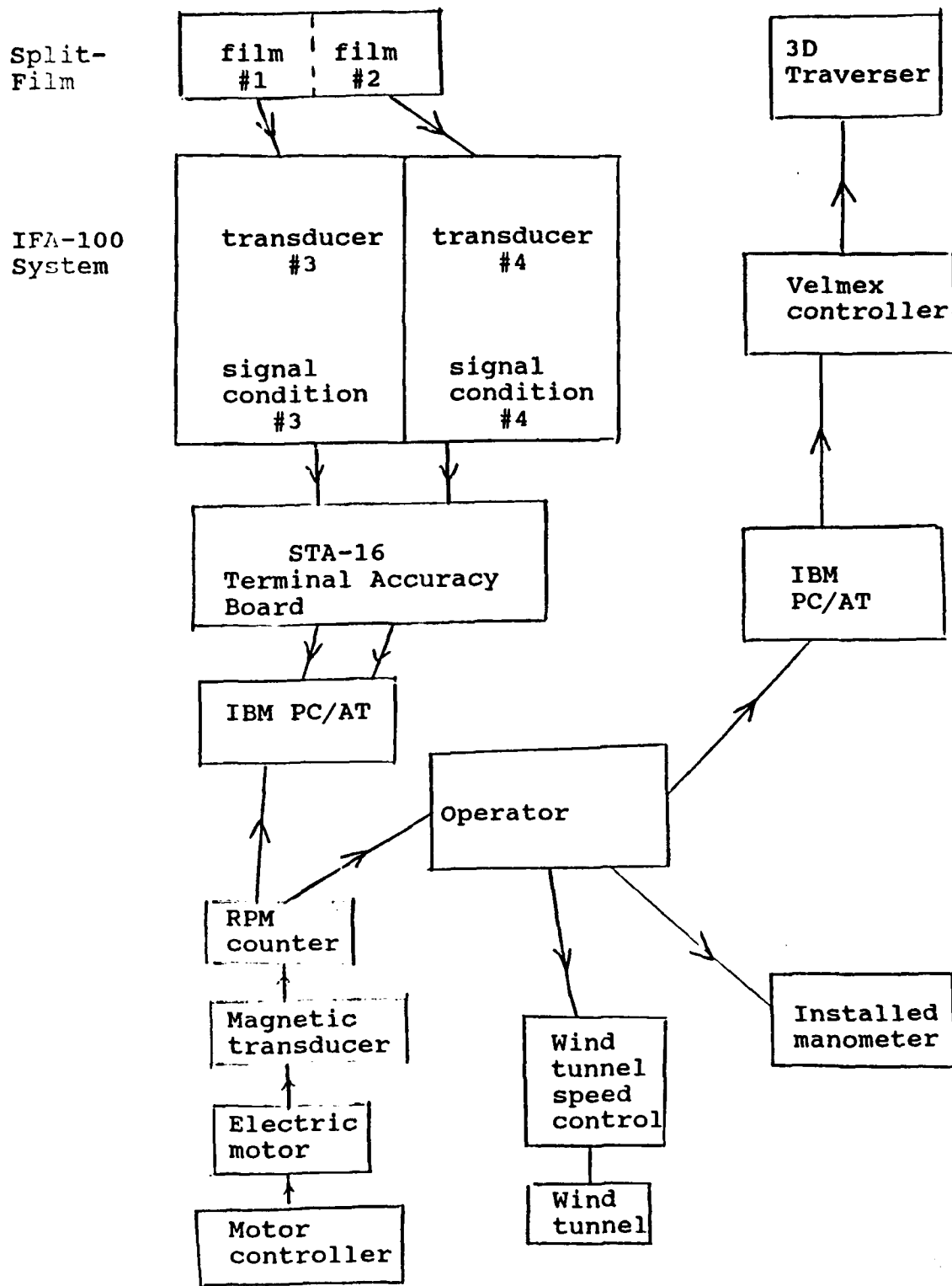
Figure 15.   Information Flow Chart

46

## IV. RESULTS

### A. SPLIT-FILM CALIBRATION

Due to the directional sensitivity associated with split-films, calibration took nearly an entire day to perform. Calibration was therefore to be conducted only twice during the investigation; once before data collection began and once upon completion. The calibration curves were then to be compared for accuracy. Unfortunately the first split-film probe was damaged during the second of four sets of data runs, requiring the use of a second probe and rendering the first set of calibration curves useless for the second, third, and fourth set. The first set of calibration curves therefore applies only to the first set of data runs, while the final curves apply to the second, third, and fourth sets.

The drift/contamination problem associated with hotwire anemometry discussed by Renoud in Ref. 10 was not studied in this investigation due to the time-consuming nature of split-film calibration. However, all literature encountered by the author agrees that contamination is either a minor or insignificant consideration for split-film anemometry. All calibration curves are contained in Appendix E.

## B. ANALYSIS OF TIME VARYING DATA

Ensemble averaging was used to represent the periodic data collected during this study. The periodic nature of the data was conducive to the collection of repetitive time histories, or pulse passage cycles, each associated with the passage of one turbulence pulse. An ensemble consists of a series of nearly-identical time histories. For accuracy a high number of pulses was desired, but was unfortunately limited due to two factors: computer space and propeller frequency. The problems concerning temporary computer storage have been mentioned previously. The pulse generator caused such oscillation of the long probe support that the author prudently decided to limit the rod rotation rate to a maximum value of 17 pulse passes per second. With storage capacity limiting the run time to about one second (at a 20,000 Hz sampling rate), only 17 propeller pulses could be collected during each run.

### 1. Ensemble Characteristics

The 17 pulse cycles from any one ensemble differed from one another somewhat due to the random nature of turbulence and the unsteadiness of separated flow. For the main data runs the velocity data were sampled at 20 KHz while the spinning rod generated turbulent pulses at 17 Hz. This sampling rate results in about 1176 points per cycle. Since each cycle has a period of about 58 milliseconds, a sample represents 50 microseconds.

48

Renoud showed for attached flows that the ensemble averaged cycle can be divided into three general "flow regions" as indicated by the dashed lines in Figure 16, which shows a time history of the velocity near the surface at 70 percent chord and zero degrees angle of attack. The specific characteristics of these regions depend somewhat on the height above the wing's surface, but the general features of these regions remain valid for any vertical position over the wing.

The undisturbed region matches very closely the conditions of the wing placed in steady flow. The pulse itself is defined by the velocity deficit. The recovery period is that area where the velocity has reached its maximum value and gradually decreases as the flow returns to its normal undisturbed state.

2. Mean Velocity Determination

The FORTRAN program SMOOTH.FOR discussed in Chapter II was used to extract the slowly varying mean velocities from an ensemble of instantaneous velocities. One specifies the amount of smoothing by selecting an appropriate window size, L, which in turn determines the cutoff frequency of the digital low pass filter within the program. The relationship is demonstrated by the following equation:

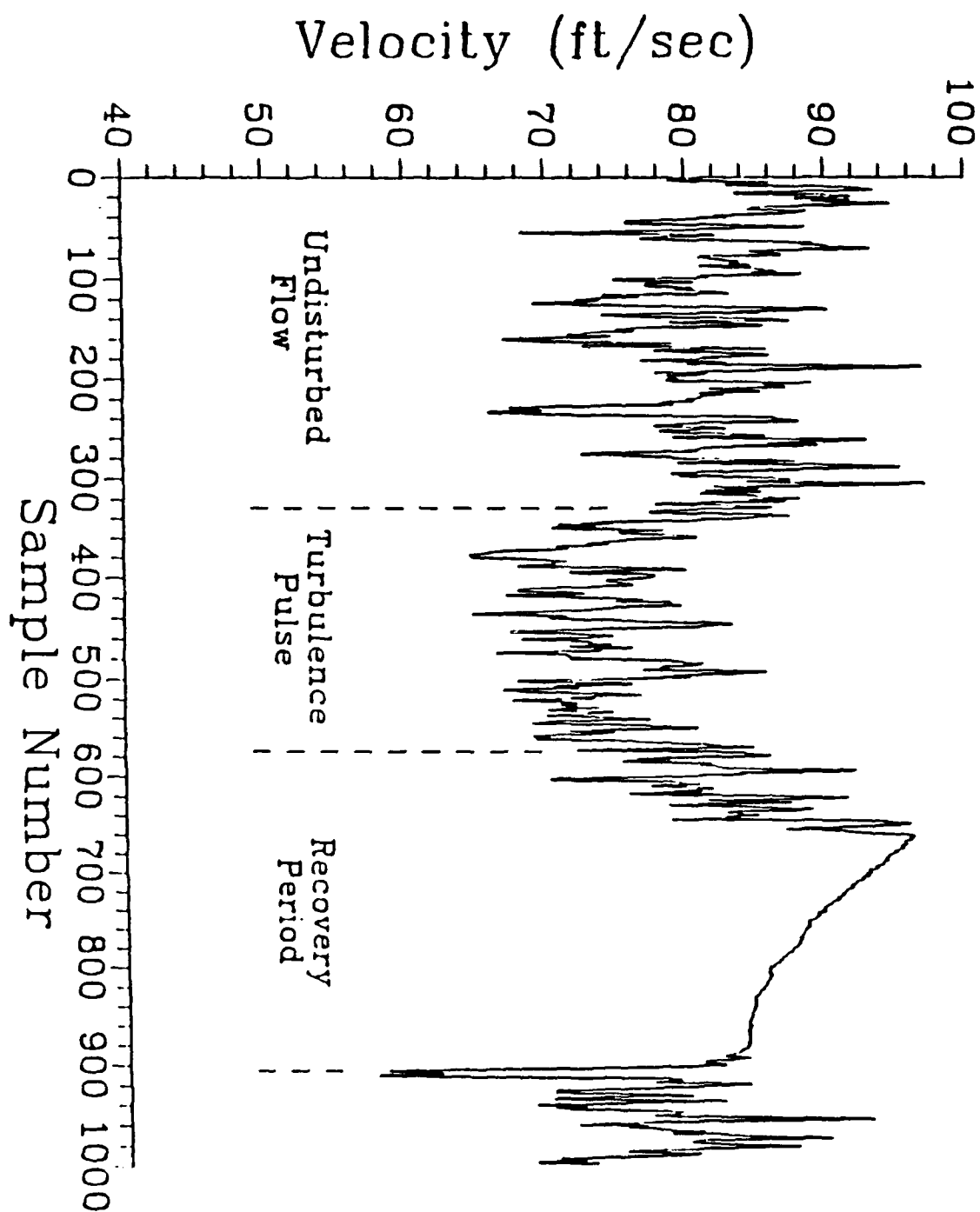$$f_c = \sqrt{0.2929 \left(\frac{f_s}{L}\right)^2} \tag{7}$$

Figure 16.   The General Regions of a Pulse Cycle [Ref. 9]

50

The cutoff frequency, $f_c$, used was 360 Hz based on the findings of Landrum and Macha [Ref. 16]. As described by Renoud [Ref. 10] their work showed that "freestream energy is contained below 200 Hz while the turbulence energy is generally contained above 550 Hz." The author chose to use 360 Hz which lies between these two values, just as Renoud did in his work.

SMOOTH.FOR was also applied to the velocity direction values. This step was needed to compensate for the crude manner in which angular data were manipulated. The limitations of this investigation's angular computations are discussed in Chapter VI.

C.   FREESTREAM ANALYSIS

In 1988 Renoud conducted a freestream analysis with all equipment removed from the test section. This analysis was not duplicated by the author for several reasons. The test section freestream conditions were assumed to be the same since Renoud's flow speed of 95 ft/sec was identical to that used by the author and there had not been any recent structural modifications of the wind tunnel. Although Renoud used a hotwire, all flow during the freestream analysis was in the horizontal plane, so the net results should be identical to those achieved had a split-film been used.

Figure 17 is the plot of velocity response over 1000 samples which Renoud obtained. The signal is flat with the high frequency turbulent component superimposed on the mean.
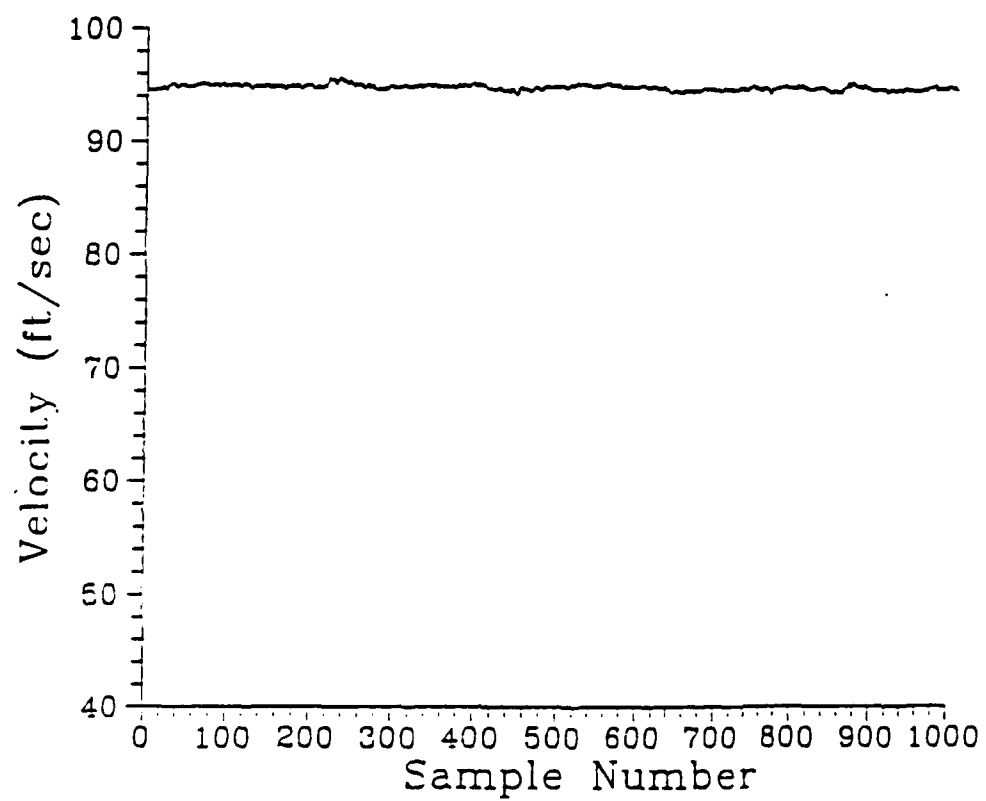
51

Figure 17.   Test Section Freestream Flow [Ref. 9]

Renoud's plotting of the freestream velocity spectrum (not shown) indicated that the most significant frequency components reside within the lower frequency ranges. This observation was what led the author to sample at 20,000 Hz rather than 50,000 Hz.

## D. ANALYSIS OF UNDISTURBED FLOW OVER THE AIRFOIL

Flow over the airfoil at a 22 degree angle of attack was investigated at 58 points above the 70 percent chord location. Velocity measurements were made to establish the specific flow behavior at this position in the absence of external disturbances. These baseline data would be crucial in analyzing any stabilizing or destabilizing effects created by imposed periodic turbulence.

Flow over the aft section of an airfoil produces an increasing pressure distribution which is referred to as an adverse pressure gradient. At high angles of attack this gradient is most pronounced. As the flow element moves downstream it may come to a stop and under the influence of the adverse pressure gradient and/or shear stress, actually reverse direction. Such a reversal causes the flow to separate and creates a wake of recirculating air downstream of the surface. Because of this flow over an airfoil at a high angle of attack can not be classified as steady, even if the freestream is left undisturbed.

To establish the behavior in this quasi-steady state of separated flow at each height above the surface the velocity magnitudes and direction of 2000 samples were averaged. The average velocity magnitude and direction values were then used to calculate average streamwise and transverse velocity components (u and v described in Fig. 18). Because the airfoil was at 22 degrees angle of attack while the sensor axis was perpendicular to the freestream flow, these components did not exactly match the actual parallel and perpendicular flow components (with respect to the airfoil surface at the 70 percent chord location). From this point forward however, for simplification of analysis, this discussion will treat the components as if they represented the actual flow parallel and perpendicular to the surface (unless otherwise stated).

The total velocity magnitude, and the streamwise and transverse velocity components for the flow at 58 separate heights above the 70 percent chord location, are plotted in Figures 19 to 21 respectively. All plots of velocity versus height generated for this investigation use nondimensional units; the height y is divided by chord length c, and the velocity values are divided by the freestream velocity, $U_\infty$. The low values of total velocity magnitude in Figure 19 (all less than half freestream) correspond to the loss of kinetic energy in the presence of an adverse pressure gradient. The lack of a significant streamwise velocity component, u, at any
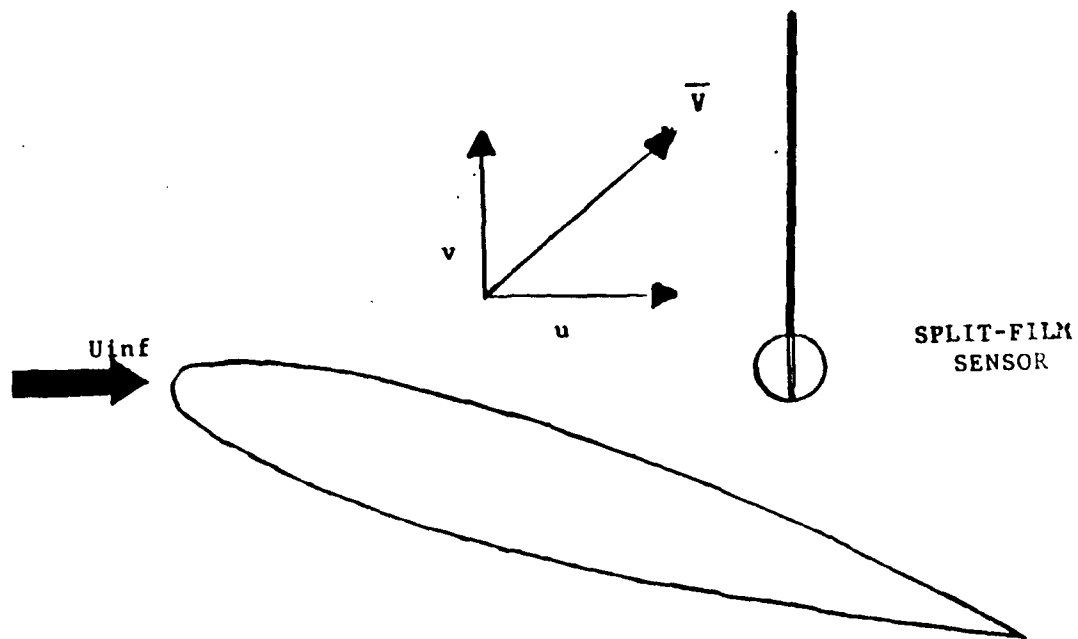
Figure 18. Definition of Flow Velocity Components

height shown in Figure 20 demonstrates separated flow at this chord location. The large values of $\overline{V}$ shown in Figure 21 and the previously noted lack of a significant streamwise component indicates that the flow is mostly vertical. Unfortunately, due to limitations of the split-film probe, the transverse velocity component values are absolute (Figure 20), and their signs cannot be determined. From the lack of any values near zero however, it can be inferred that the flow is either all positive (upward) or negative (downward) at this chord and span location.

Figure 19.   Average Total Velocity Profile,
Undisturbed Flow, 70% Chord,
22° Angle of Attack

Figure 20.   Average Streamwise Velocity Profile,
Undisturbed Flow, 70% Chord,
22° Angle of Attack
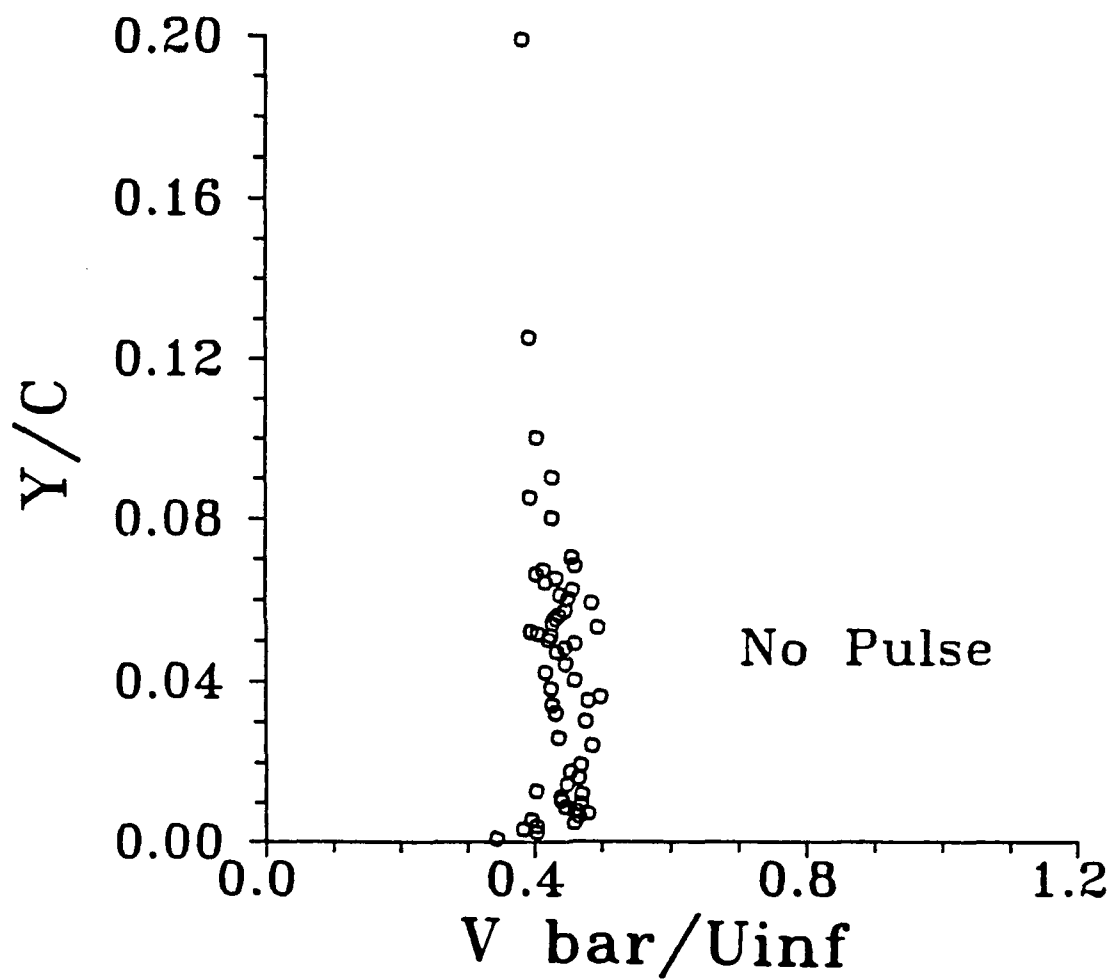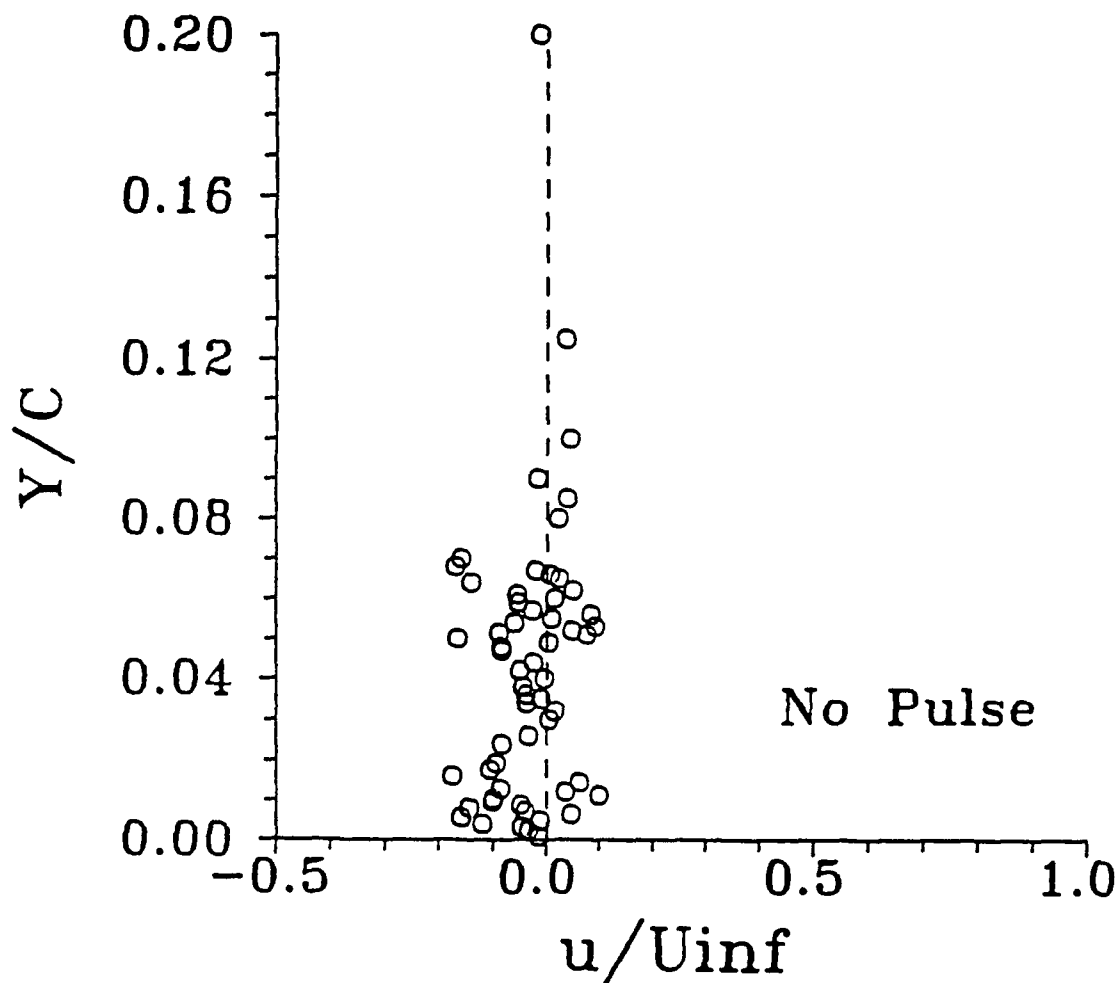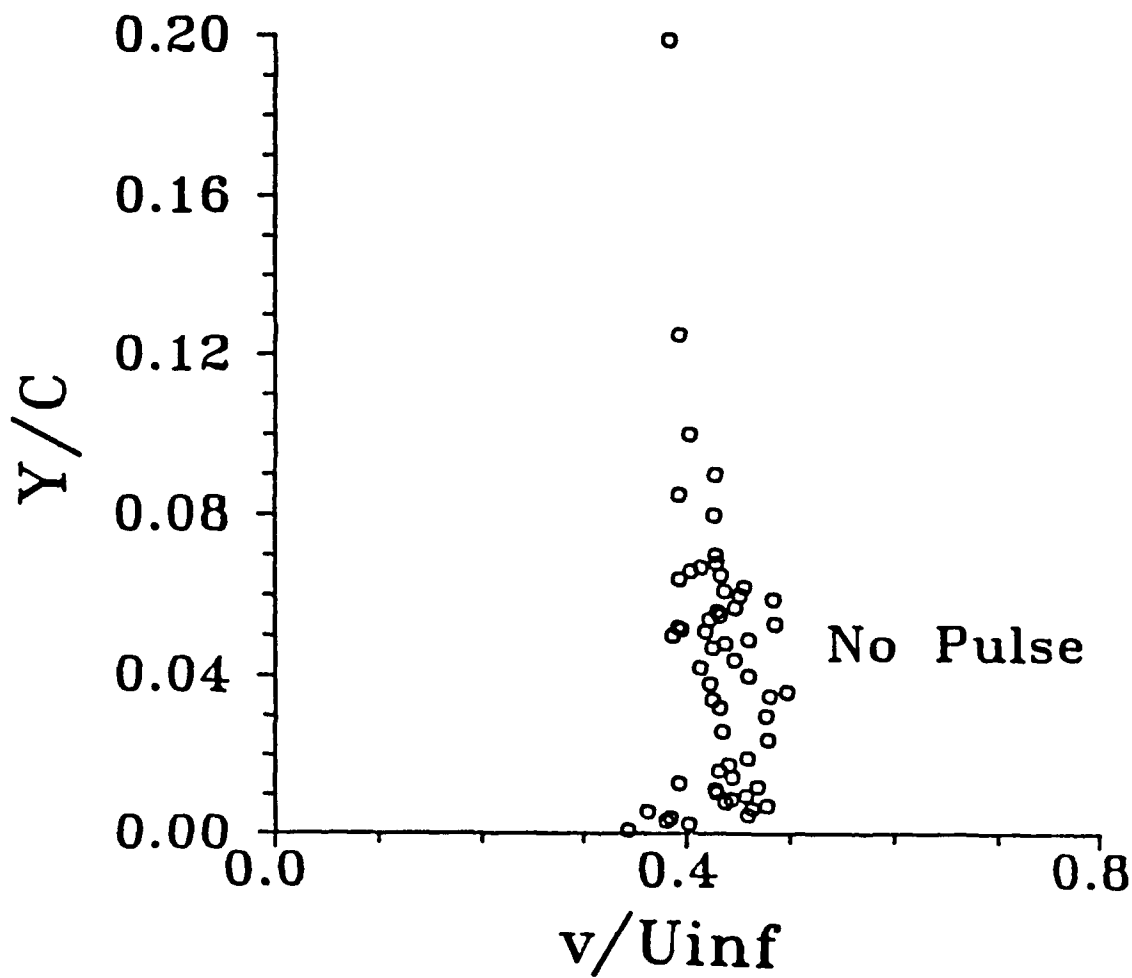
57

Figure 21.   Average Transverse Velocity Profile,
Undisturbed Flow, 70% Chord,
22° Angle of Attack

A time history of the total velocity in this undisturbed case is shown in Figure 22.  The unsmooth nature of these plots shows the unsteadiness present due to separation.

E.  RESPONSE TO FREESTREAM DISTURBANCES AT HIGH ANGLES OF ATTACK

The response to the turbulence pulse was examined at the 70% chord location under the following sets of conditions:

1.  22 degrees angle of attack, k = .47

2.  22 degrees angle of attack, k = .09

3.  12 degrees angle of attack, k = .47.

The symbol k listed for each setup represents the reduced frequency and is defined in the following equation:

$$k = \frac{\omega \, c}{2 \, U_\infty} \tag{8}$$

where $\omega$ is the rotational or oscillating frequency, c is the chord length, and $U_\infty$ is the freestream velocity.  Carr [Ref. 4], whose work with oscillating airfoils and dynamic stall is discussed in Chapter I, documented the response of a pitching airfoil to changes in this reduced frequency.  Among other things he found that the maximum lift coefficient increased as k was increased.

Variation of the reduced frequency of an oscillating airfoil is known to alter the lift coefficient as well as other aspects of the flow response.  In this investigation, where the impinging flow was oscillating as opposed to the
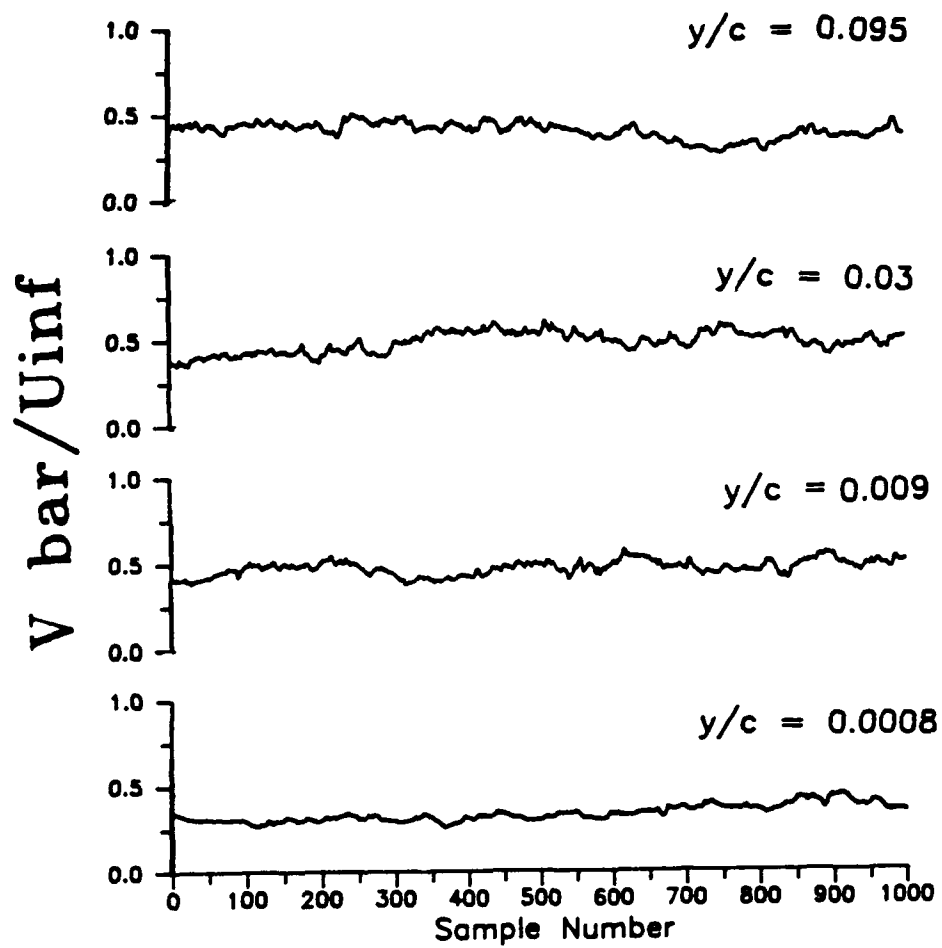
59

Figure 22. Undisturbed Flow, Total Velocity Time Histories (AOA = 22°)

airfoil (due to the generation of periodic disturbances) a similar situation exists. The purpose of introducing a different reduced frequency during the second set of data runs was to document a reduced frequency variation influence on a separating boundary layer.

The third set of data runs listed above (k = .47, angle of attack = 12 degrees) was made to determine how periodic turbulence might affect attached flow near separation. All conditions, except angle of attack, were the same as those used in the first set of data runs.

1.   <u>22 Degree Angle of Attack, k = .47</u>

Figures 23 through 25 contain plots of the total velocity versus the height above the surface. Each plot represents the velocity profile at a particular point within the pulse cycle. From the 100th to 500th sample most heights show a very slight velocity decrease. By the 999th sample the velocities have generally increased back to the 100th sample values, indicating the cyclical nature of a passing pulse. The cyclical nature of the pulse passage was expected but the changes in the character of these profiles were surprisingly subtle.

While a cyclic nature in the total velocity plots is barely noticeable, there is no discernible cyclic trend exhibited by the horizontal velocity component plots of Figures 26 through 28. Regardless of the sample number each plot is similar in its general nature to the no pulse baseline

Figure 23.    Ensemble Average Profile, Imposed
              Periodic Turbulence (17 Hz), 70%
              Chord, 22° Angle of Attack

Figure 24.   Ensemble Average Profile, Imposed
             Periodic Turbulence (17 Hz), 70%
             Chord, 22° Angle of Attack

Figure 25. Ensemble Average Profile, Imposed
Periodic Turbulence (17 Hz), 70%
Chord, 22° Angle of Attack
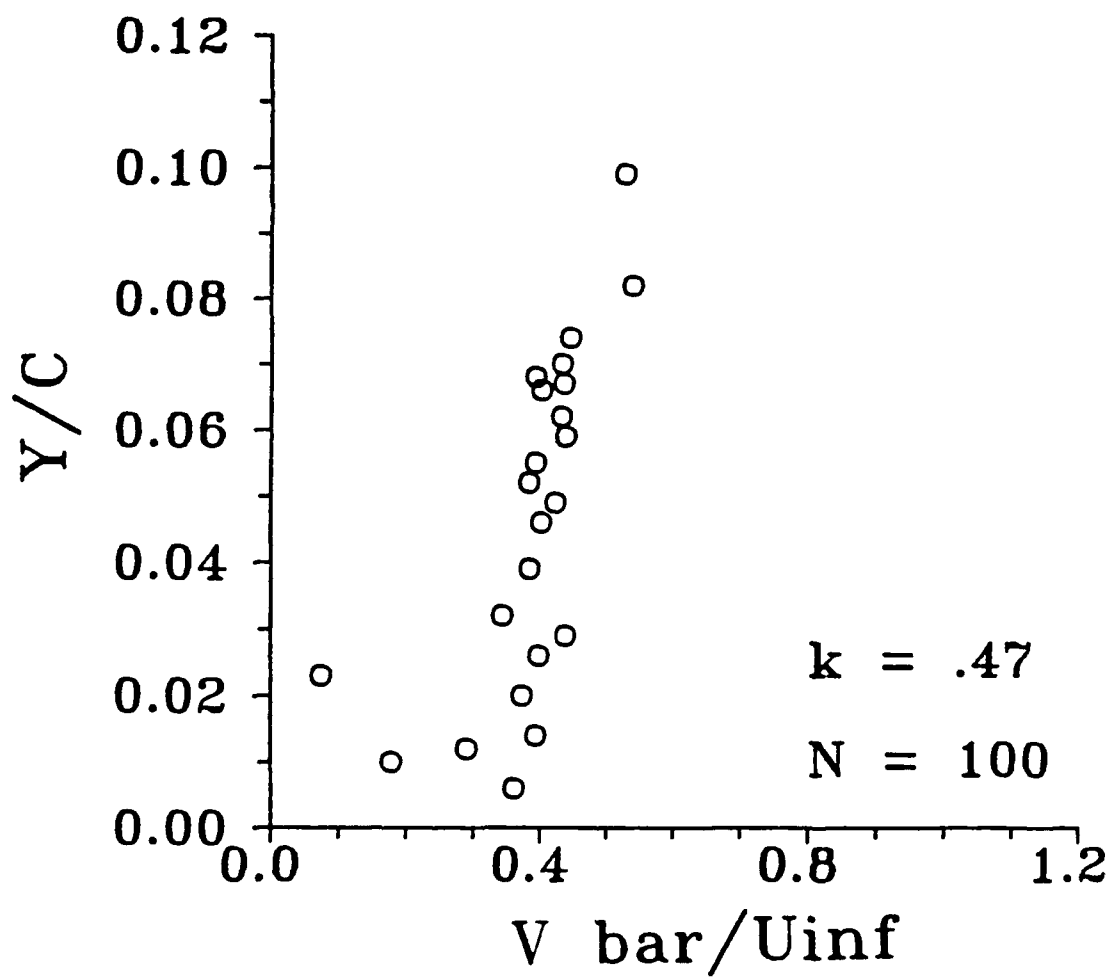
Figure 26.    Ensemble Average Profile, Imposed
              Periodic Turbulence (17 Hz), 70%
              Chord, 22° Angle of Attack

Figure 27. Ensemble Average Profile, Imposed
Periodic Turbulence (17 Hz), 70%
Chord, 22° Angle of Attack

66

Figure 28.    Ensemble Average Profile, Imposed
             Periodic Turbulence (17 Hz), 70%
             Chord, 22° Angle of Attack

67

case discussed previously. Possible explanations for a lack

of any real difference between these plots and the plot of the

no pulse case could be:

1.  periodic pulses in general have little net effect on the
    highly separated flow at this chord position and angle
    of attack

2.  the frequency of the pulse was too high to influence the
    highly separated flow.

Plots of v versus height in Figures 29 and 30 also

show no cyclic nature. However, they do exhibit one important

difference from the no pulse case. In both of the plots two

of the lower heights show values which are much less than any

of those values in the no pulse case (see Figure 21). In

fact, looking back at the plots of $\bar{V}$ versus height (Figures

23-25) one notices that there are two points (on all plots)

which have much lower velocities than similar heights of the

no pulse case. These two points also show a much lower

velocity than others do on the same plot at nearby heights.

The separation bubble sketched in Figure 31 offers a

possible explanation for this phenomenon. At the lowest point

measured the split-film sensor is at point A. Here there is

a large vertical velocity, about 40 percent freestream. For

the next measurement the sensor is raised to point B which is

on or near the vertical stagnation line, where the velocity is

much less than the surrounding flow. By the time the sensor

reaches point C it is far enough from the stagnation line so

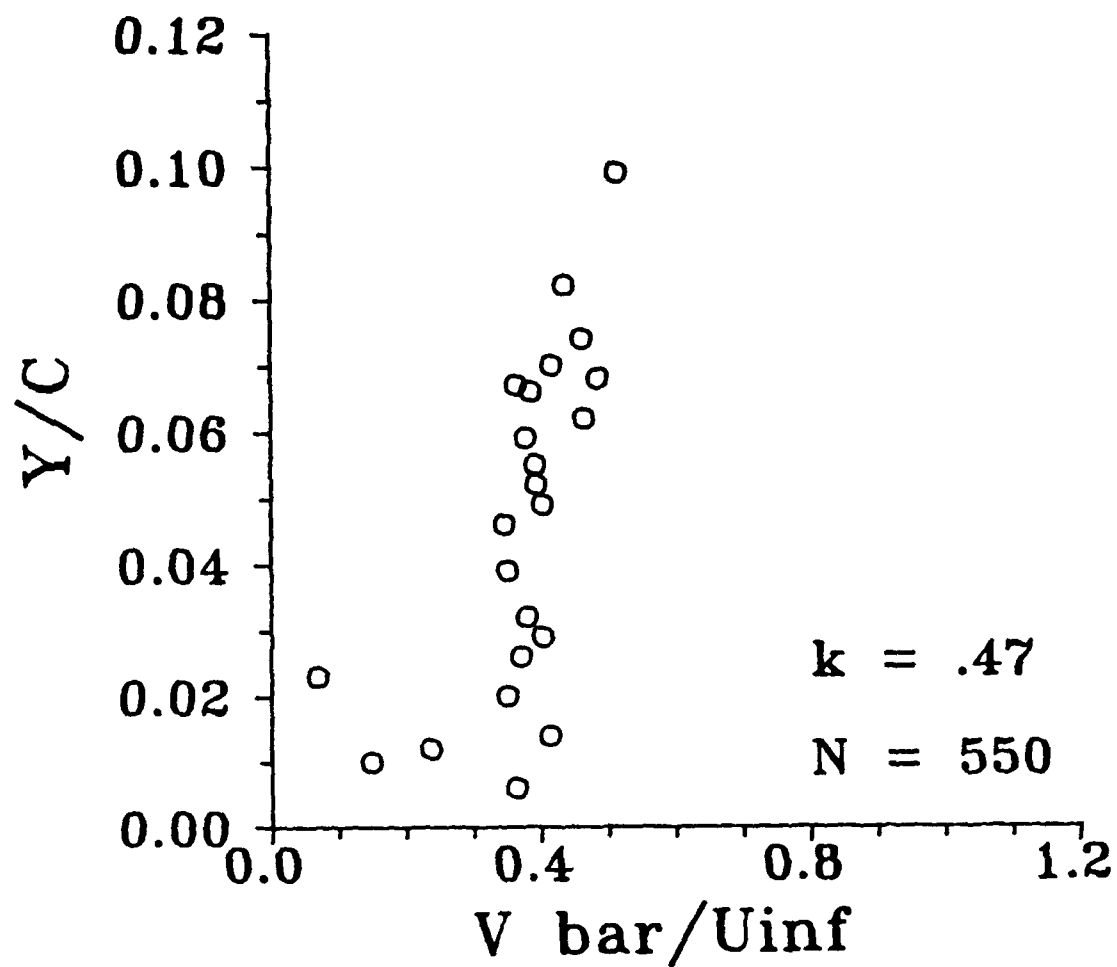that the total velocity is restored to a  value  in  the rough

68

Figure 29.  Ensemble Average Profile, Imposed
Periodic Turbulence (17 Hz), 70%
Chord, 22° Angle of Attack
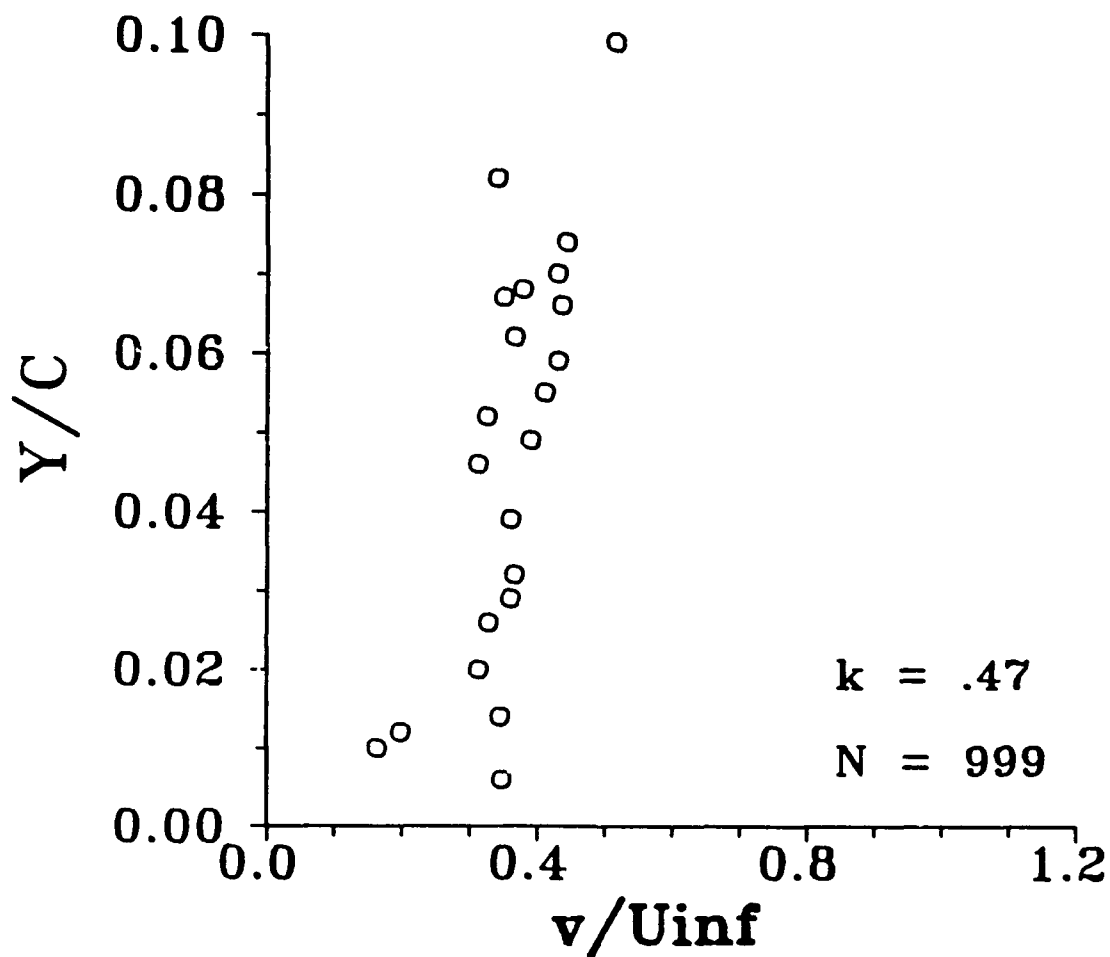
Figure 30.  Ensemble Average Profile, Imposed
            Periodic Turbulence (17 Hz), 70%
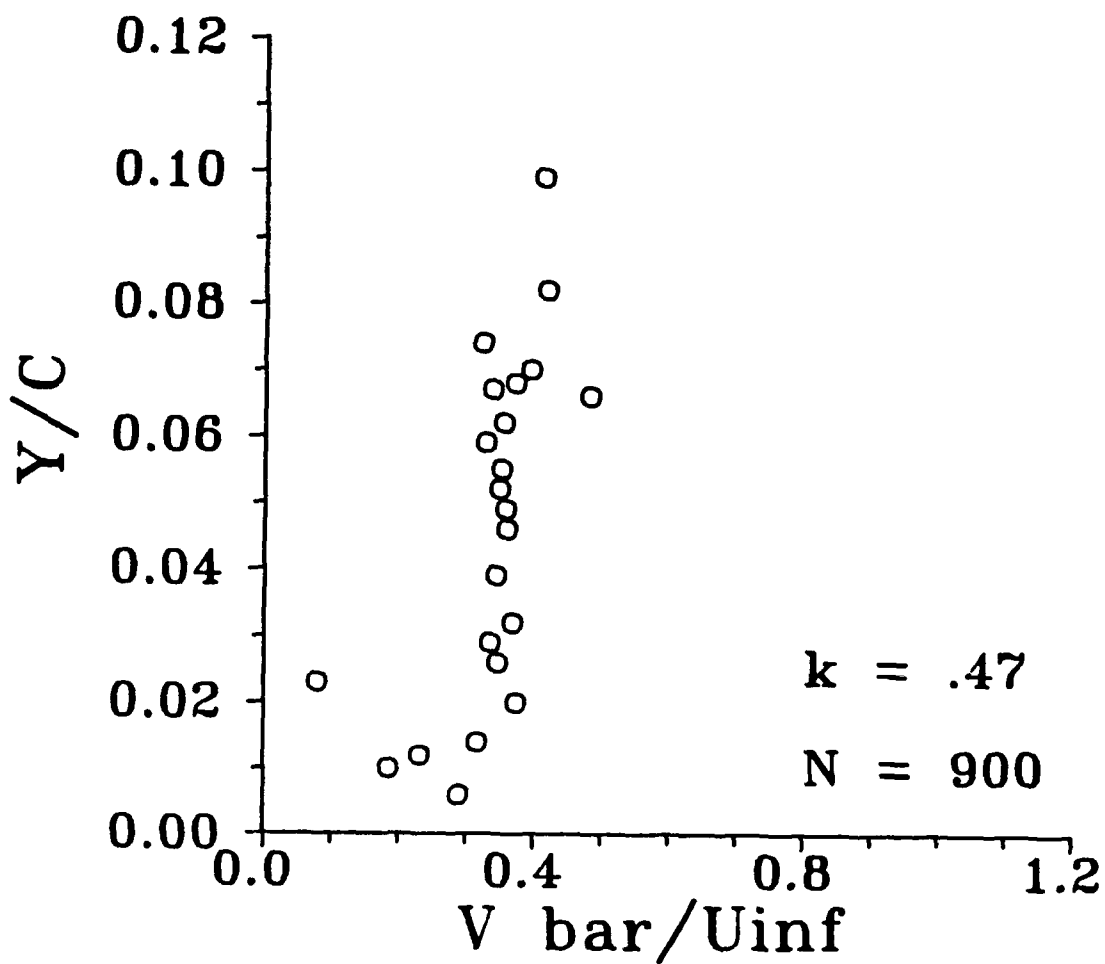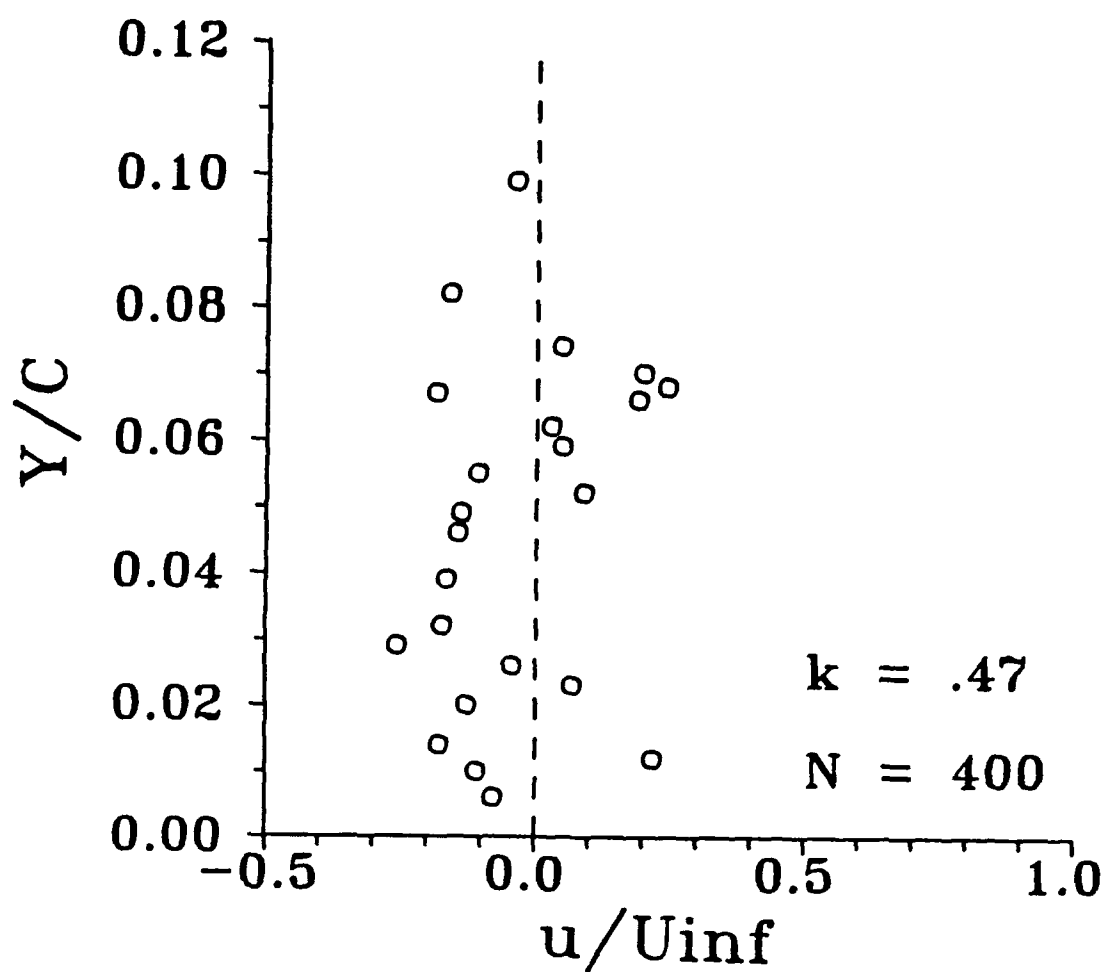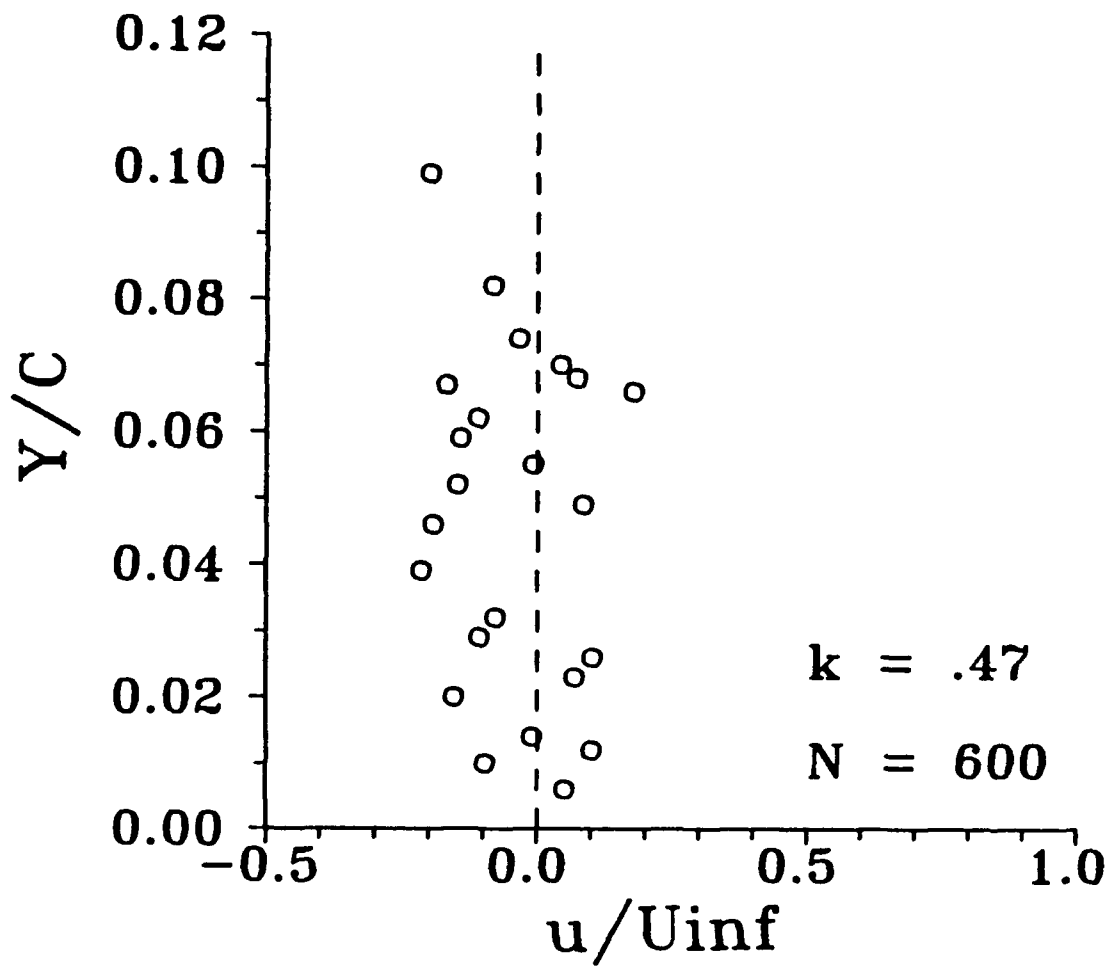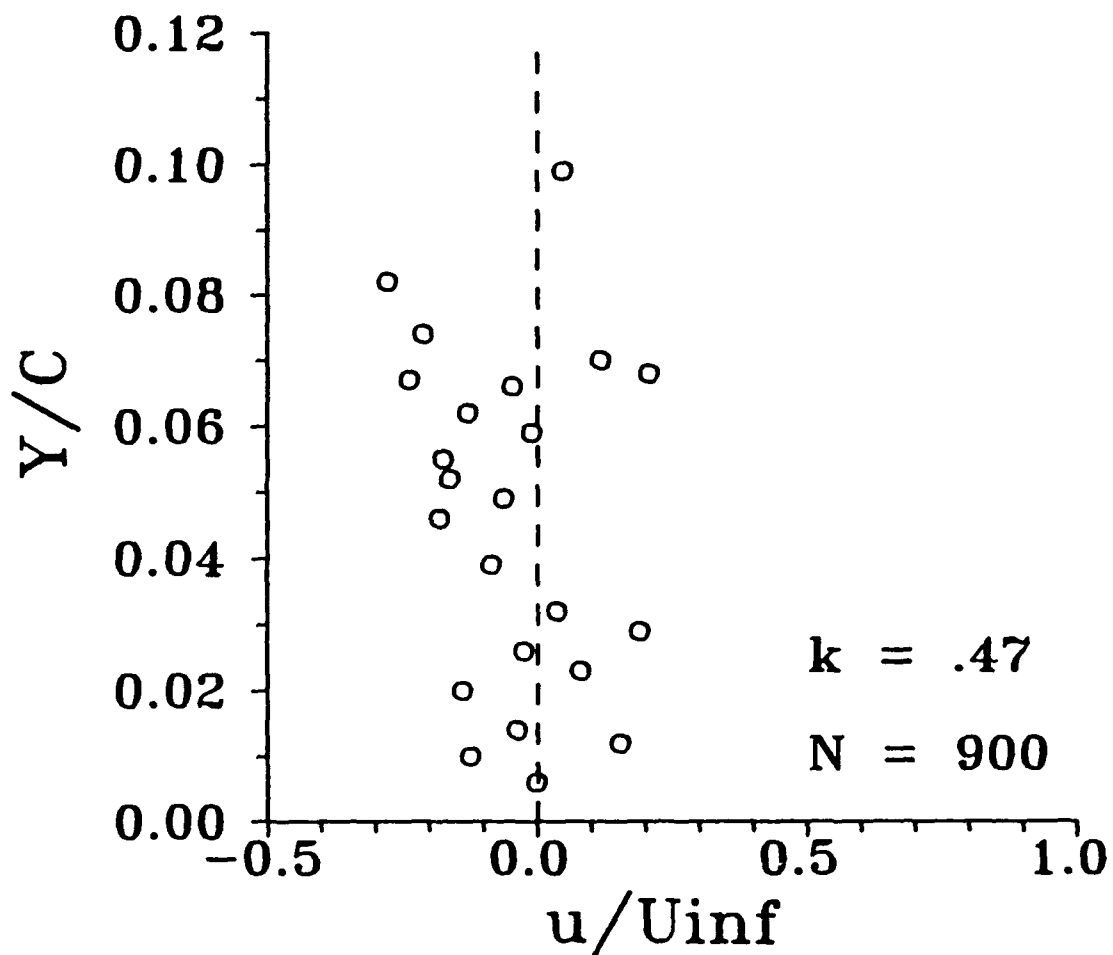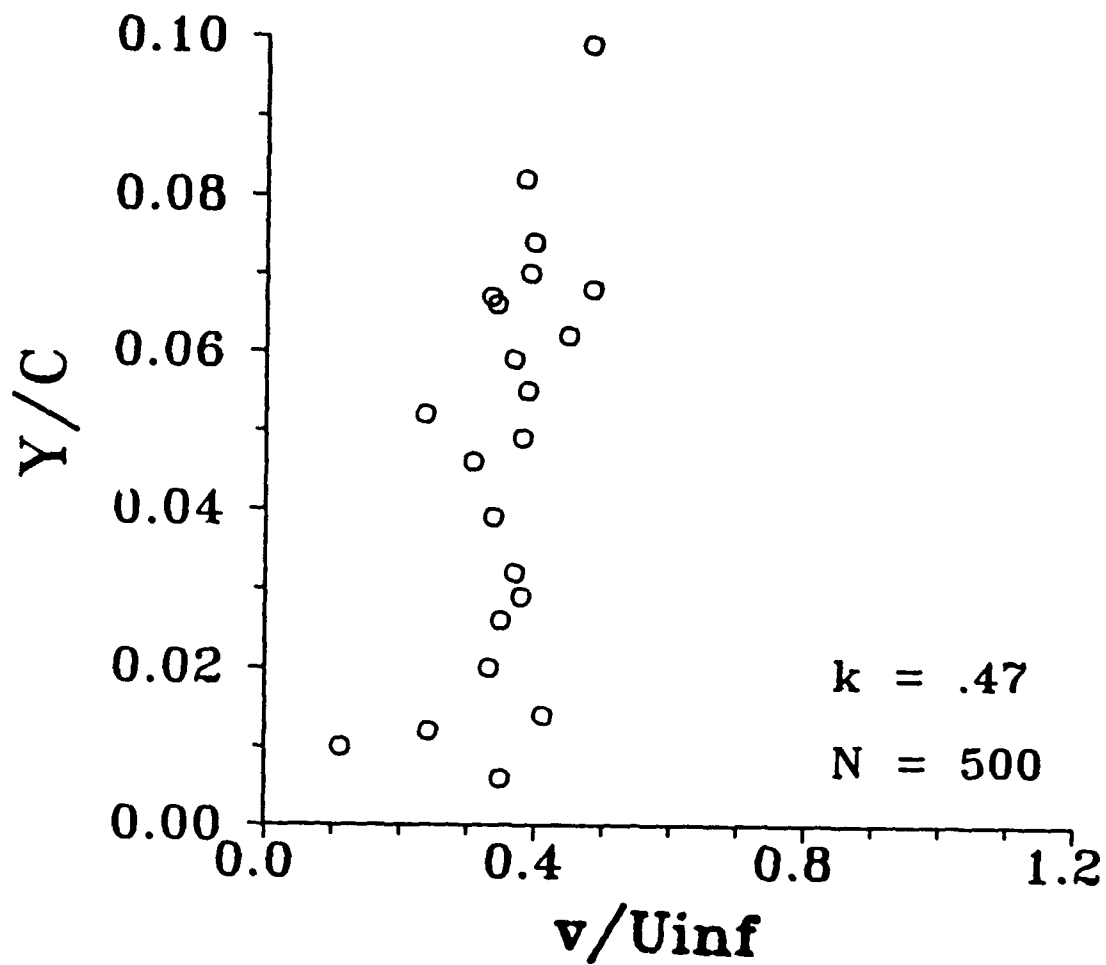            Chord, 22° Angle of Attack

70
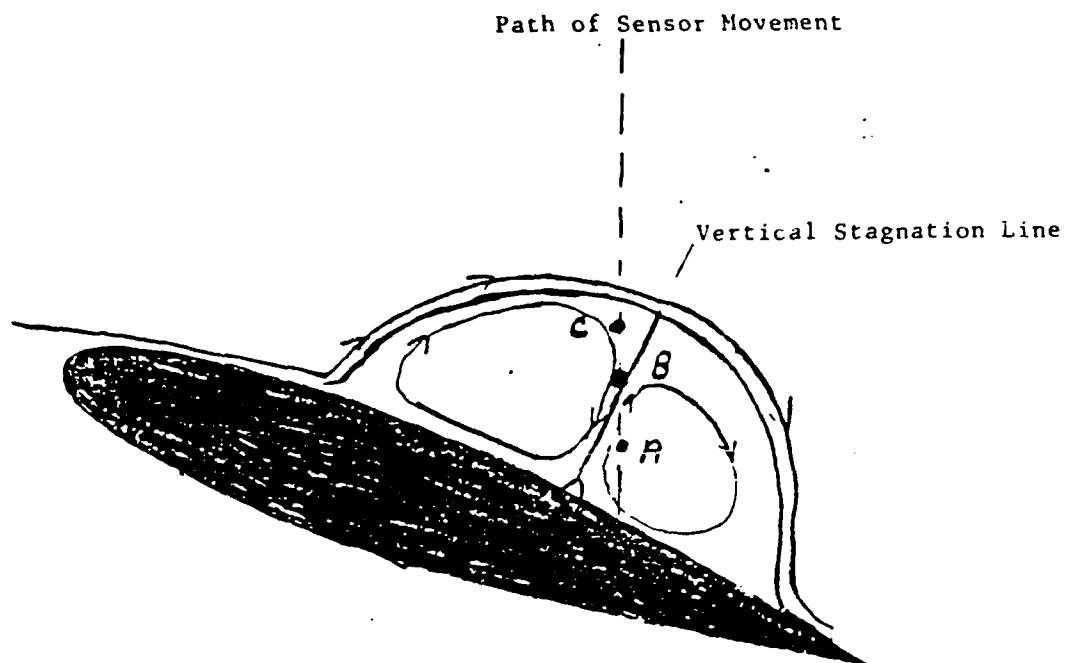
Figure 31.  Laminar Separation Bubble and Its
           Possible Effect on Velocity
           Measurements

71

vicinity of 40 percent freestream. This phenomenon does not occur in the no pulse case. Perhaps its separation bubble is different from the one hypothesized to exist in the induced pulse case.

When considering the above explanation one should keep in mind that all measured u components were near zero and that the v measurements are only indicative of magnitude, not sign. Also one should keep in mind that this hypothesis is plausible only if a separation bubble similar to the one drawn exists. Also, the phenomenon could simply be caused by unsteadiness near the surface though the repetition of this behavior indicates otherwise.

Smoothed mean velocity time histories (total velocity and the u components) of the pulse passage cycle are shown in Figures 32 and 33. These plots represent the time histories at various vertical distances (Y/C) above the wing surface. The bottom trace shows the time history closest to the wing while the top plot shows a record of flow at the highest measured point above the surface. Figure 32 contains a plot of flow in the horizontal direction ($u/U_\infty$) while the plot on Figure 33 is of total flow.

As in the case of the velocity profiles, these plots show the rapidly changing nature of separated flow but do not show any outward presence of an imposed low frequency disturbance. In addition, the plot of $\overline{V}$ vs time indicates that the total flow energy remains relatively constant throughout

72
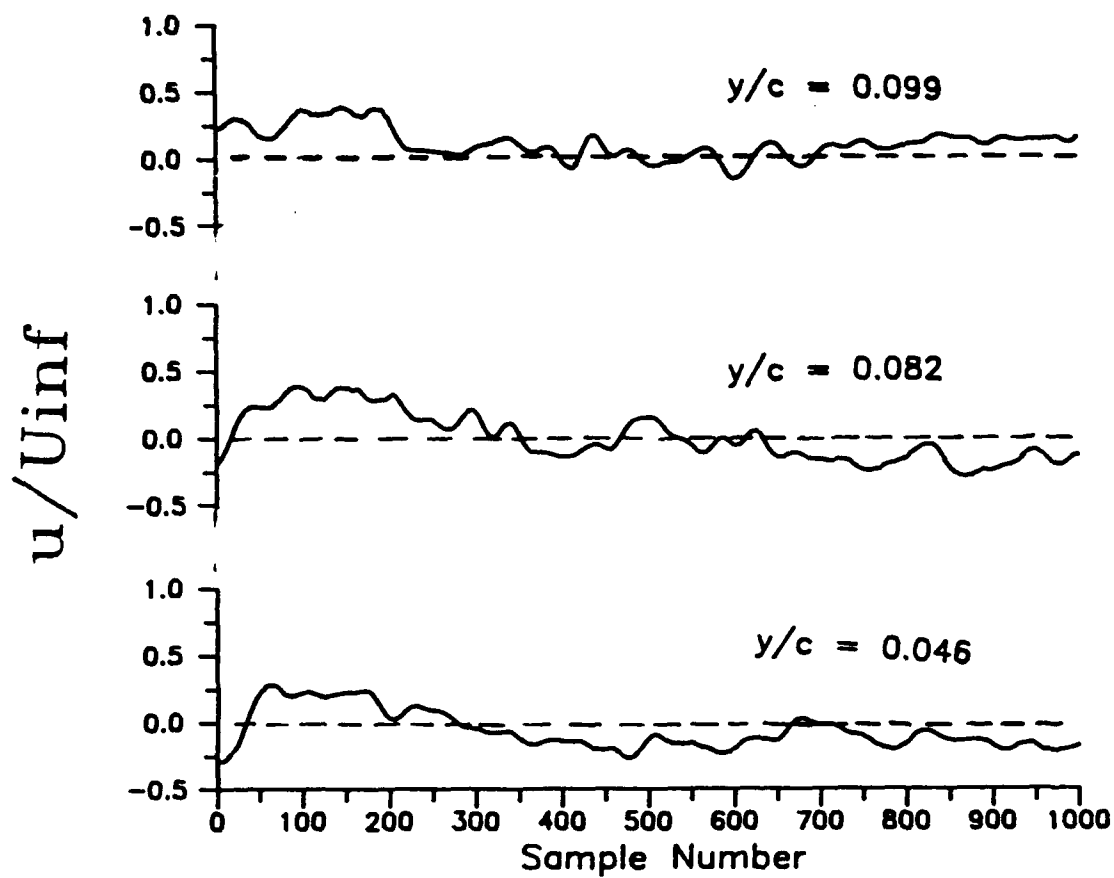
Figure 32.   Streamwise Velocity Time Histories
            (AOA = 22°,  k = .47)

73
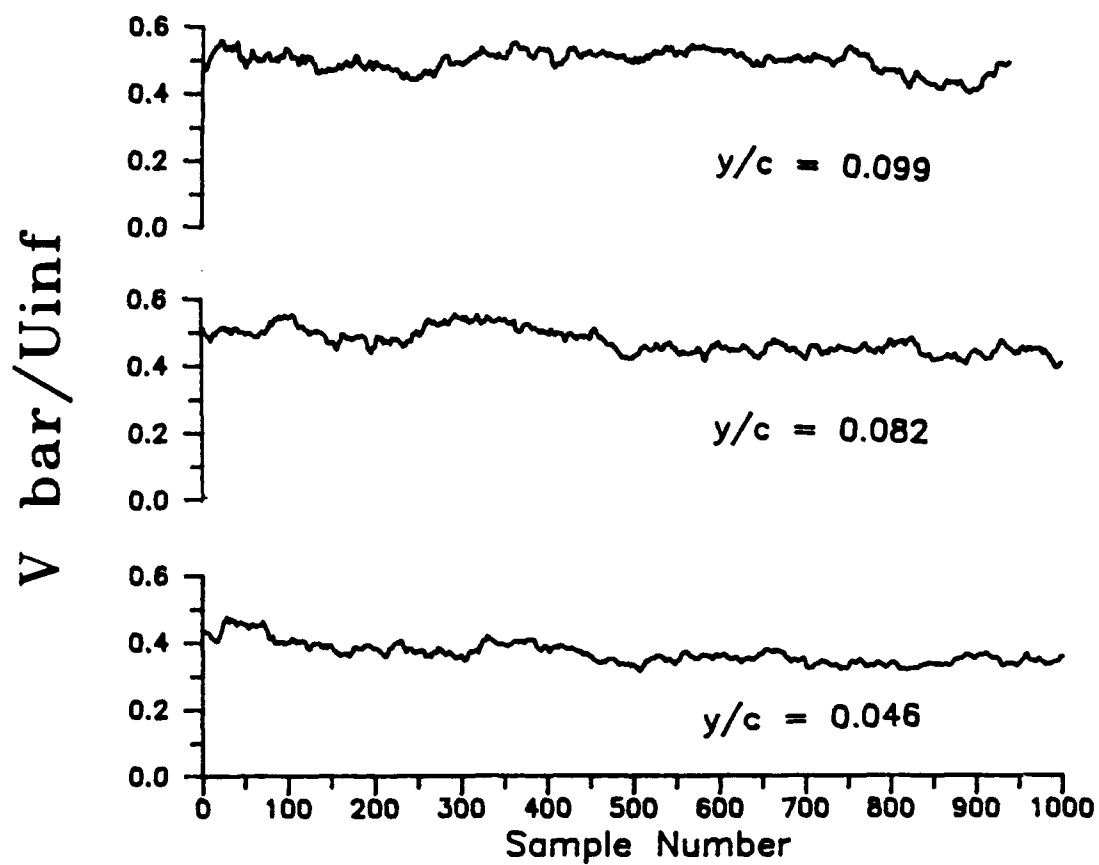
Figure 33. Total Velocity Time Histories
(AOA = 22°, k = .47)

74

throughout the pulse passage. Analysis of the next scenario in which a lower pulse generation frequency was used may help explain why these time histories and velocity profiles show no clear presence of disturbance.

An observation worth mentioning is the possible indication of turbulence at this reduced frequency. Careful inspection of the streamwise velocity time histories shows a repetitive wavelike pattern which occurs about ten times during each pulse cycle. Recalling that the sampling rate was 20,000 Hz:

$$20,000 \frac{\text{samples}}{\text{sec}} \times \frac{\text{cycle}}{100 \text{ samples}} = 2000 \frac{\text{cycles}}{\text{sec}} = 2000 \text{ Hz} \tag{9}$$

Repetition at this high rate is not indicative of separation vortices. It does, however, appear to imply the strong presence of turbulence in the separation region at this frequency.

2.  <u>22 Degree Angle of Attack, k = .09</u>

Figures 34 through 39 contain the ensemble-average total velocity profiles for the slowly generated turbulent pulse. Unlike the reduced frequency case of .47 just discussed, here the imposed pulse had an extremely dramatic effect. The total velocity profiles after sample 50 indicate an increase in magnitude with the passage of time. This increase was most dramatic at larger distances from the surface. At the 450th sample the velocity values peaked. The

75

Figure 34.   Ensemble Average Profile, Imposed
             Periodic Disturbance (3 Hz), 70%
             Chord, 22° Angle of Attack

Figure 35. Ensemble Average Profile, Imposed
Periodic Disturbance (3 Hz), 70%
Chord, 22° Angle of Attack

Figure 36.  Ensemble Average Profile, Imposed
Periodic Disturbance (3 Hz), 70%
Chord, 22° Angle of Attack

Figure 37.   Ensemble Average Profile, Imposed
Periodic Disturbance (3 Hz), 70%
Chord, 22° Angle of Attack

79

Figure 38.   Ensemble Average Profile Imposed
             Periodic Disturbance (3 Hz), 70%
             Chord, 22° Angle of Attack

Figure 39.   Ensemble Average Profile, Imposed
            Periodic Disturbance (3 Hz), 70%
            Chord, 22° Angle of Attack

81

passage of the pulse may be a stabilizing influence, since it allows the flow to overcome the adverse pressure gradient. By the 700th sample the values were once again close to those of sample 50. This profile also corresponds very closely to the no pulse case shown previously in Figure 28, indicating that sample 50 represents the undisturbed portion of the cycle.

Inspection of the horizontal velocity component profiles (Figures 40-48) confirms this. Once again at sample 50 the profile is very similar to the no pulse case. With passage of time, more and more heights show nonreversed flow until sample 250 when virtually all flow is in the streamwise direction. The effect further from the surface is also more pronounced. From samples 250 to 450, the outer flow increases in magnitude, while the inner flow begins to proceed moving in the reversed direction. The trend continues to swing the opposite way, until sample 650 where all flows are reversed. The plot of sample 850 shows the flow as it is returning to the undisturbed portion of the cycle at sample 50. To summarize the behavior of flow these profiles have been smoothed and sketched by hand and are shown in Figure 49.

The analysis of $u/U_\infty$ seems to indicate that the pulse gradually causes the flow reversal (similar to the no pulse, undisturbed case) to cease, but then actually intensifies the reversal before finally allowing the flow to return to the undisturbed state. This pattern is similar to the one Renoud discovered associated with the periodic disturbance effect on
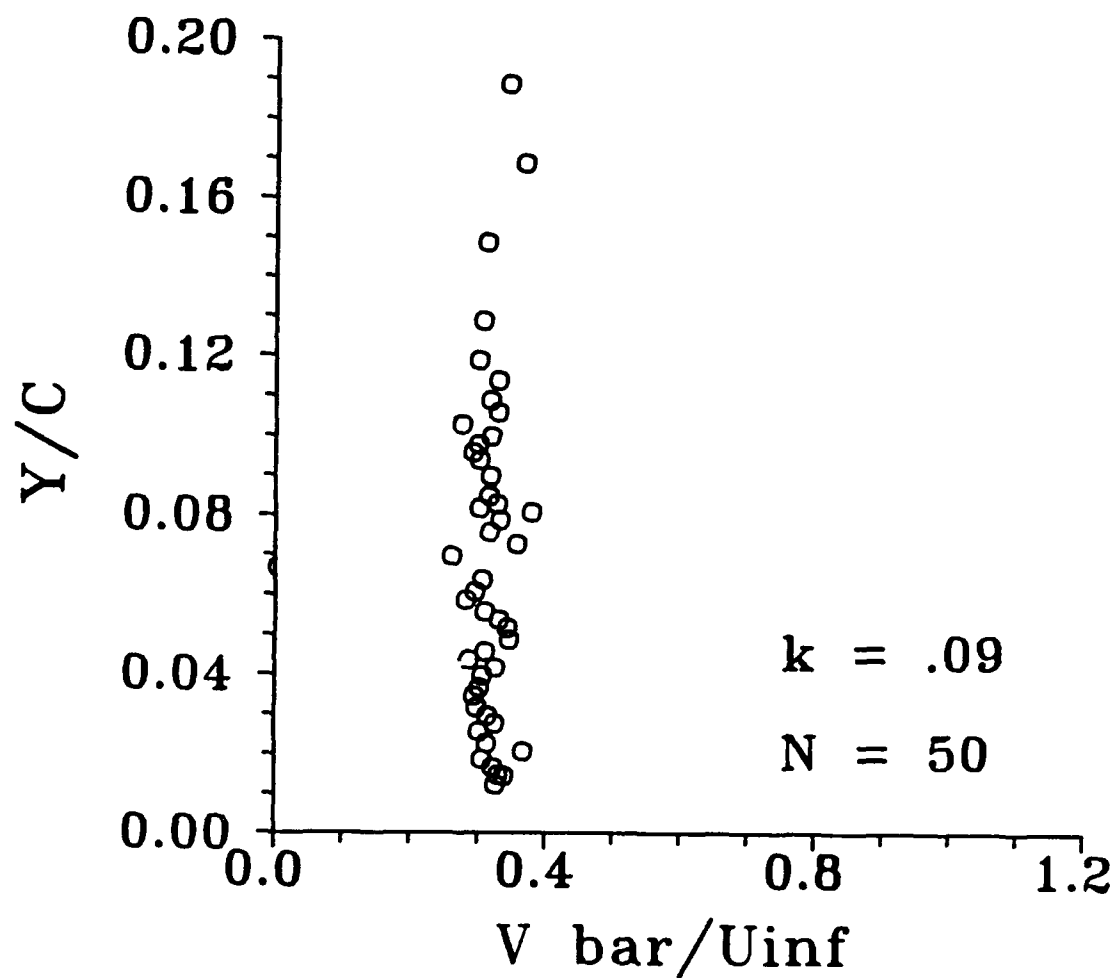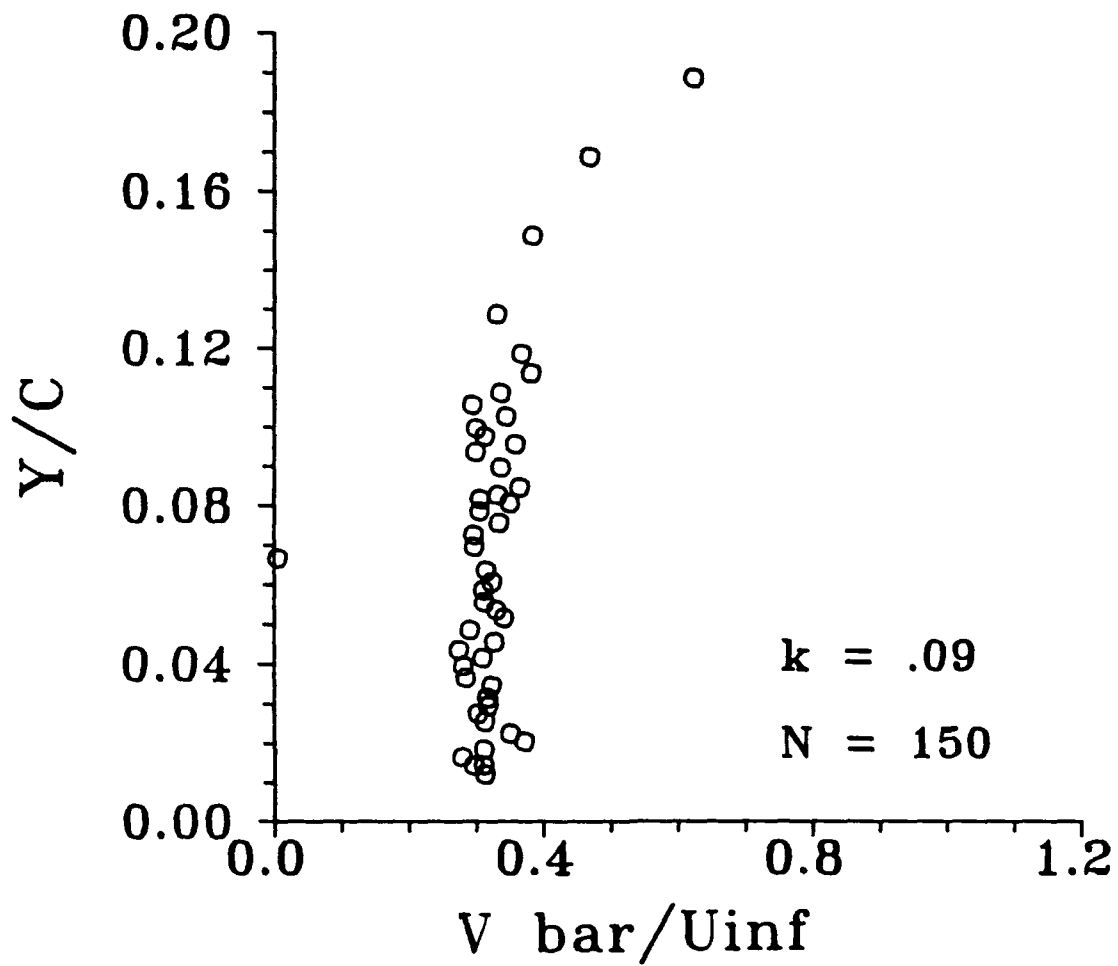
82

Figure 40.  Ensemble Average Profile, Imposed
Periodic Disturbance (3 Hz), 70%
Chord, 22° Angle of Attack
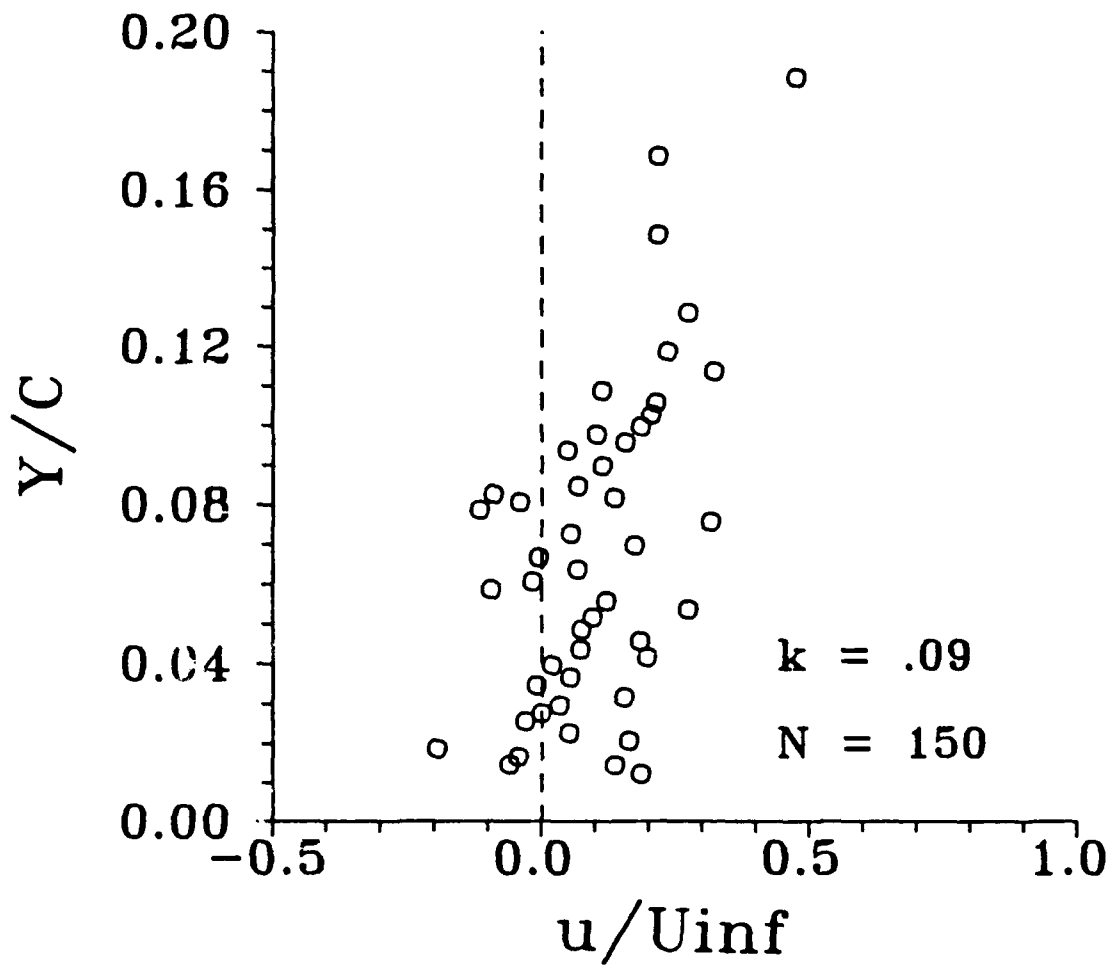
Figure 41.   Ensemble Average Profile, Imposed
             Periodic Disturbance (3 Hz), 70%
             Chord, 22° Angle of Attack

84
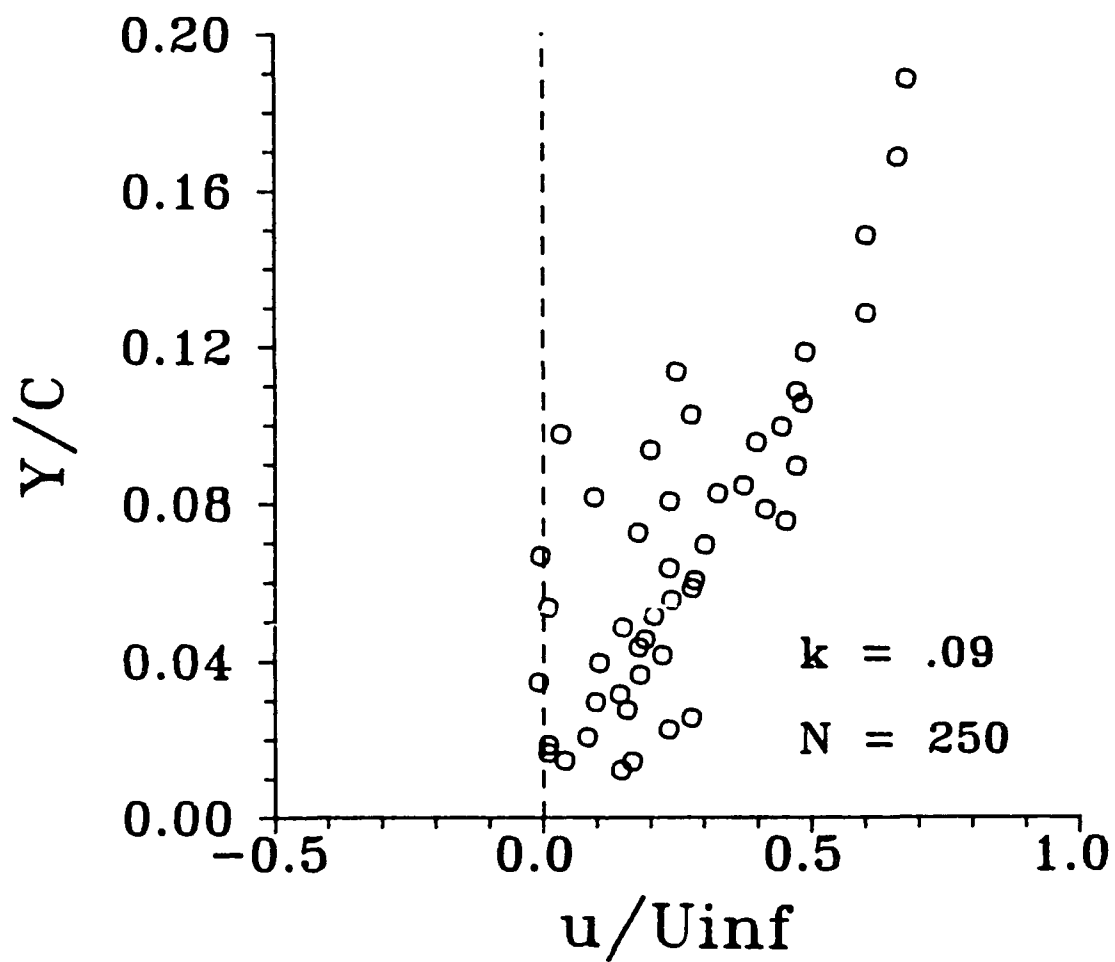
Figure 42.  Ensemble Average Profile, Imposed
            Periodic Disturbance (3 Hz), 70%
            Chord, 22° Angle of Attack
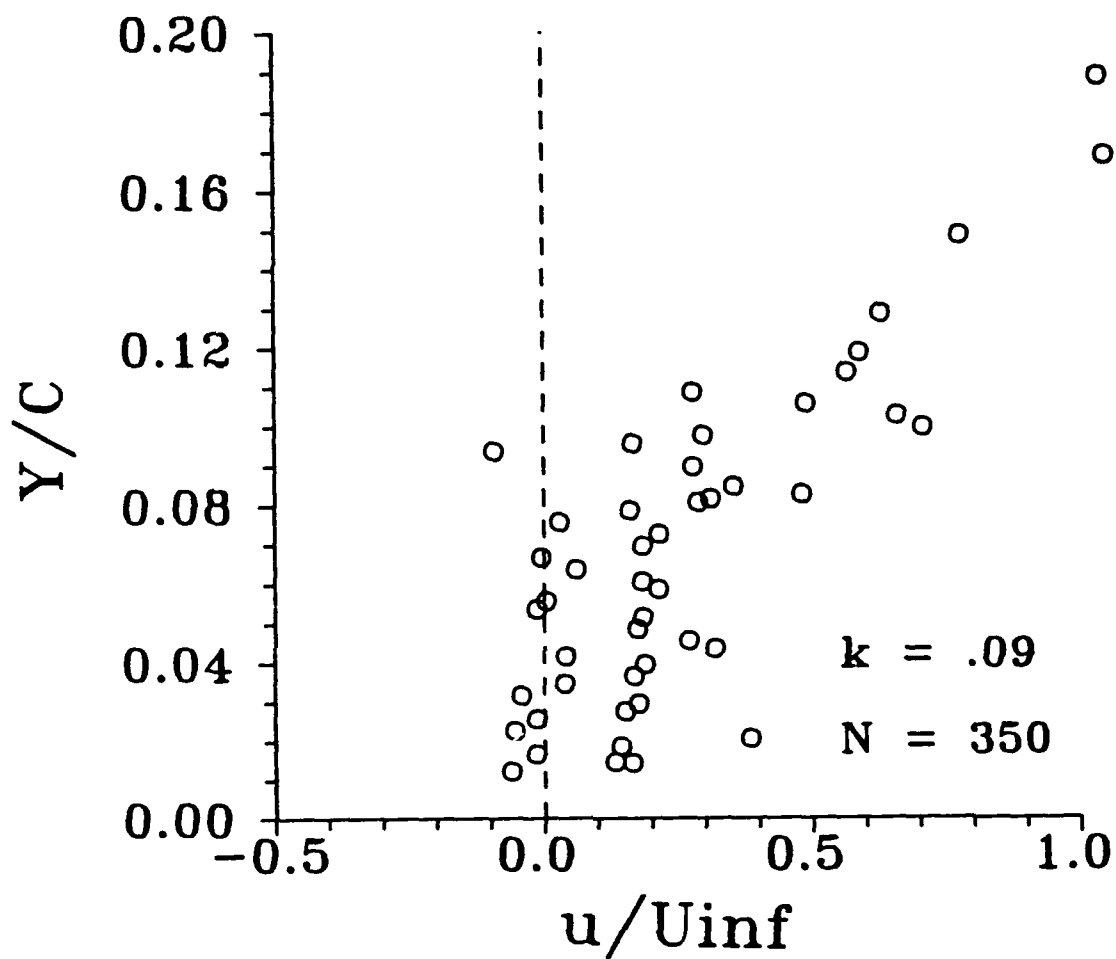
Figure 43.    Ensemble Average Profile, Imposed
             Periodic Disturbance (3 Hz), 70%
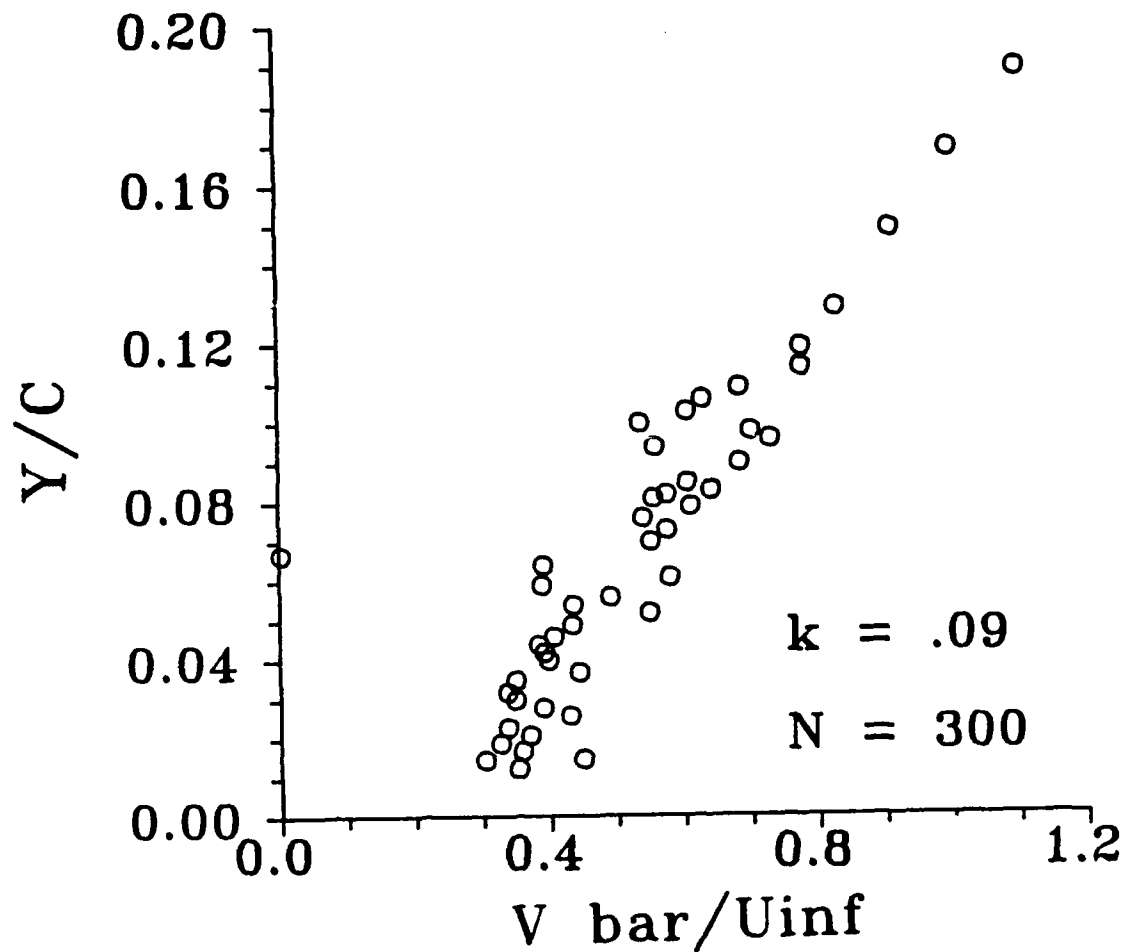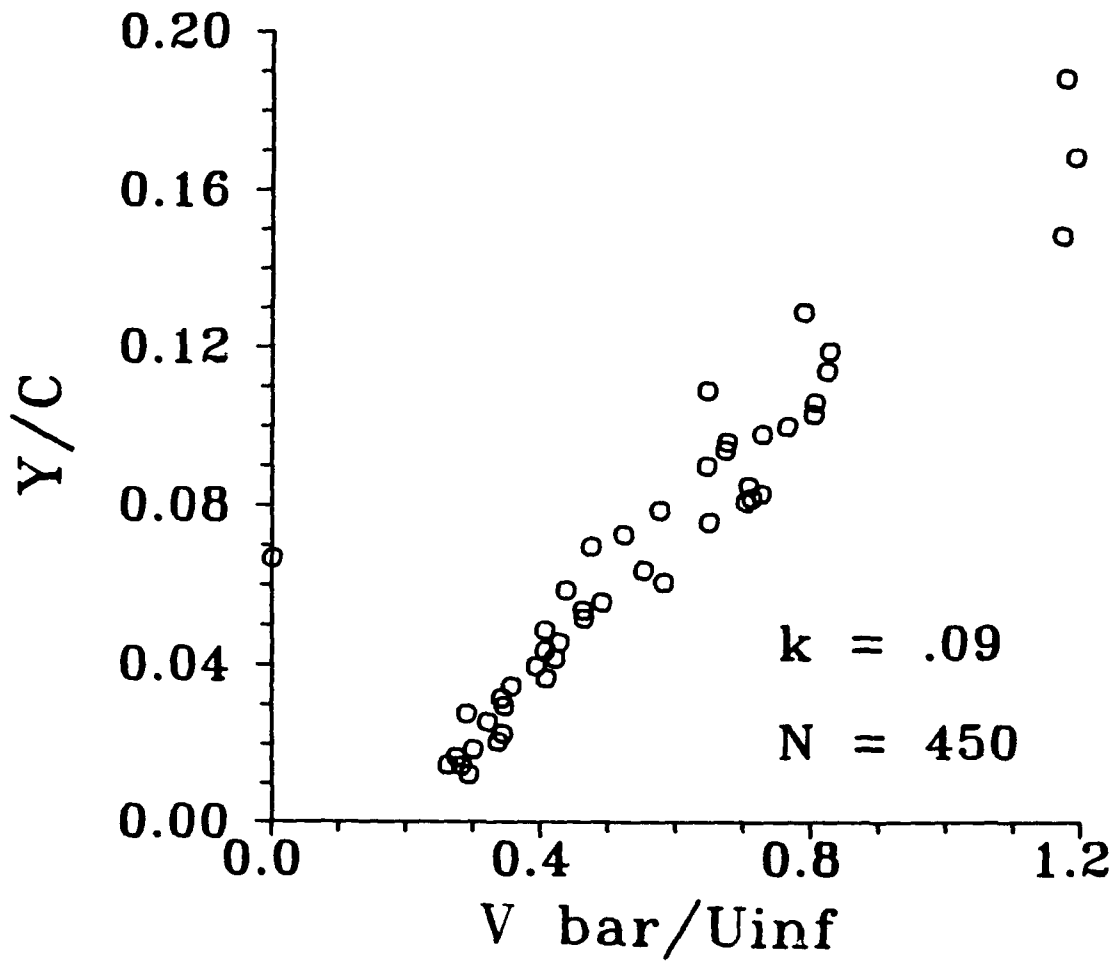             Chord, 22° Angle of Attack
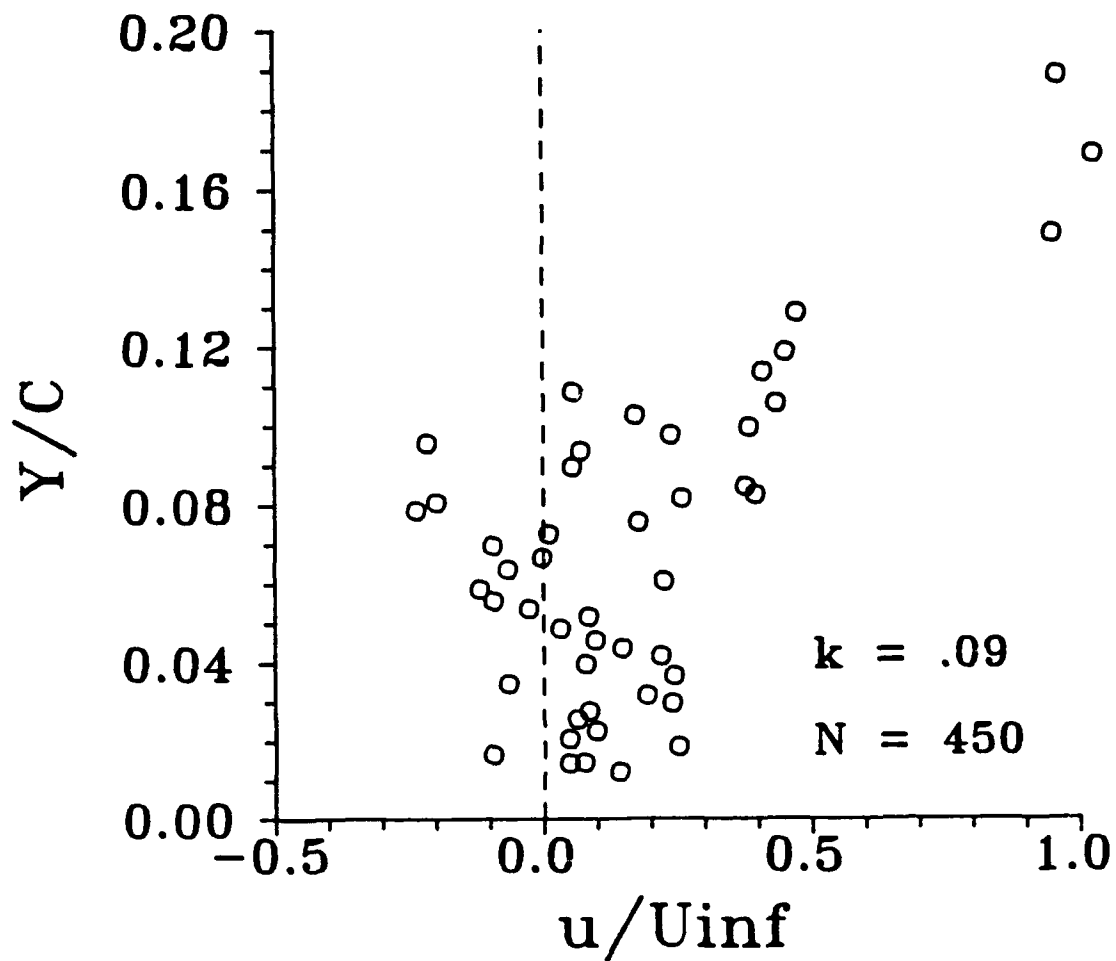
Figure 44.    Ensemble Average Profile, Imposed
              Periodic Disturbance (3 Hz), 70%
              Chord, 22° Angle of Attack
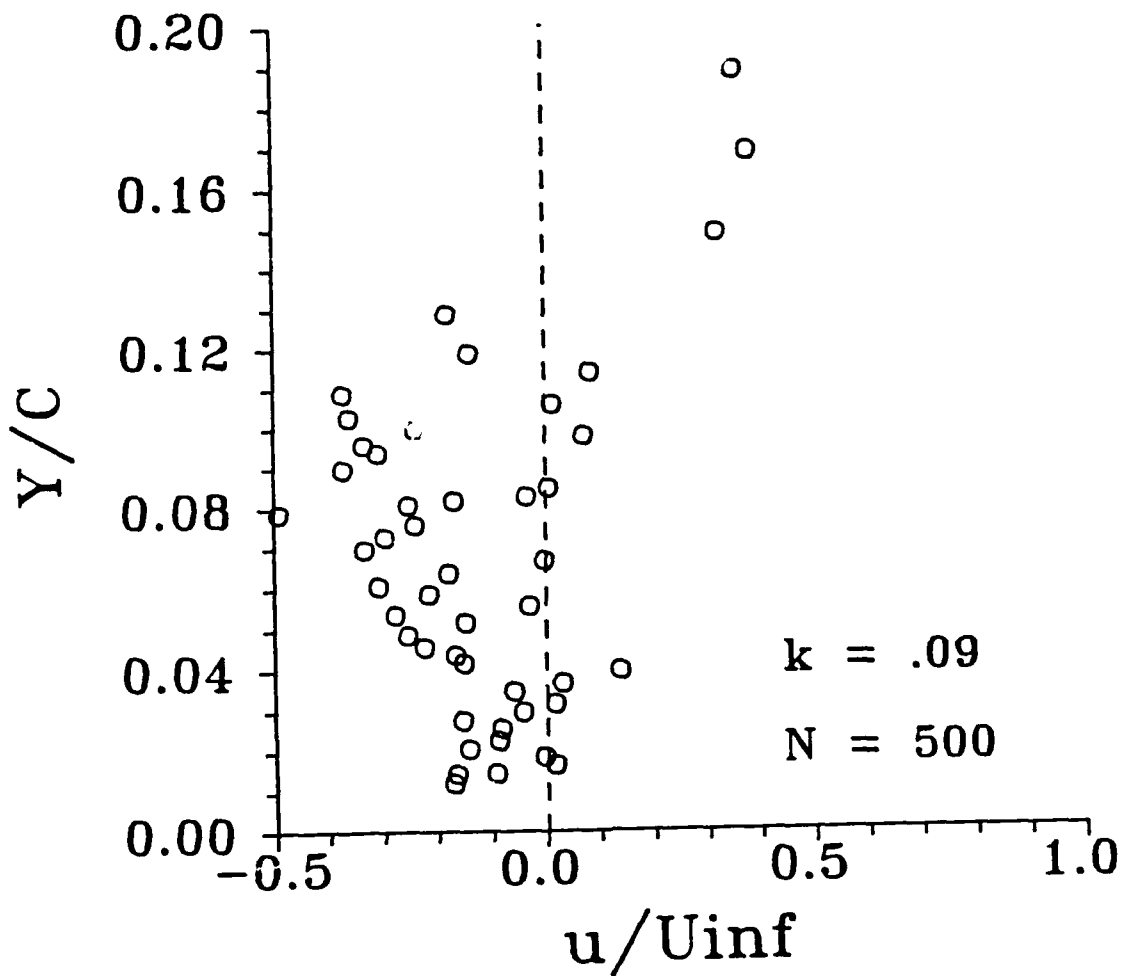
Figure 45. Ensemble Average Profile, Imposed
Periodic Disturbance (3 Hz), 70%
Chord, 22° Angle of Attack
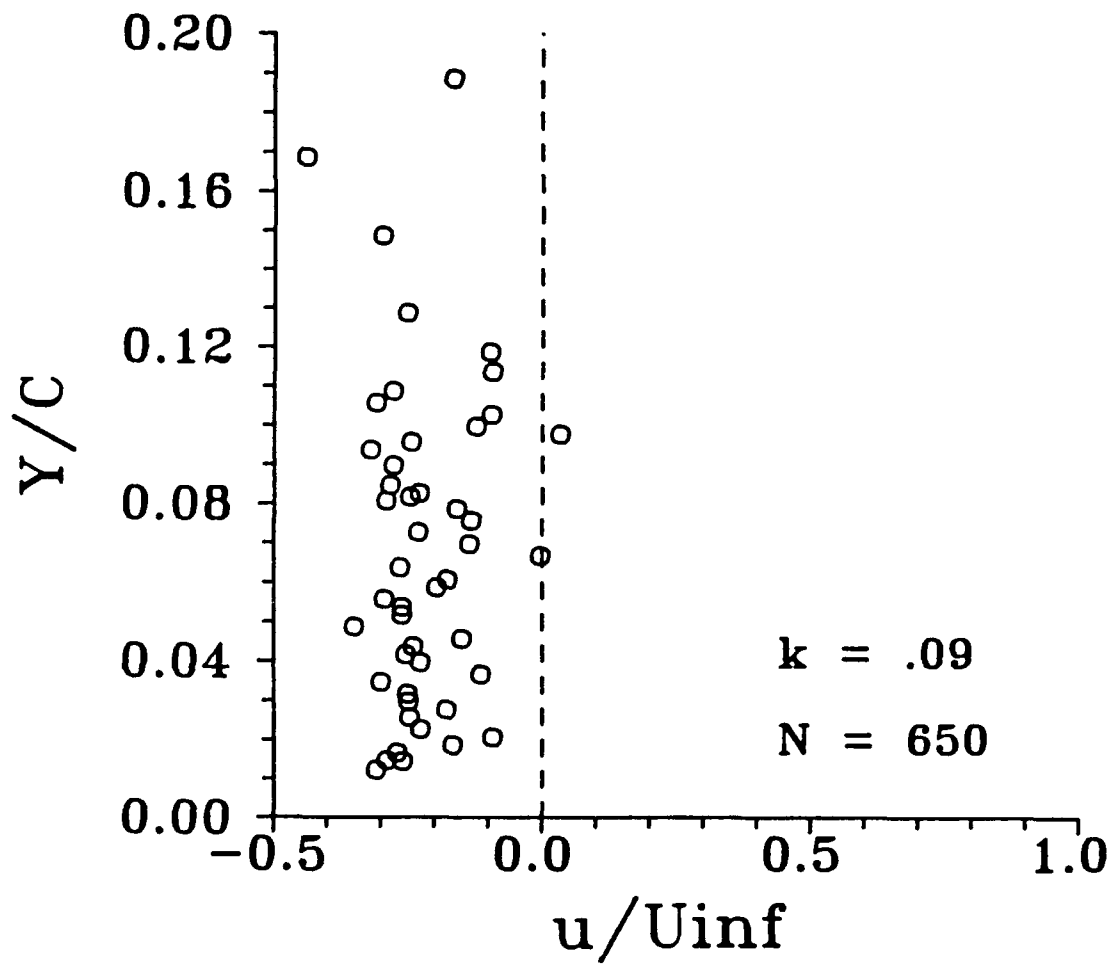
Figure 46.   Ensemble Average Profile, Imposed
Periodic Disturbance (3 Hz), 70%
Chord, 22° Angle of Attack

Figure 47.   Ensemble Average Profile, Imposed
             Periodic Disturbance (3 Hz), 70%
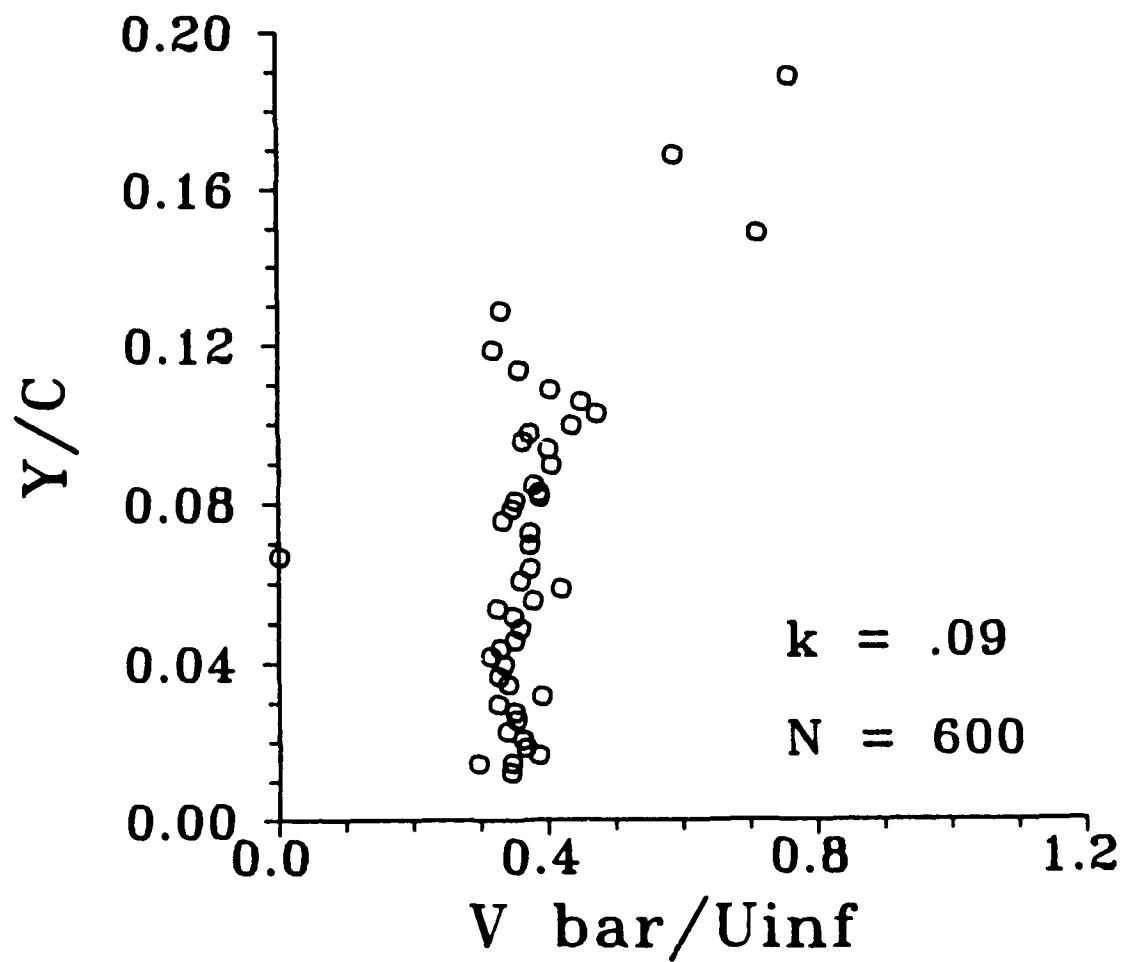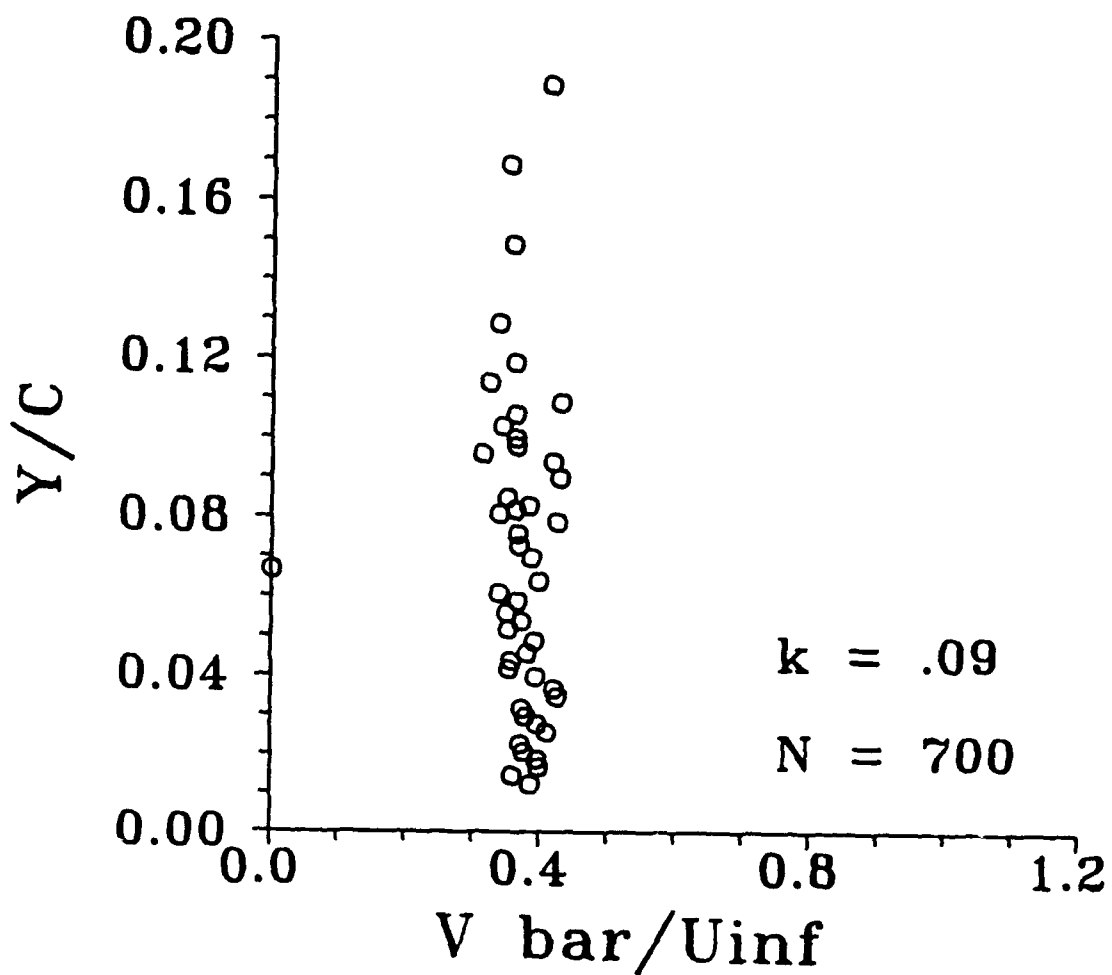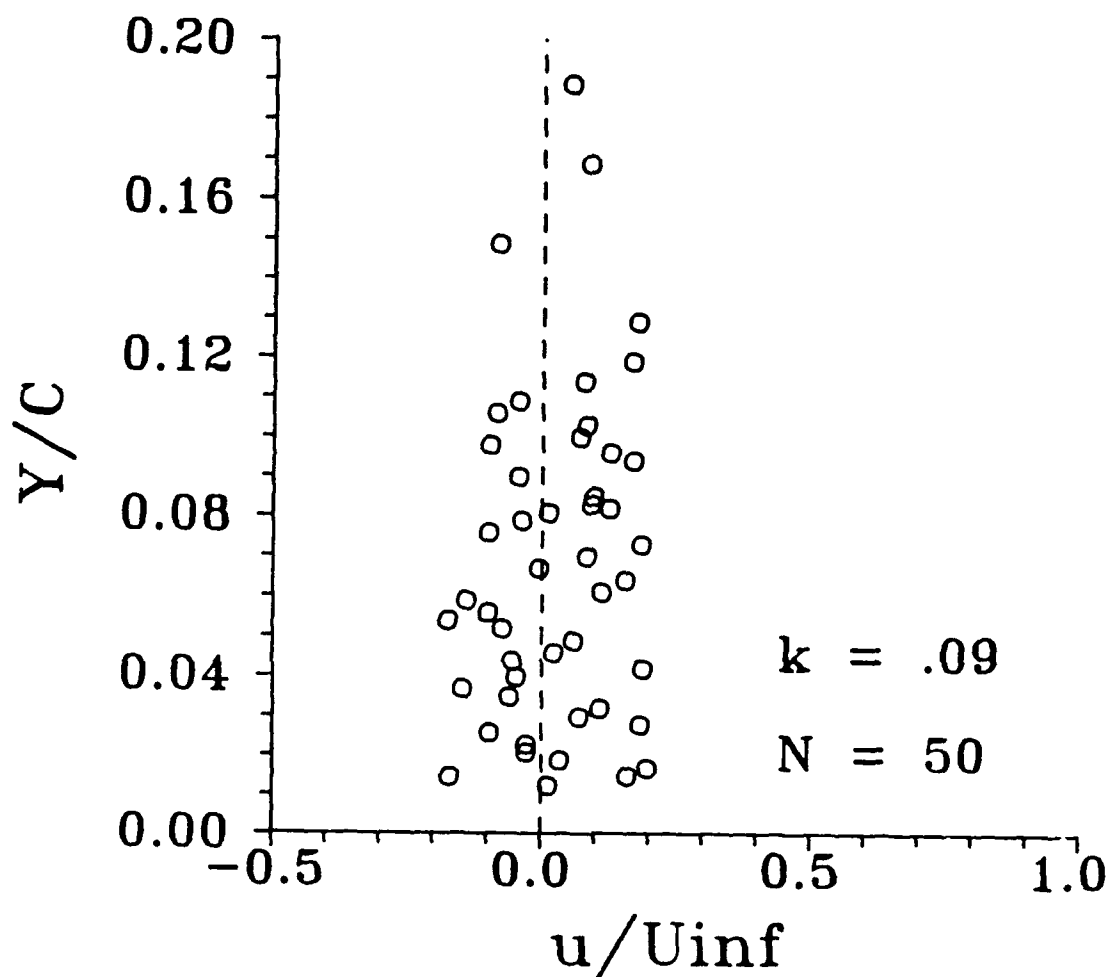             Chord, 22° Angle of Attack

90
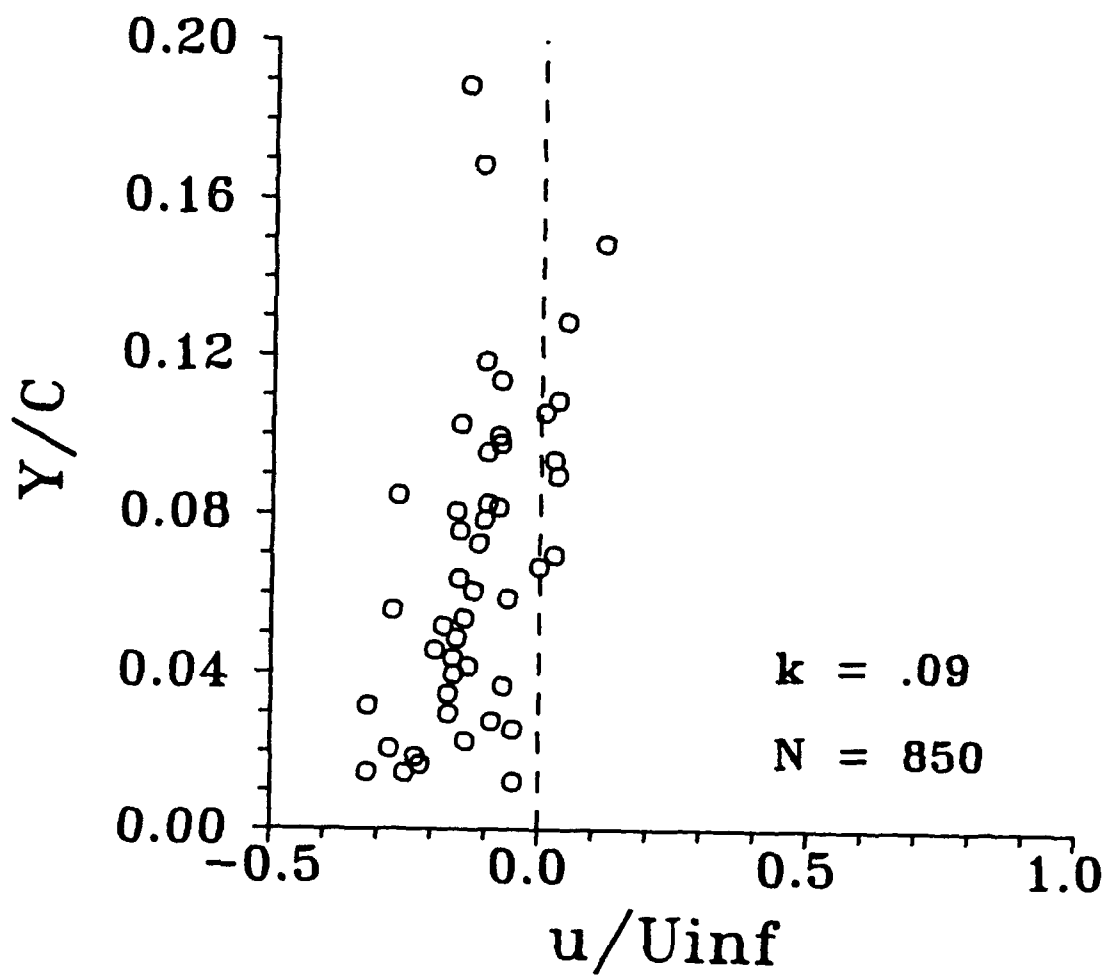
Figure 48.    Ensemble Average Profile, Imposed
Periodic Disturbance (3 Hz), 70%
Chord, 22° Angle of Attack
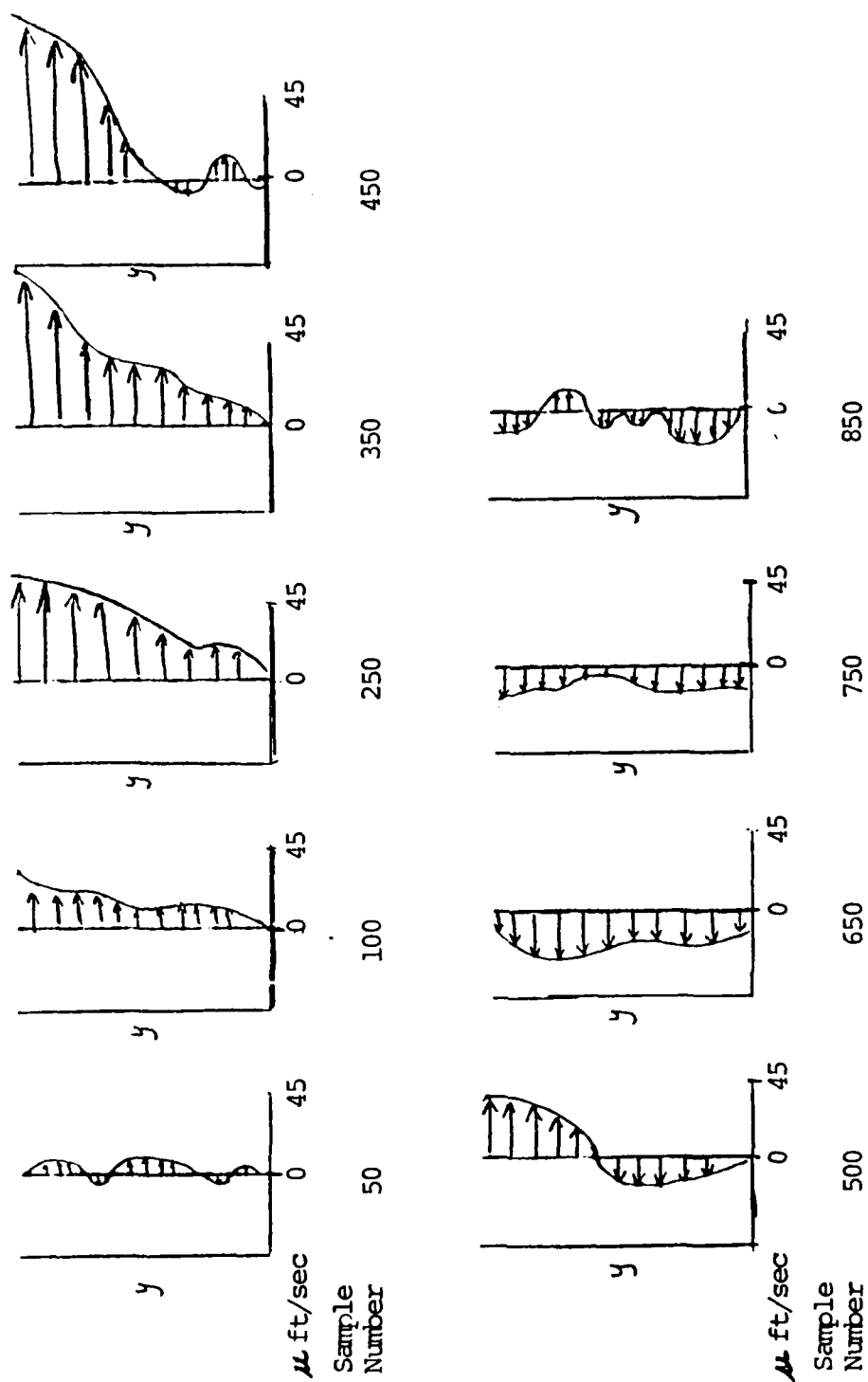
Figure 49. Summary of Ensemble Average Profiles, k = .09

attached flow [Ref. 9]. In the turbulent region of the airfoil, Renoud found that the passage of the pulse did not merely return the flow to its undisturbed, turbulent state; he found that there was a recovery period the effect of which was to laminarize flow. This could be analogous to what is being shown in these velocity profiles. The undisturbed case of sample 50 is altered by the pulse and is stabilized. However, before returning to the undisturbed case the flow reversal is actually intensified to greater than its undisturbed value (analogous to how Renoud's flow was laminarized to a greater extent then its undisturbed level). The author realizes that this analogy is a loose one since Renoud was studying a different type of flow; however, it is still an important observation.

Another interesting aspect of these profiles is the distinction between the horizontal velocities at different heights. For all sample times except for those which look similar to the undisturbed case, the measurements taken above 1.2 inches indicate large positive streamwise flow. The most obvious observation associated with this is that the pulse is bringing the separated region down to a lower height (this was also indicated in the plots of $\bar{V}$). Also interesting to note is sample 450 where the change in velocity at 1.2 inches is very abrupt. This could be an indication of reversed flow near the surface and a massive shedding of flow at a forward portion of the airfoil.

Inspection of the total velocity time histories of Figure 50 shows that at a height of .1216 inches it is difficult to distinguish the effect of the pulse at any sample number. At a height of .6316 inches the effect of a pulse can be seen to be centered at sample 400. As height is increased the effect became much more pronounced.

Inspection of the horizontal velocity component histories (Figure 51) shows a similar pattern. It appears that the pulse is present between samples 100 and 500. This presence is indicated by an increase in velocity and may be a stabilizing influence which causes the flow to attach. From samples 500 to 800 the flow reversal returns and is more pronounced than the undisturbed region near sample 50.

Finally, the flow is returned to the undisturbed, separated flow region seen at the end and the beginning of each history. The reader should keep in mind that as many as 150 samples at the end of the cycle are not shown. During data reduction, pulse cycles which contained more data points than those of the shortest pulse cycle within the data run were truncated so that the pulses could be ensemble averaged together.

The original purpose of generating pulses with a reduced frequency of .09 was to document the effect, if any, that variation of reduced frequency had on separated flow. The differences between the results of this case and those of the .47 reduced frequency case are major. Somehow the slower

94
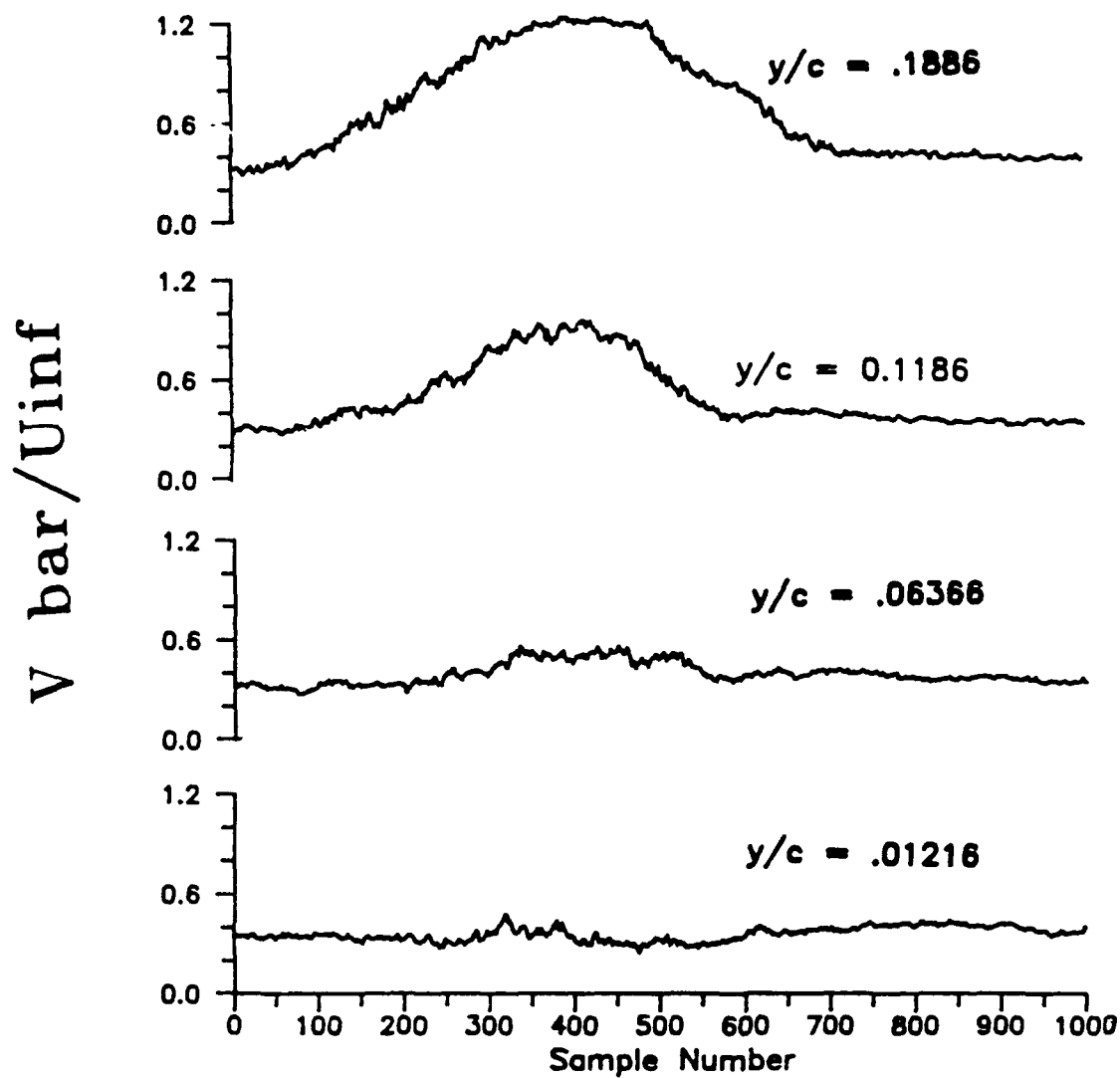
Figure 50.    Total Velocity Time Histories
(AOA = 22°,  k = .09)
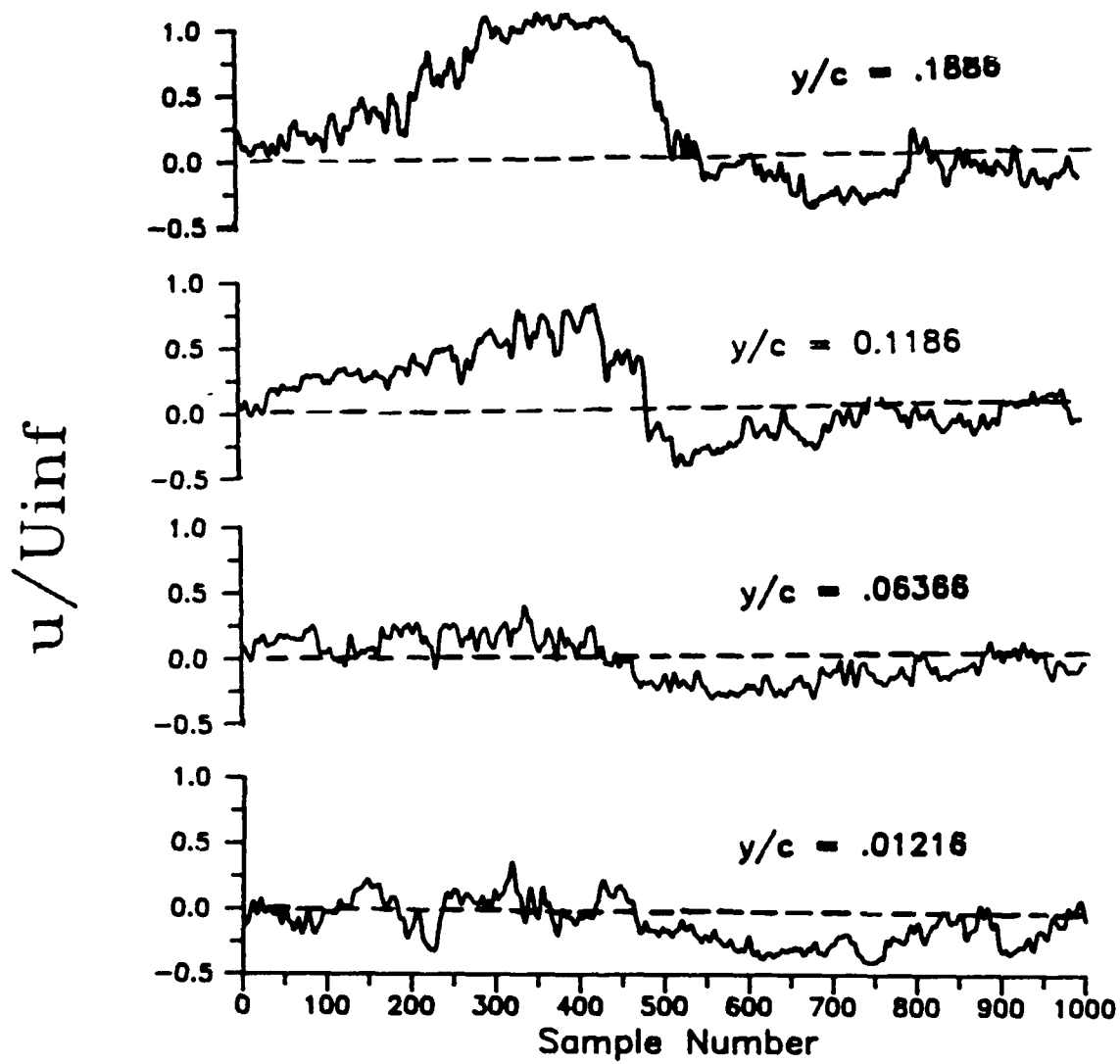
Figure 51.   Streamwise Velocity Time Histories
             (AOA = 22°, k = .09)

generation of pulses makes the flow response quite sensitive to the pulse influence. Perhaps the time constant associated with the high frequency pulses was too large for the separated boundary layer to respond. Or perhaps the reduced frequency of .47 used in this investigation was at some "critical" value which in some way caused the effects to be masked by the separated flow. Because only one chord location was investigated these speculations are of a preliminary nature. An understanding of the mechanics of the undisturbed separated flow, based on measurement of various chord and possibly span locations will be required to arrive at more definitive conclusions.

3.   <u>12 Degrees Angle of Attack, k = .47</u>

The total velocity profiles shown in Figures 52 and 53 and the streamwise velocity profiles shown in Figures 54 to 56, as well as the total velocity time history of Figure 57 indicate that under the influence of a turbulent periodic pulse the flow was at no time approaching separation. This discovery was surprising as the flow visualization photograph (see Figure 9) indicated that the 12 degrees angle of attack condition consisted of flow near separation.

Either the flow visualization gave a false indication of such a condition in the undisturbed case, or the periodic disturbance caused the flow to become more attached rather than separated. The first explanation is unlikely given the success that flow visualization had in demonstrating

97

Figure 52.   Ensemble Average Profile, Imposed
Periodic Disturbance (17 Hz), 70%
Chord Location

98
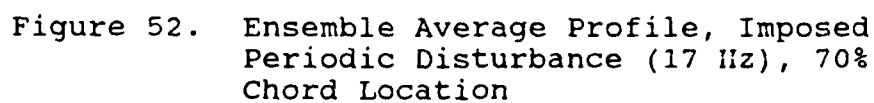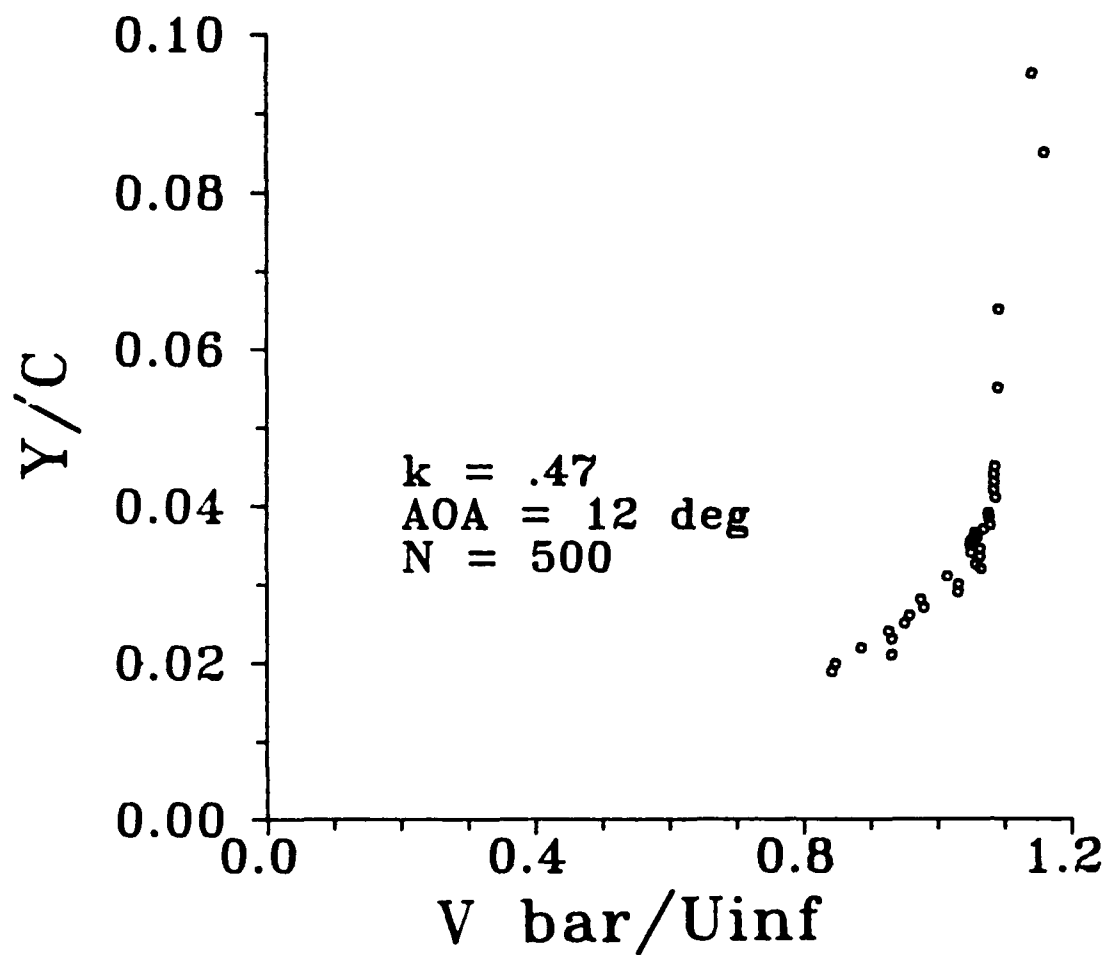
Figure 53. Ensemble Average Profile, Imposed
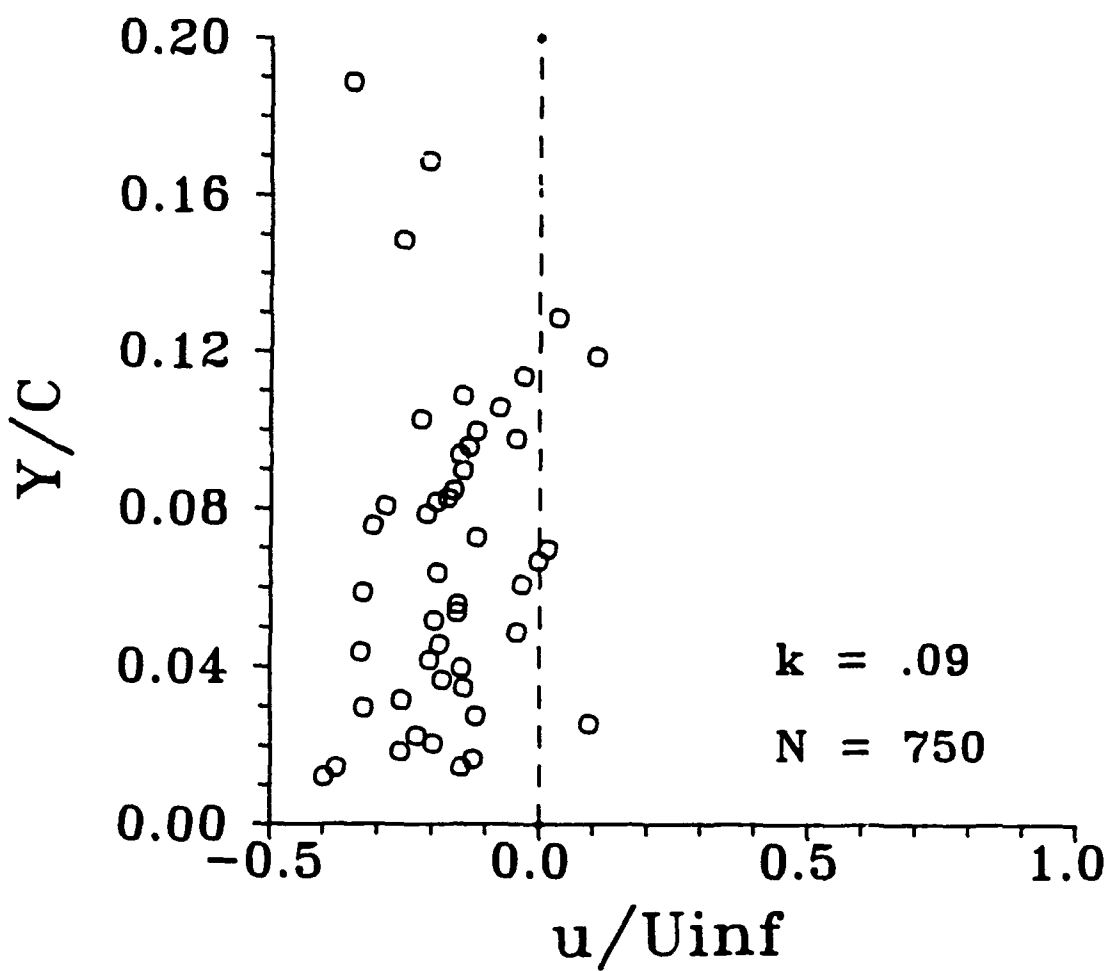Periodic Disturbance (17 Hz),
70% Chord Location
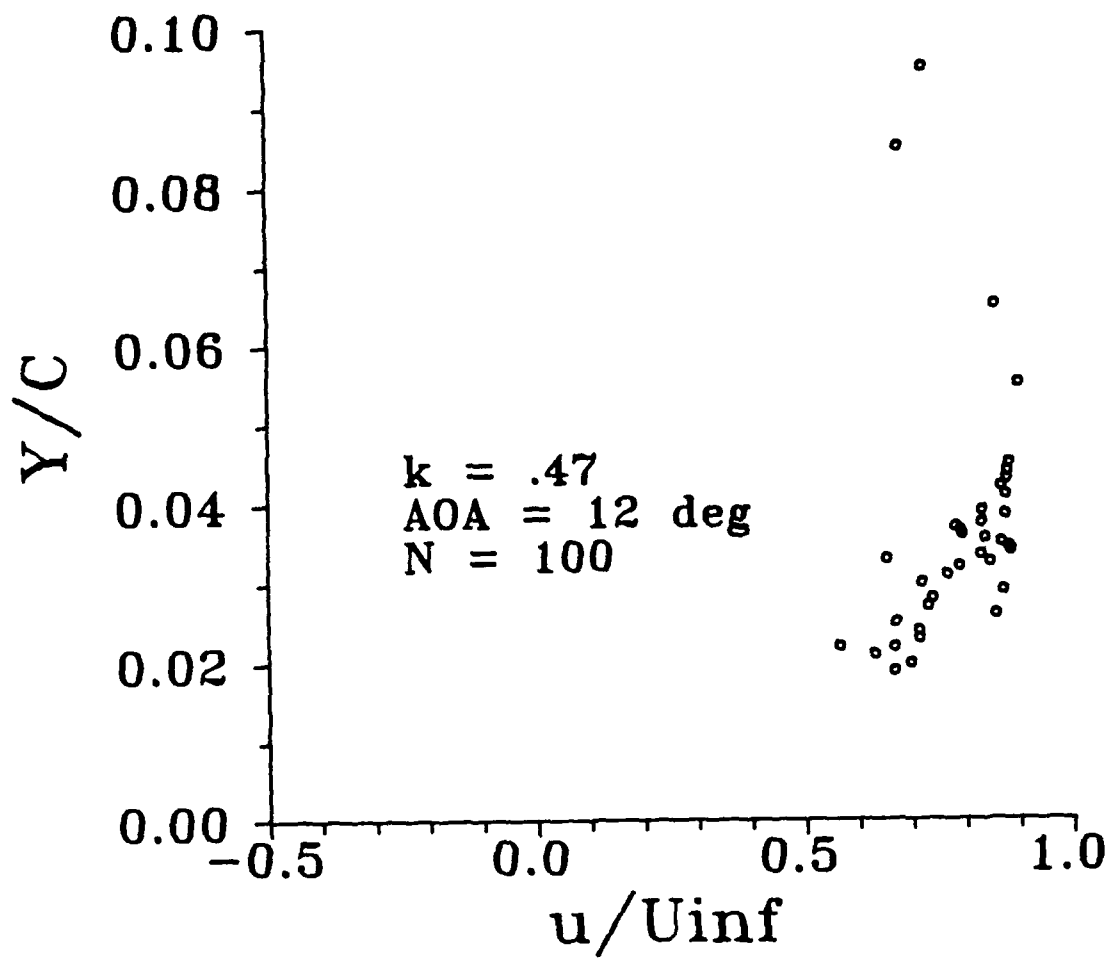
Figure 54. Ensemble Average Profile, Imposed
Periodic Disturbance (17 Hz),
70% Chord Location
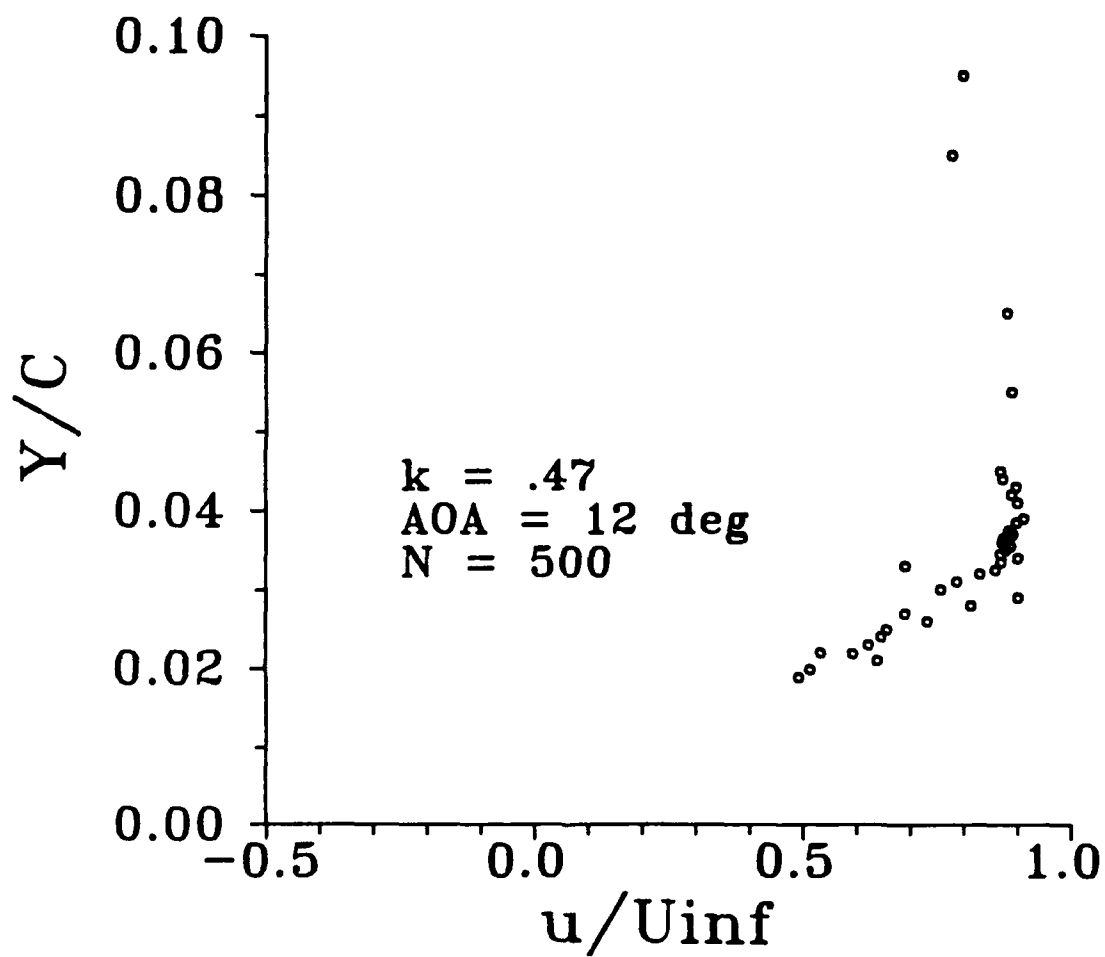
Figure 55.   Ensemble Average Profile, Imposed
             Periodic Disturbance (17 Hz),
             70% Chord Location

101
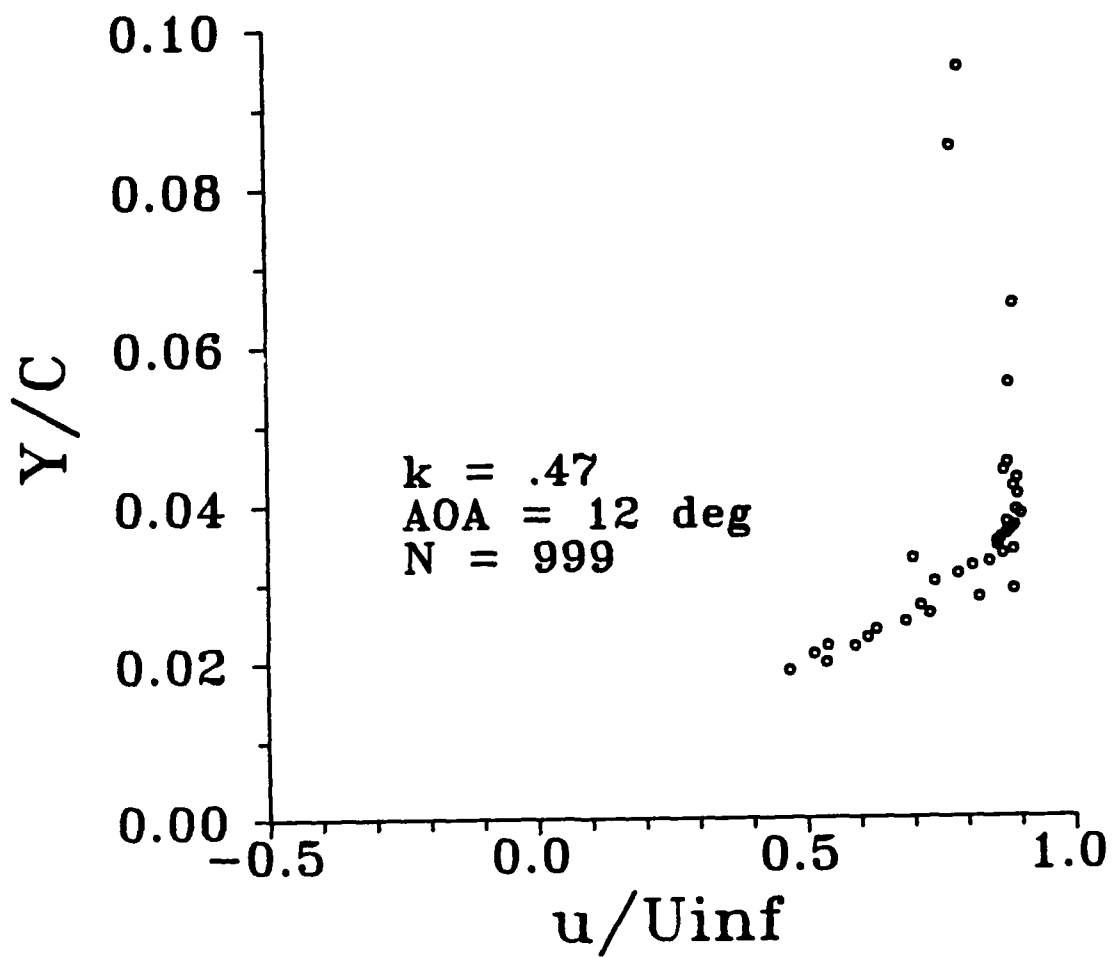
Figure 56.    Ensemble Average Profile, Imposed
              Periodic Disturbance (17 Hz),
              70% Chord Location
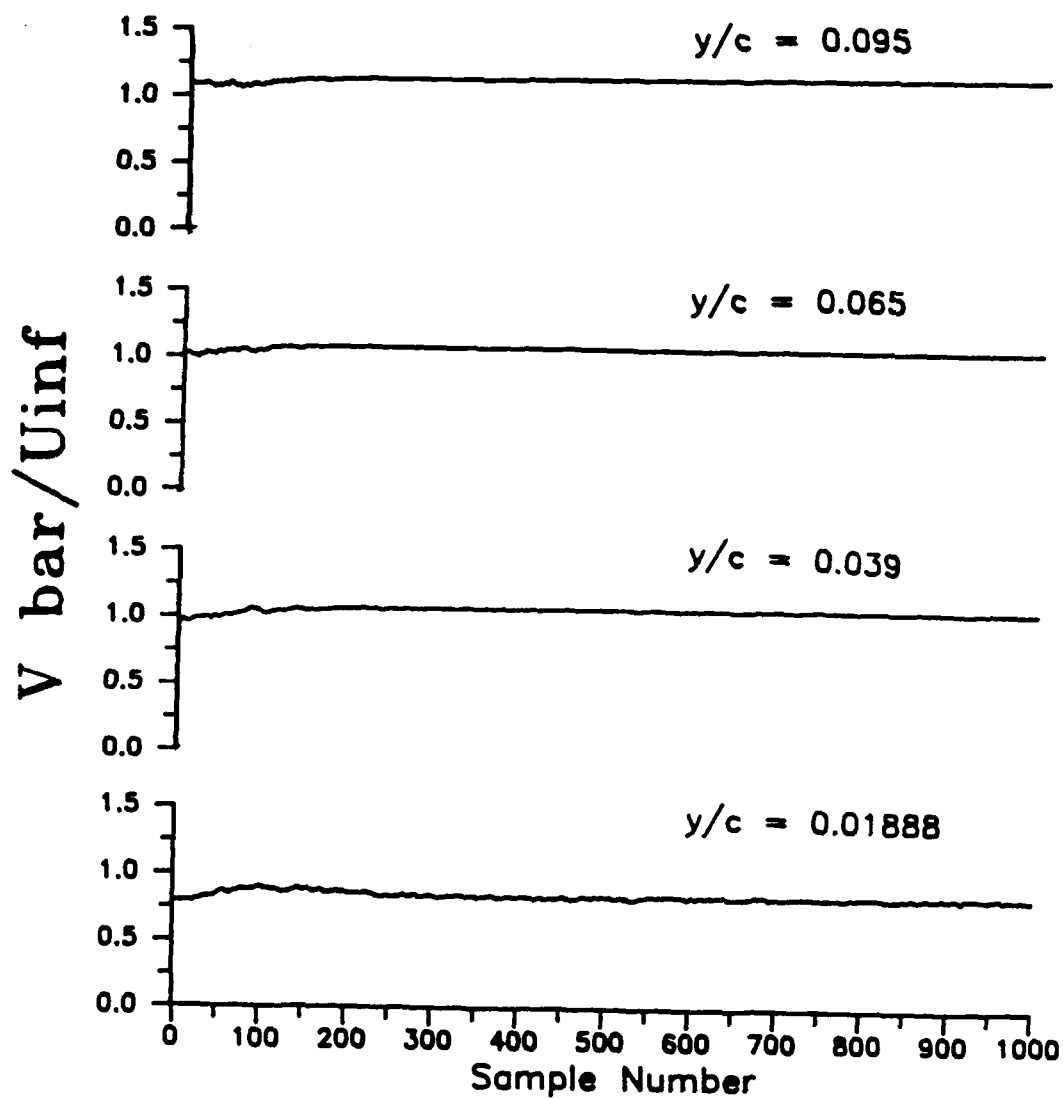
Figure 57.    Total Velocity Time Histories,
AOA = 22°, k = .47

separation at the 22 degree angle of attack and the fact that wings of similar dimensions are close to stall at 12 degrees. Perhaps at low angles of attack, pulses of high enough frequencies cause the flow to attach. Unfortunately, there were no non-pulse runs made at this angle of attack for comparison. The lack of any significant flow variation during the passage of the pulse cycle is not surprising, considering that such effects were not noticed in the 22 degree angle of attack case either. These two cases support the notion that as the disturbance frequencies increase the influence of the pulse is diminished. As previously discussed, an abstract hypothetical model for this phenomenon could be that the pulses, when produced at such a frequency where the time between them is low enough, act as a "steady" stream of turbulence.

While the velocity profiles show no outward evidence of a periodic disturbance, their time histories do (see Figures 57 and 58). The slight velocity deficit at about the 50th sample of the cycle indicates the presence of a periodic disturbance imposed on the attached flow. It is important to realize that the typical pulse has well over 1100 samples so that the time histories, which in this thesis include only 1000 samples may not include a significant portion of the pulse. The fact that the velocity deficit exists means that the pulse is noticed, while the presence of highly attached flow indicates that a separating effect is minimal or

104
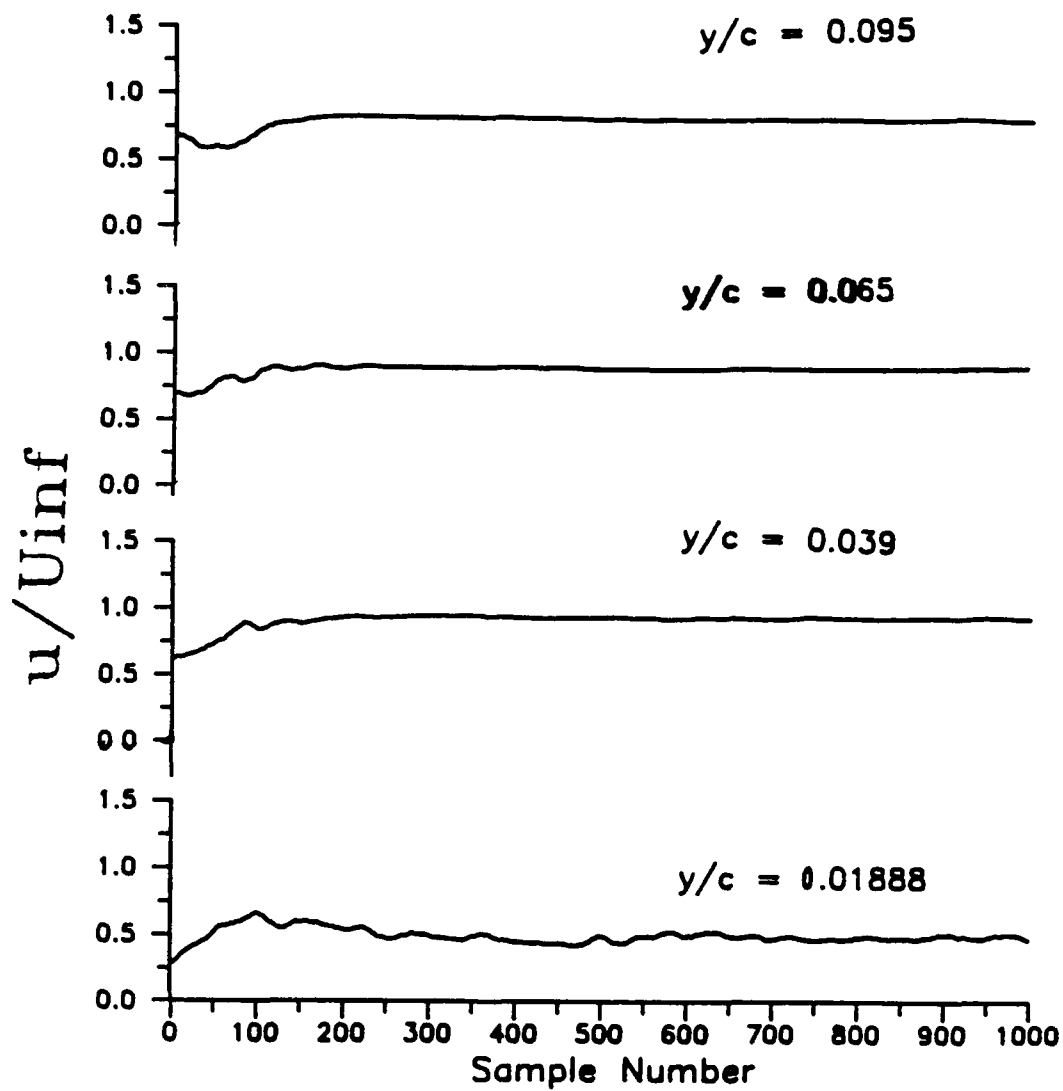
Figure 58.   Streamwise Velocity Time Histories,
             AOA = 22°, k = .47

105

nonexistant.  In fact, the possibility of a stabilizing effect

cannot be discounted.

# V. CONCLUSIONS

The response of a separating boundary layer of a wing to periodically-varying turbulent disturbances in the mean flow (Reynolds Number of about 500,000) was investigated.

The results indicate a pronounced response only to those disturbances of certain reduced frequencies. In general, the separating boundary layer (22 degrees AOA) was much more sensitive to those disturbances generated at a reduced frequency of .09 than it was to those of .47. These conclusions were made by comparing both of the cases to one in which there were no imposed disturbances. It is proposed that as the reduced frequency of the pulse increases to a certain rate the changing nature of the disturbance becomes too rapid to elicit a discernible response by a separating boundary layer.

The response of the separating boundary layer brought about by the slower of the two reduced frequencies was complicated in its nature. The pulse initially caused the flow reversal of the undisturbed case to cease as it imparted energy in the positive streamwise direction and reduced the vertical distance of the separated region. Then, instead of just returning the flow to its undisturbed state, it intensified its reverse direction to a greater extent than in the undisturbed case. Finally, the flow returned to its

107

undisturbed form. This pattern (dealing with separation) is analogous to the relaminarization effect, which deals with transition, discovered by Renoud [Ref. 9].

The effect of periodic turbulence on flow thought to be near separation in its undisturbed state (12 degrees angle of attack) could not be fully determined because an undisturbed, mean flow analysis was not done. However, the discovery that under the influence of such a disturbance the flow was at all times attached and far from separation showed that the induced turbulence had little or no separating affect or may have had a stabilizing effect.

# VI.  RECOMMENDATIONS

This study attempted to determine the effect a periodic disturbance has on flows near or at separation. All attention was focused at one chord location (70 percent) of a single airfoil. The turbulent disturbance frequencies were used to document the response of a separating boundary layer to reduced frequency variation. A second angle of attack of lower value then the first was used to investigate the possibility that periodic turbulence could induce separation in a flow which was not quite separated.

The investigation demonstrated that periodic turbulence of a reduced frequency of .09 has a strong influence on the flow, while disturbances of reduced frequency .47 had no discernible effect. While the study strongly suggests that higher frequency pulses have less of an effect on flow response than lower ones, the results do not constitute absolute proof that the $k = .47$ response had no effect. Had a small but significant effect existed, the lack of its detection could be the fault of some of the cruder aspects of the data collection process. As mentioned earlier, data collection was limited by the failure of the split-film anemometer to output two channels simultaneously. A sychronization mechanism was used which partially compensated for this inadequacy. However, since the flow velocity was a function of the square of both

split film voltages taken simultaneously, slight errors in the synchronization process could cause significant errors in the output.

The velocity direction was less reliable than the magnitude because of the manner in which it was obtained. The interpolation data (see Appendix E) used to find the direction of flow, based upon entering arguments of speed and the difference $(E_4^2 - E_3^2)$, had little resolution between the voltage values. A small error in the value obtained from the circuitry for $E_3$ and/or $E_4$ could easily cause an incorrect angle to be output. While the author can discern no better way to calculate the velocity direction, he strongly recommends that in the future the calibration data be taken by automated digital techniques over a short sample period and then averaged to give a single value. This method should be much better than the manual method used in which the resolution of each of the potentials ($E_3$ or $E_4$) were read to only plus or minus 0.01 volts. Using a digital calibration procedure and an anemometer circuit which outputs simultaneous split-film channels should provide an extremely accurate way to resolve both flow velocity magnitude and direction. In addition, it would provide the means to develop good time histories of the baseline, no pulse case. These histories would aid greatly in the study of the effects of imposed disturbances.

Well after data collection was completed, the author was informed by TSI Corporation of a way in which the IFA-100 system could be altered to accomplish simultaneous output. A follow-up of this idea could be beneficial to future investigations.

The patterns and trends detected in this study, which were evident in spite of data collection limitations, may well be in large part due to the large volume of data collected, the use of ensemble averaging, and the application of digital low pass filter smoothing. All of these aspects should be included if follow-up research is performed. Ensemble averaging is particularly important, and its implementation should include the use of more than the 17 pulses used here. To do so the simultaneous output just described must be implemented to save storage space and a high amount of RAM capacity must be secured (see problems concerning RAM in Chapter II). It is recommended to make dry runs using all equipment at some time just prior to actual data collection in order to ensure that the system is collecting the desired amount of data. Steps must be taken to limit the data collection time. If using LABTECH NOTEBOOK, RAM capacity must be sufficient to download all data during a single collection run.

Another goal of follow-up research could attempt to find the reasons why a lower frequency had a much stronger effect on flow than a higher one did. A first step could be to vary

the frequency over a continuous range and note at which value it had a discernible influence on the flow. Measurement of the undisturbed separated flow at 22 degrees angle of attack at more transverse, span, and chord locations will be needed to determine the mechanics of the unsteady flow response.

The extremely attached flow found on a 12 degree angle of attack airfoil at the 70 percent chord location was a surprising discovery. Was the periodic disturbance responsible for this or was the flow already attached? This investigation could not answer the question since there was no undisturbed baseline case available for comparison. Future work could document the same flow under freestream conditions for comparisons.

# APPENDIX A

## AIRFOIL COORDINATES

| UPPER | | LOWER | |
|---|---|---|---|
| x/c | y/c | x/c | y/c |
| 1.000 | .0000 | 1.000 | .0000 |
| .990 | .0008 | .990 | -.0002 |
| .980 | .0015 | .980 | -.0005 |
| .970 | .0022 | .970 | -.0008 |
| .960 | .0030 | .960 | -.0010 |
| .950 | .0039 | .950 | -.0011 |
| .940 | .0050 | .940 | -.0011 |
| .930 | .0064 | .930 | -.0009 |
| .920 | .0080 | .920 | -.0007 |
| .910 | .0100 | .910 | -.0003 |
| .900 | .0121 | .900 | .0000 |
| .890 | .0142 | .890 | .0006 |
| .850 | .0220 | .880 | .0010 |
| .800 | .0310 | .850 | .0023 |
| .750 | .0400 | .800 | .0042 |
| .700 | .0483 | .750 | .0056 |
| .650 | .0561 | .700 | .0066 |
| .600 | .0635 | .650 | .0071 |
| .550 | .0704 | .600 | .0072 |
| .500 | .0766 | .550 | .0067 |
| .450 | .0816 | .540 | .0065 |
| .400 | .0858 | .530 | .0063 |
| .350 | .0894 | .520 | .0061 |
| .300 | .0918 | .510 | .0059 |
| .250 | .0927 | .500 | .0056 |
| .240 | .0926 | .490 | .0053 |
| .230 | .0923 | .480 | .0050 |
| .220 | .0919 | .470 | .0047 |
| .210 | .0914 | .460 | .0044 |
| .200 | .0907 | .450 | .0040 |
| .190 | .0900 | .440 | .0036 |
| .180 | .0888 | .430 | .0031 |
| .170 | .0876 | .420 | .0027 |
| .160 | .0862 | .410 | .0022 |
| .155 | .0854 | .400 | .0018 |
| .150 | .0846 | .390 | .0013 |
| .145 | .0837 | .380 | .0009 |
| .140 | .0828 | .370 | .0004 |
| .135 | .0818 | .360 | .0000 |
| .130 | .0808 | .340 | -.0008 |
| .125 | .0797 | .320 | -.0015 |
| .120 | .0785 | .300 | -.0020 |
| .115 | .0773 | .280 | -.0025 |
| .110 | .0760 | .260 | -.0029 |
| .105 | .0746 | .240 | -.0032 |
| .100 | .0731 | .220 | -.0034 |

| | | | |
|---|---|---|---|
| .095 | .0716 | .210 | -.0035 |
| .090 | .0700 | .200 | -.0034 |
| .085 | .0684 | .180 | -.0033 |
| .080 | .0666 | .150 | -.0030 |
| .075 | .0647 | .100 | -.0016 |
| .070 | .0628 | .080 | -.0008 |
| .060 | .0585 | .060 | -.0000 |
| .050 | .0537 | .050 | .0002 |
| .040 | .0481 | .040 | .0003 |
| .030 | .0415 | .030 | .0000 |
| .020 | .0335 | .025 | -.0002 |
| .015 | .0286 | .020 | -.0008 |
| .010 | .0233 | .015 | -.0016 |
| .005 | .0169 | .010 | -.0008 |
| | | .005 | .0020 |

## PROGRAM CONVERTS.FOR

```
      PROGRAM CONVERTS
C********************************************************************
CTHIS PROGRAM CONVERTS VOLTAGES TAKEN FROM TWO DIFFERENT
CDATA FILES INTO VELOCITY SPEED AND DIRECTION BASED ON KING'S
CLAW.  VOLTAGE E3 IS READ FROM ONE DATA FILE WHILE E4 IS
CREAD FROM THE OTHER.  WHEN THE SPINNING ROD IS AT A
CCERTAIN POSITION, A THIRD VOLTAGE RECIEVED FROM A MAGNETIC
CTRANSDUCER PEAKS.  THIS PROGRAM CONVERTS THE ANALOG PEAKING
COF THIS VOLTAGE INTO A DISCRETE DIGITAL SIGNAL.  THE
CSIGNAL MARKS THE BEGINNING OF A PULSE.  E3 AND E4 ARE
CCONVERTED INTO SPEED.  THE SUBROUTINE INTERP IS CALLED
CTO DETERMINE FLOW DIRECTION.  INTERP SCANS THE CALIBRATION
CTABLE CAL.DAT (LOADED AT THE BEGINNING OF THE PROGRAM) WITH
CENTERING ARGUMENTS OF SPEED AND THE DIFFERENCE BETWEEN E3
CSQUARED AND E4 SQUARED. IF THE ENTERING ARGUMENTS DO NOT
CFIT ON THE CORRECT LINE IN THE INTERPOLATION TABLE, VALUES OF
CPLUS OR MINUS 90 DEGREES ARE DETERMINED, DEPENDING ON THE
CCLOSEST CASE.  THE FLOW DIRECTION IS THEN HANDED BACK TO THE
CMAIN PROGRAM AND THE PULSES ARE SUPERIMPOSED ON ONE ANOTHER TO
CFORM ONE ENSEMBLE AVERAGE PULSE, WHICH IS WRITTEN TO AN OUTPUT
CFILE.
C********************************************************************
C
$DEBUG
$STORAGE:2
REAL E3,E4,DAT,THETA,SPEED,DIR
INTEGER CHOICE,K,LIMIT,SAMPLES,BADDAT
      CHARACTER*14 AINFILE,BINFILE,OUTFILE
      DIMENSION DAT(2000,2),VEL(14),ANG(19),VOLTS(14,19)
      OPEN(2,FILE='C:CAL.DAT')

DO 10 I=1,14
      READ (2,*)VEL(I)
10CONTINUE

      DO 20 I=1,19
      READ (2,*)ANG(I)
20    CONTINUE

      DO 30 I=1,14
      READ (2,*)(VOLTS(I,J),J=1,19)
```

```
30CONTINUE

      CLOSE(2)

5SPEED=0.0
THETA=0.0
SAMPLE=0
BADDAT=0
DIR=0.0
      WRITE(*,*)'ENTER THE FILE CONTAINING '
WRITE(*,*)'CHANNEL THREE DATA'
READ(*,'(a)')AINFILE
C
WRITE(*,*)'ENTER THE NAME OF THE FILE CONTAINING'
WRITE(*,*)'CHANNEL FOUR VOLTAGE DATA'
READ(*,'(A)')BINFILE

WRITE(*,*)'ENTER THE OUTPUT DATA FILE NAME'
READ(*,'(A)')OUTFILE
C
OPEN(10,FILE=AINFILE,STATUS='OLD')
OPEN(11,FILE=OUTFILE,STATUS='NEW')

DO 40 J=1,2000
    READ(10,*,END=50,ERR=50)DAT(J,1)
40CONTINUE
50CONTINUE
C
CLOSE (10)
C
OPEN(12,FILE=BINFILE,STATUS='OLD')
C
DO 60 K=1,2000
      READ(12,*,END=150,ERR=150)DAT(K,2)
60CONTINUE
150CONTINUE

IF (J .LT. K) THEN
    LIMIT=J
      ELSE
    LIMIT=K
ENDIF

DO 70 I=1,LIMIT-1
HOLDER=DAT(I,1)
DAT(I,1)=((DAT(I,1)**2+DAT(I,2)**2-3.47)/1.441)**2
DAT(I,2)=(DAT(I,2)**2-HOLDER**2)
CALL INTERP(DAT(I,1),DAT(I,2),THETA,VEL,VOLTS,ANG)
IF (THETA .EQ. 90.0 .OR. THETA .EQ. -90.0)THEN
          BADDAT=BADDAT+1
      ELSE
          SAMPLES=SAMPLES+1
          SPEED=SPEED+DAT(I,1)
          DIR=DIR+THETA
```

```
70CONTINUE
C
SPEED=SPEED/(94.75*SAMPLES)
THETA=DIR/SAMPLES
C
WRITE(11,80) SPEED,THETA
WRITE(*,*)'SPEED IS',SPEED
WRITE(*,*)'THETA IS',THETA
SAMPLES=SAMPLES+BADDAT
WRITE(*,*)BADDAT,'BAD SAMPLES OUT OF',SAMPLES
CLOSE(12)
CLOSE(11)
WRITE(*,*)'TYPE (1) FOR ANOTHER RUN, (2) TO ESCAPE'
READ(*,*)CHOICE
        IF (CHOICE .EQ. 1)GOTO 5
STOP
END
C
SUBROUTINE INTERP(VI,EI,THETA,VEL,VOLTS,ANG)
REAL VI,EI,NEWVOL(19),SPACE,VOLTS(14,19),ANG(19),VEL(14),THETA
INTEGER M,N,ROW,COL
M=14
N=19
C
DO 99 I=1,M
IF (VEL(I) .LE. VI) ROW=I
99CONTINUE
C
11SPACE=(VI-VEL(ROW))/(VEL(ROW+1)-VEL(ROW))
C
DO 110 J=1,N
NEWVOL(J)=SPACE*(VOLTS(ROW+1,J)-VOLTS(ROW,J))+VOLTS(ROW,J)
110      CONTINUE
DO 120 J=1,N
    IF ( NEWVOL(J).LE. EI) COL=J
120      CONTINUE
IF(COL .EQ. N .OR. NEWVOL(COL+1) .LE.NEWVOL(COL))THEN
    THETA=ANG(COL)
  ELSE
THETA=ANG(COL)+((EI-NEWVOL(COL))/(NEWVOL(COL+1)-NEWVOL(COL)))*
     +    10
ENDIF
IF(EI .LE.NEWVOL(1)) THETA=-90
RETURN
END
```

# APPENDIX C

## PROGRAM PROPCONV.FOR

```
C     THIS PROGRAM IS USED TO CONVERT THE SPLIT-FILM VOLTAGES
C     ASSOCIATED WITH THE IFA-100 ANEMOMETER SYSTEM INTO FLOW
C     SPEED AND DIRECTION.  DATA IS READ FROM TWO DIFFERENT INPUT
C     FILES AND SYCHRONIZED.  WHEN THE SPINNING ROD IS AT A CERTAIN
C     POSITION,THE VOLTAGE RECIEVED FROM A MAGNETIC TRANSDUCER PEAKS.
C     THIS PROGRAM CONVERTS THE ANALOG PEAKING OF THE VOLTAGE INTO A
C     DISCRETE DIGITAL SIGNAL.  THESE  SIGNALS FROM THE THIRD COLUMN
C          OF TWO DATA FILES ARE USED TO MATCH THE PERIODS OF THE
C     PULSE CYCLE.  PULSE CYCLES WHICH LAST LONGER THAN THE SHORTEST
C          ONE YET ENCOUNTERED ARE TRUNCATED.  ALL DATA IS STORED IN
C     ASCII INTEGER FORM ON DISK. IT IS CONVERTED INTO REAL NUMBERS
C      AND THEN, USING KING'S LAW, IS CONVERTED INTO FLOW SPEED.
C     THE VALUE OF E3 COMES FROM ONE DATA FILE WHILE E4 COMES FROM
C     THE OTHER INPUT FILE. THE SYNCHRONIZATION PROCESS ENSURES THAT
C     THE INDIVUAL VALUES FOR THESE VARIABLES REPRESENT THE EXACT
C          SAME POINT IN THIER RESPECTIVE PULSE CYCLES. FOLLOWING THIS
C     THE SUBROUTINE INTERP IS THEN CALLED TO DETERMINE FLOW
C     DIRECTION.  THE CALIBRATION TABLE CAL.DAT, READ AT THE BEGINING
C     OF THE PROGRAM, IS SCANNED BY INTERP WITH THE ARGUMENTS
C     OF FLOW SPEED AND THE DIFFERENCE BETWEEN THE SQUARED VOLTAGES
C     E3 AND E4).  IF THE ENTERING ARGUMENTS DO NOT FIT ON THE
C     SAME LINE IN THE INTERPOLATION TABLE, VALUES OF PLUS OR MINUS
C     90 DEGREES ARE DETERMINED, DEPENDING ON THE CLOSEST CASE.
C     THE FLOW DIRECTION IS THEN HANDED BACK TO THE MAIN PROGRAM
C     AND THE PULSES ARE SUPERIMPOSED ON ONE ANOTHER TO FORM ONE
C          ENSEMBLE AVERAGED PULSE, WHICH IS WRITTEN TO AN OUTPUT FILE.
C************************************************************************
C
$DEBUG
$STORAGE:2
          REAL BULL,PREVA,PREVC,FLAGC,FLAGA,DATP,MATP
          INTEGER COUNT,PULSE,I,J,CHOICE,PMIN,PMAX,PASS
          CHARACTER*14 AINFILE,BINFILE,OUTFILE,DINFILE,CINFILE
          DIMENSION PAT(2000,2),VEL(14),ANG(19),VOLTS(14,19)
          DIMENSION SUM(2000,2)
               PREV=0.0
               PULSE=0
               COUNT=0
               PMAX=1
               PMIN=10000

      OPEN(2,FILE='C:SECOND')
      DO 10 I=1,14
          READ(2,*)VEL(I)
```

```
10      CONTINUE

        DO 20 I=1,19
          READ (2,*)ANG(I)
20      CONTINUE

        DO 30 I=1,14
            READ (2,*)(VOLTS(I,J),J=1,19)
30   CONTINUE
        CLOSE(2)

        WRITE(*,*)'ENTER THE OUTPUT FILE NAME'
                READ(*,'(a)')OUTFILE
        WRITE(*,*)'ENTER FIRST CHANNEL 3 INPUT FILE'
                READ(*,'(A)')AINFILE
        WRITE(*,*)'ENTER NEXT CHANNEL 3 INPUT FILE'
                READ(*,'(A)')CINFILE
        WRITE(*,*)'ENTER THE FIRST CHANNEL 4 INPUT FILE'
                READ(*,'(A)')BINFILE
        WRITE(*,*)'ENTER THE NEXT CHANNEL 4 INPUT FILE'
                READ(*,'(A)')DINFILE

        OPEN(10,FILE=AINFILE,STATUS='OLD')
        OPEN(13,FILE=OUTFILE,STATUS='NEW')
        OPEN(12,FILE=BINFILE,STATUS='OLD')

40      READ(10,*,END=90)DATP,BULL,FLAGA
      datp=(datp*5.)/4095.
      flaga=(flaga*5.)/4095.
          TIC=0.0
          IF(FLAGA.GT.1.0 .AND. FLAGA .LT. PREVA .AND.(COUNT .GT.
     +    100 .OR. COUNT.EQ.0))TIC=2.0
          PREVA=FLAGA
          FLAGA=TIC
          IF (FLAGA .NE. 2.0)GOTO 40

50      READ(12,*,END=90)BULL,MATP,FLAGC
      matp=(matp*5.)/4095.
      flagc=(flagc*5.)/4095.
          CIC=0.0
          IF(FLAGC.GT.1.0 .AND. FLAGC .LT. PREVC .AND.(COUNT .GT.
     +    100 .OR. COUNT.EQ.0))CIC=2.0
          PREVC=FLAGC
          FLAGC=CIC
          IF (FLAGC .NE. 2.0)GOTO 50

55      VI=((DATP**2 + MATP**2 -4.48)/1.325)**2
        EI=MATP**2-DATP**2
        PULSE=PULSE+1
        COUNT=COUNT+1
        CALL INTERP(VI,EI,THETA,VEL,VOLTS,ANG)
        PAT(COUNT,1)=VI
        PAT(COUNT,2)=THETA

60      READ(10,*,END=89)DATP,BULL,FLAGA
```

```
            datp=(datp*5.)/4095.
            flaga=(flaga*5.)/4095.
                  TIC=0.0
                  IF(FLAGA.GT.1.0 .AND. FLAGA .LT. PREVA .AND.(COUNT .GT.
            +     100 .OR. COUNT.EQ.0))TIC=2.0
                  PREVA=FLAGA
                  FLAGA=TIC
                  IF (FLAGA .EQ. 2.0)GOTO 70

               READ(12,*,END=89)BULL,MATP,FLAGC
            matp=(matp*5.)/4095.
            flagc=(flagc*5.)/4095.
                  CIC=0.0
                  IF(FLAGC.GT.1.0 .AND. FLAGC .LT. PREVC .AND.(COUNT .GT.
            +     100 .OR. COUNT.EQ.0))CIC=2.0
                  PREVC=FLAGC
                  FLAGC=CIC
                  IF (FLAGC .EQ. 2.0)GOTO 70
                  COUNT=COUNT+1
                  VI=((DATP**2 + MATP**2-4.48)/1.325)**2
                  EI=MATP**2-DATP**2
                  CALL INTERP(VI,EI,THETA,VEL,VOLTS,ANG)
                        PAT(COUNT,1)=VI
                        PAT(COUNT,2)=THETA
                        GOTO 60

      70                  IF (PMIN .GT. COUNT) PMIN=COUNT
                          IF (PMAX .LT. COUNT) PMAX=COUNT

                          DO 75 I=1,PMIN
                          SUM(I,1)=SUM(I,1)+PAT(I,1)
                          SUM(I,2)=SUM(I,2)+PAT(I,2)
      75      CONTINUE

                  COUNT=0
                  IF(FLAGA .EQ. 2.0) GOTO 50
      80      READ(10,*,END=90) DATP,BULL,FLAGA
            datp=(datp*5.)/4095.
            flaga=(flaga*5.)/4095.
                  TIC=0.0
                  IF(FLAGA.GT.1.0 .AND. FLAGA .LT. PREVA .AND.(COUNT .GT.
               +     100 .OR. COUNT.EQ.0))TIC=2.0
                  PREVA=FLAGA
                  FLAGA=TIC
                  IF (FLAGA .NE. 2.0) GOTO 80
                  GOTO 55

      89    PULSE=PULSE-1
      90        CLOSE (10)
                CLOSE (12)
            IF (PASS .GT. 0)GOTO 100
            OPEN(10,FILE=CINFILE,STATUS='OLD')
            OPEN(12,FILE=DINFILE,STATUS='OLD')
            COUNT=0
            PASS=1.0
```

```
      GOTO 40

100       DO 110 I=1,PMIN
          SUM (I,1)=SUM(I,1)/(PULSE*94.75)
          SUM (I,2)=SUM(I,2)/PULSE
          WRITE(13,*) SUM(I,1),SUM(I,2)
110       CONTINUE
          CLOSE (13)

          STOP
          END

          SUBROUTINE INTERP(VI,EI,THETA,VEL,VOLTS,ANG)
          REAL VI,EI,NEWVOL(19),SPACE,VOLTS(14,19),ANG(19),VEL(14)
     REAL THETA
          INTEGER M,N,ROW,COL
          M=14
          N=19
C
          DO 99 I=1,M
          IF (VEL(I) .LE. VI) ROW = I
99        CONTINUE
C
11        SPACE=(VI-VEL(ROW))/(VEL(ROW+1)-VEL(ROW  ))
C
          DO 110 J=1,N
          NEWVOL(J)=SPACE*(VOLTS(ROW+1,J)-VOLTS(ROW,J))+VOLTS(ROW  ,J)
110       CONTINUE

          DO 120 J=1,N
              IF (NEWVOL(J) .LE. EI) col=j
120       CONTINUE

          IF( COL .EQ. N .OR. NEWVOL(COL+1) .LE. NEWVOL(COL)) THEN
              THETA = ANG(COL)
          ELSE
         THETA=ANG(COL)+((EI-NEWVOL(COL))/(NEWVOL(COL+1)-newvol(col)))
     +    *10
          ENDIF

     IF(EI .LE. NEWVOL(1)) THETA=-90
          RETURN
          END
```
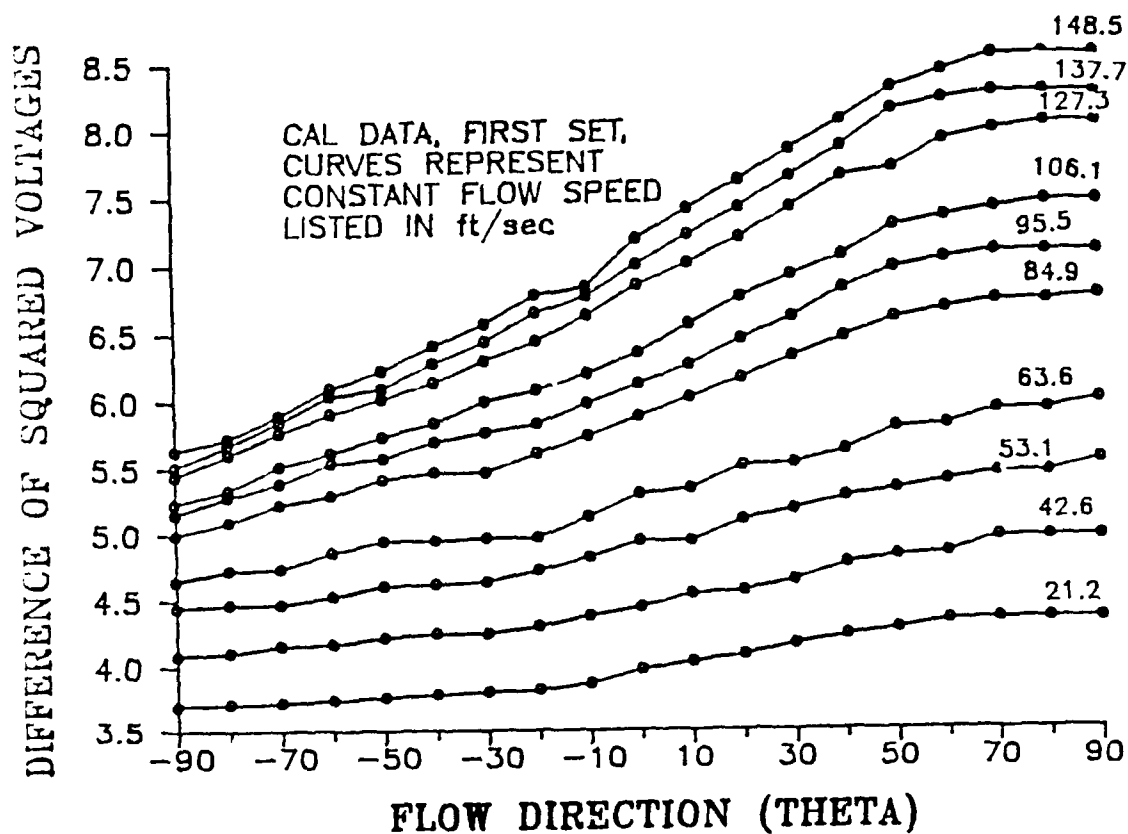
121

# APPENDIX D

## PROGRAM READIN.FOR

```fortran
      PROGRAM READIN
C*****************************************************************
C     THIS PROGRAM READS IN A CALIBRATION TABLE TO BE USED FOR THE
C     PROGRAMS CONVERTS.FOR AND PROPCONV.FOR.   THE USER IS ASKED
C     TO INPUT THE VELOCITY AND ANGLE VALUES USED DURING CALIBRATION.
C     IT THEN ASKS FOR VOLTAGE DATA, THE DIFFERENCES OF THE SQUARE
C     VOLTAGES E3 AND E4. THE CALDATA FILE NAME MUST BE ENCLOSED IN
C     QUOTES. EACH ROW OF VOLTAGE DATA SHOULD BE ON THE SAME LINE,
C     SEPARATED BY A SPACE, AND ENTER SHOULD NOT BE DEPRESSED
C     UNTIL THE ENTIRE LINE HAS BEEN TYPED. THE CALIBRATION TABLE
C     IS A 14 BY 19 ARRAY.
C*****************************************************************
C
      REAL DAT,VOLTS(19)
      CHARACTER*14 FNAME
      PRINT *, 'ENTER CALDATA FILENAME'
      READ(*,*) FNAME
      OPEN(2,FILE=FNAME)
      PRINT *,'ENTER VELOCITY DATA (14 VALUES)'
      DO 10 I=1,14
      READ *,DAT
      WRITE (2,*)DAT
10    CONTINUE
      PRINT *,'ENTER ANGLE DATA (19 VALUES)'
      DO 20 I=1,19
      READ *,DAT
      WRITE(2,*)DAT
20    CONTINUE
      PRINT*,'ENTER VOLTAGE DATA (19 VALUES)'
      DO 30 I=1,14
      READ *,(VOLTS(J),J=1,19)
      WRITE (2,*)(VOLTS(J),J=1,19)
30    CONTINUE
      CLOSE(2)
      STOP
      END
```
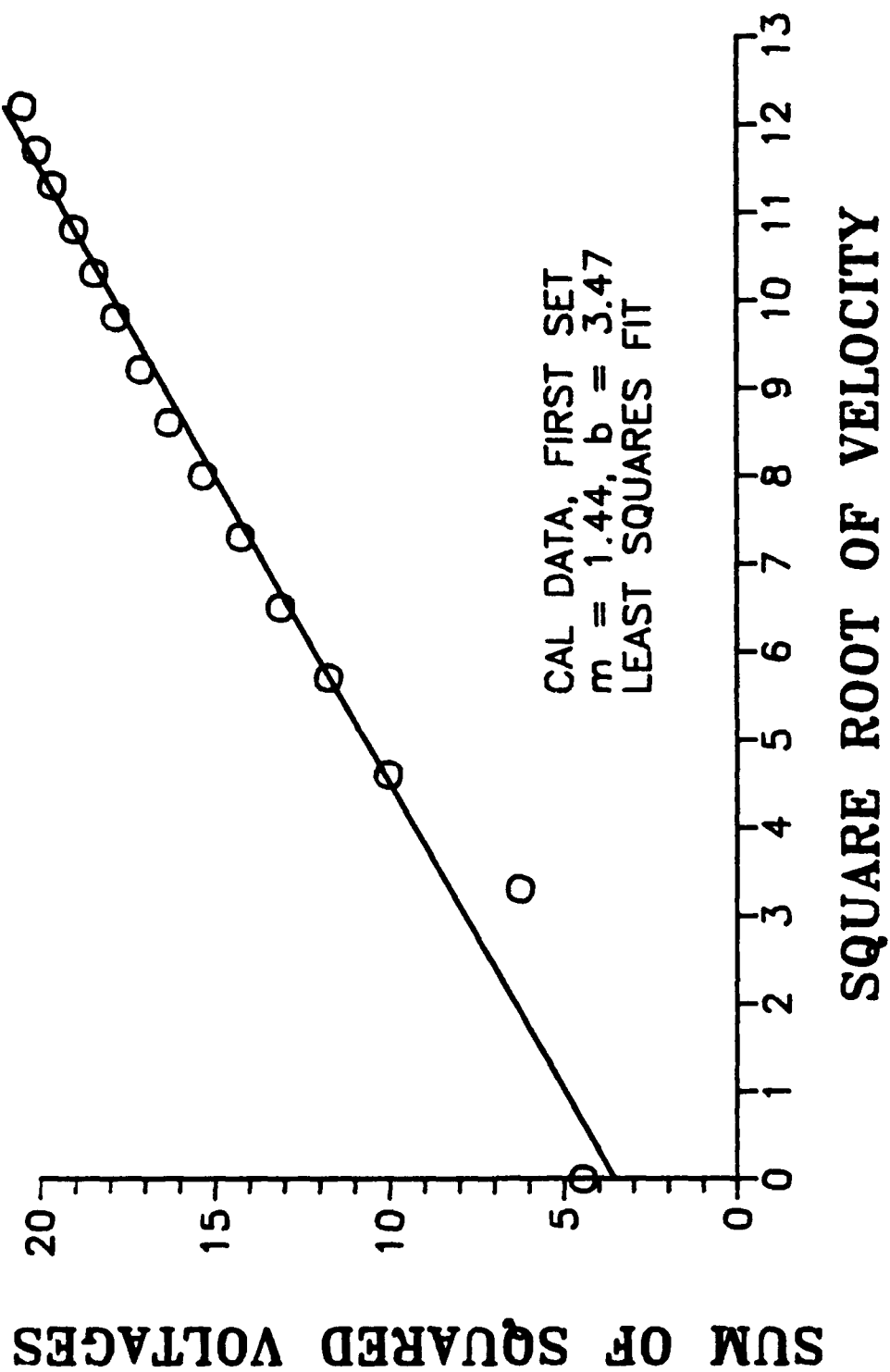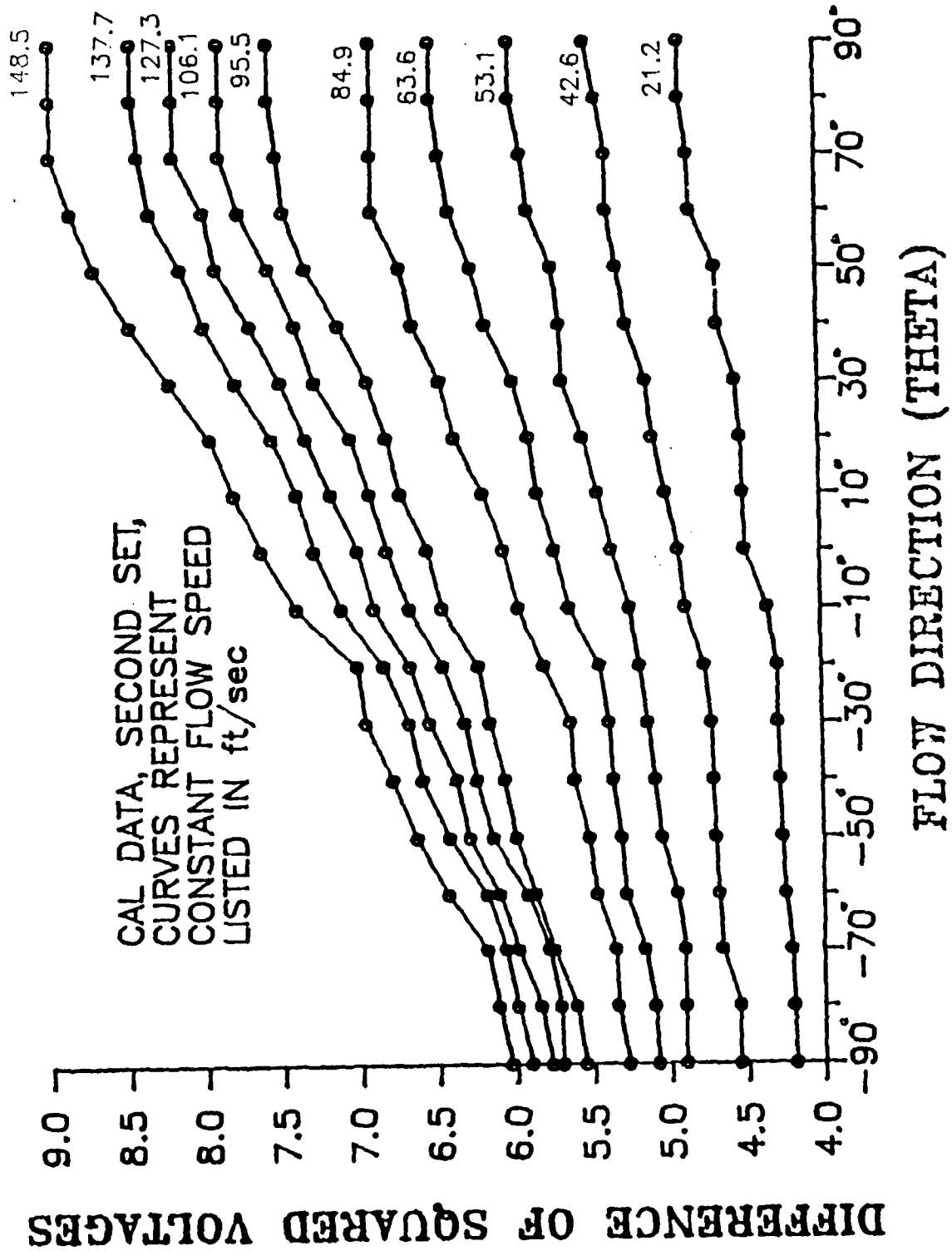
## CALIBRATION DATA

CAL DATA, FIRST SET
m = 1.44, b = 3.47
LEAST SQUARES FIT

SUM OF SQUARED VOLTAGES

SQUARE ROOT OF VELOCITY

CAL DATA, SECOND SET,
CURVES REPRESENT
CONSTANT FLOW SPEED
LISTED IN ft/sec

148.5
137.7
127.3
106.1
95.5
84.9
63.6
53.1
42.6
21.2

DIFFERENCE OF SQUARED VOLTAGES

9.0 8.5 8.0 7.5 7.0 6.5 6.0 5.5 5.0 4.5 4.0

FLOW DIRECTION (THETA)

-90° -70° -50° -30° -10° 10° 30° 50° 70° 90°

125

CAL DATA, SECOND SET
m = 1.33, b = 4.44
LEAST SQUARES FIT

SQUARE ROOT OF VELOCITY

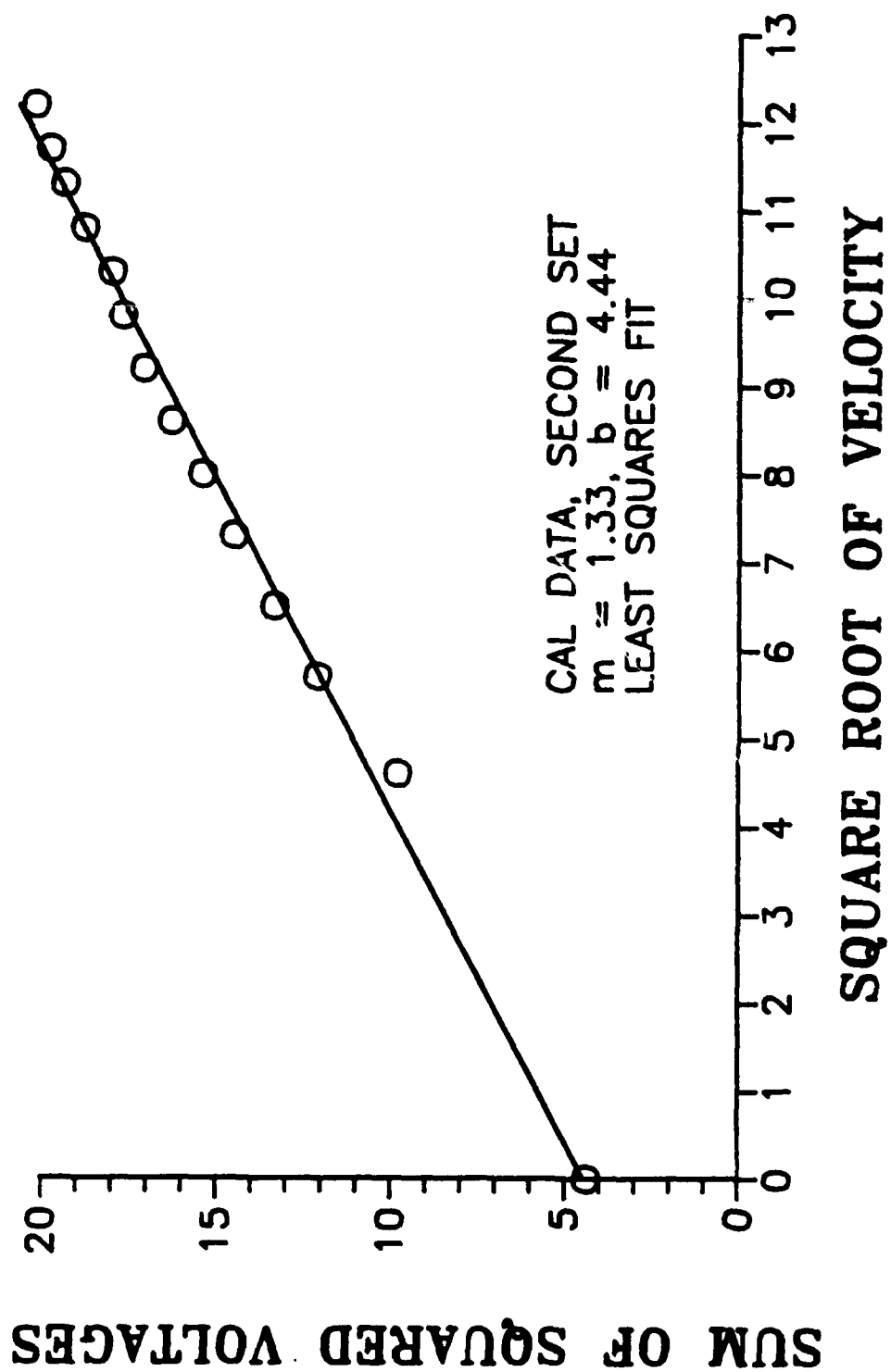SUM OF SQUARED VOLTAGES

# LIST OF REFERENCES

1. Meier, H.U., and Kreplin, H.P., "Influence of Freestream Turbulence on Boundary-Layer Development," *AIAA Journal*, Vol. 18, No. 7, pp. 11-15, January 1980.

2. National Aeronautics and Space Administration Final Report (NASA-CR-180638), "The Influence of Free-Stream Turbulence on Separation of Turbulent Boundary Layers in Incompressible, Two-Dimensional Flow," by J.L. Potter et al., pp. 1-42, 22 December 1986.

3. Kindelspire, D.W., *The Effects of Freestream Turbulence on Airfoil Boundary Layer Behavior at Low Reynolds Numbers*, Master's Thesis, Naval Postgraduate School, Monterey, California, September 1988.

4. Carr, L.W., "Progress in Analysis and Prediction of Dynamic Stall," *Journal of Aircraft*, Vol. 25, No. 1, pp. 6-17, January 1988.

5. Brendel, M., *Experimental Study of the Boundary Layer on a Low Reynolds Number Airfoil in Steady and Unsteady Flow*, Ph.D. Dissertation, University of Notre Dame, Notre Dame, Indiana, May 1986.

6. Miley, S.J., and Howard, R.M., and Holmes, B.J., "Wing Laminar Boundary Layer in the Presence of a Propeller Slipstream," *Journal of Aircraft*, Vol. 25, No. 7, pp.606-611, July 1988.

7. Howard, R.M., and Miley, "Time Dependent Boundary Layer Response in a Propeller Slipstream," *Journal of Aircraft*, Vol. 26, No. 9, pp. 863-869, September 1989.

8. DISA Information Sheet, Types 55R55, 55R56, 55R57, and 55R58 Split-Fiber Probes for 2-dimensional Flow Field Measurements, DISA Electronics, Marina Del Rey, California.

9. Howard, Richard M., *An Investigation of the Effects of the Propeller Slipstream on a Wing Boundary Layer*, Ph.D. Dissertation, Texas A&M University, College Station, Texas, May 1987.

10. Renoud, R.W., <u>Boundary Layer Response to an Unsteady Turbulent Environment</u>, Master's Thesis, Naval Postgraduate School, Monterey, California, September 1988.

11. Department of Aeronautics and Astronautics, Laboratory Manual for Low-Speed Wind-Tunnel Testing, Naval Postgraduate School, Monterey, California, October 1983.

12. TSI Incorporated, IFA 100 System Instruction Manual, Revision C, St. Paul, Minnesota, August 1987.

13. Laboratory Technologies Corporation, LABTECH NOTEBOOK, Version 4, Wilmington, Massachusetts, January 1988.

14. Johnson, D.K., <u>A Data Analysis System for Unsteady Turbulence Measurements</u>, Master's Thesis, Naval Postgraduate School, Monterey, California, September 1988.

15. TSI Incorporated, Technical Bulletin TB 20 TSI Split Film Sensor Calibration and Application, St Paul, Minnesota.

16. Landrum, D.B., and Macha, J.M., "Influence of a Heated Leading Edge on Boundary Layer Growth, Stability and Transition," paper presented at the AIAA 19th Fluid Dynamics, Plasma Dynamics and Lasers Conference, Honolulu, Hawaii, 8-10 June 1987.

## INITIAL DISTRIBUTION LIST

No. Copies

1. Defense Technical Information Center   2
   Cameron Station
   Alexandria, Virginia   22304-6145

2. Library, Code 0142   2
   Naval Postgraduate School
   Monterey, California   93943-5002

3. Chairman, Code 67   2
   Department of Aeronautics and Astronautics
   Naval Postgraduate School
   Monterey, California   93943-5000

4. Commander   1
   Naval Air Systems Command
   Washington, D.C.   20360

5. NASA Langley Research Center   1
   MS/1285 Technical Library
   Hampton, Virginia   23665

6. NASA Ames Research Center   1
   Technical Library
   Moffett Field, California   94035

7. Dr. Bruce J. Holmes   1
   Head, Flight Applications Branch
   NASA Langley Research Center
   MS 247
   Hampton, Virginia   23665

8. Mr. Benjy Nuemann   2
   Naval Air Systems Command
   Aircraft Division--Research and Technology
   Air 931K
   Washington, D.C.   20360

9. Prof. R.M. Howard, Code 67 Ho   10
   Department of Aeronautics and Astronautics
   Naval Postgraduate School
   Monterey, California   93943-5000

10. LT David J. Gwilliam Jr.                    2
    145 Monroe Street
    E. Hartford, Connecticut  06118